UNCLASSIFIED

AD NUMBER
AD254847
LIMITATION CHANGES
TO: **Approved for public release; distribution is unlimited.**
FROM: **Distribution authorized to U.S. Gov't. agencies and their contractors; Administrative/Operational Use; DEC 1960. Other requests shall be referred to Army Transportation Research Command, Fort Eustis, VA.**
AUTHORITY
TRECOM per DTIC form 55

THIS PAGE IS UNCLASSIFIED

12 600

U. S. ARMY
TRANSPORTATION RESEARCH COMMAND
FORT EUSTIS, VIRGINIA

TREC TECHNICAL REPORT 61-19

INVESTIGATION OF TILTING DUCT AND FAN-WING IN TRANSITION FLIGHT

Project 9R38-11-009-12

Contract Number DA-44-177-TC-486

December 1960

prepared by :

MASSACHUSETTS INSTITUTE OF TECHNOLOGY
Boston, Massachusetts

61-2-6
XEROX

2494-60

AEROELASTIC AND STRUCTURES RESEARCH LABORATORY
MASSACHUSETTS INSTITUTE OF TECHNOLOGY

TECHNICAL REPORT 90-1

INVESTIGATION OF TILTING DUCT AND FAN-WING IN TRANSITION FLIGHT

BY

JEAN F. DUVIVIER
ROBERT B. McCALLUM

FOR

USA TRECOM
FT. EUSTIS, VIRGINIA
CONTRACT NUMBER DA-44-177-TC-486, J. O. No. 3

DECEMBER 1960

TREC TECHNICAL REPORT 61-19

ABSTRACT

A study of the ducted fan as a lifting device in forward flight, as a tilting duct and as a wing enclosed fan showed that significant changes in lift and power occur when inlet separation occurs; that sizable crossflow exists in the duct in all cases; that an increase in lift and power and a decrease in drag occur with forward speed after inlet separation is established which cannot be accounted for by momentum considerations alone. In the case of the fan-wing, the lift curve slope and C_{M_α} are not changed by the fan operation. A comparison of an articulated and a rigid rotor does not show significant changes in total pitching moments. Comparatively less lifting power is required under similar conditions for the fan-wing than for the tilting duct.

Additional force, velocity and pressure data are presented.

FOREWORD

The study presented in this report was undertaken by the Aeroelastic and Structures Research Laboratory, Massachusetts Institute of Technology, Cambridge 39, Massachusetts and sponsored by the U. S. Army Transportation Research Command under Contract Number DA-44-177-TC-486, Job Order No. 3. The authors, Mr. Jean F. Duvivier and Mr. Robert B. McCallum are members of the Division of Sponsored Research Staff at M.I.T. This research program was carried out under the supervision of Professor Rene H. Miller of the Department of Aeronautics and Astronautics with Mr. Duvivier as project leader. This study began in July 1959 and was completed in September 1960. Mr. James Scheiman of the U. S. Army Transportation Research Command was the Project Officer.

The authors are indebted to Professor Rene Miller for his supervision and advice, to the Personnel of the Model Shop under Mr. Oscar Wallin, to Mr. Fred Merlis of the Electronic Shop, and to Mrs. Adele Holevas for the preparation of the report.

TABLE OF CONTENTS

TABLE OF CONTENTS (Continued)

LIST OF FIGURES

LIST OF FIGURES (Continued)

NOMENCLATURE

A	rotor disc area (ft.^{2})
b	wing span (ft.)
c	airfoil chord (ft.)
C_D	drag coefficient $\left(= \frac{D}{\frac{\rho}{2} S V^2}\right)$
C_L	lift coefficient $\left(= \frac{L}{\frac{\rho}{2} S V^2}\right)$
C_M	moment coefficient $\left(= \frac{M_{.3c}}{\frac{\rho}{2} S c V^2}\right)$
C_D^*	$= \frac{D}{\rho A (\Omega R)^2}$ — used for static tests, $V = 0$
C_L^*	$= \frac{L}{\rho A (\Omega R)^2}$ — used for static tests, $V = 0$
C_M^*	$= \frac{M}{\rho A (\Omega R)^2 R}$ — used for static tests, $V = 0$
D	drag (lb.)
D_R	rotor diameter (ft.)
H	"horizontal" force (lb.), defined in Eq. 4
i	tilt angle (degree), positive nose down
L	lift (lb.)
$\dot{m}$	mass flow (slugs/sec.)
M	moment (ft.-lb.) about point 0 (Fig. 3, 4) $(= M_{.3c})$
n	number of rotor blades
P	power (ft.-lb./sec.)
r	radius (in. or ft.)
R	rotor radius (ft.)
S	wing area (ft.^{2})
T	thrust (lb.) along rotor axis
$\bar{u}$	mean inflow through the rotor (ft./sec.)
V	forward flight velocity (ft./sec.)
α	wing angle of attack, positive nose up
β	blade flapping angle
Δ	aerodynamic load increase (= total load with fan operating - load with fan inoperative)

NOMENCLATURE (Continued)

σ	$\dfrac{n\,C_b}{\pi(R + r_h)}$ rotor solidity
ρ	air density (lb. sec.^{2}/ft.^{4})
Ω	rotational velocity (rad./sec.)
ψ	azimuth angle measured in the directions of rotation from the aft position
η	inlet recovery factor

Subscripts

b	blade
$(\ )_i$	induced
p	parasite
R	rotor
S	shroud
x, z	components along x, z axes
1	inlet
2	outlet
h	hub

1. INTRODUCTION

The interest existing in the field of Vertical Take-Off Aircraft (VTOL) has led to the study of various means of achieving adequate lift during take-off and hovering as well as during transition to forward flight. Besides the well-known helicopters, test aircraft embodying tilting rotors, tilting wings, vertical jet engines, deflected slipstream and ducted fans, have been designed and flown, with varying degrees of success.

The object of the present study is limited to ducted fans, and to achieving a better fundamental understanding of the mechanisms whereby thrust, moment and drag are generated and related to each other. The expression "ducted fan" used herein refers to a rotor or propeller located within the boundaries of a circular cylindrical surface. Equivalent expressions also found in the literature are: "shrouded propeller", "ducted propeller", and "lift fan". Two applications are considered: the "tilting duct" alone and the "fan-wing" in which the ducted fan is buried inside a wing body.

The U. S. Army TRECOM-MIT Symposium on Ducted Fans held at MIT, Cambridge, Massachusetts in December 1958 showed that most test data and theories proposed dealt with the propulsive rather than the lifting use of ducted fans. Since then various reports have been published, (Refs. 1, 3, 7, 13, 16, 21) which have added to the data available. Unfortunately no results of flight tests of actual test vehicles such as the DOAK VZ-4DA and the Piasecki VZ-5P have been published.

The difficulties involved in establishing a theory for the prediction and evaluation of aerodynamic loads on ducted fans are manifold. The flow around and into the duct is three-dimensional, viscous effects are present (boundary layer separation at the inlet, interaction between wall boundary layer and rotor tip vortices) and the wake does not extend linearly to infinity, (curves back in forward flight, and spreads out in all directions in hovering). The purpose of this program has been to obtain experimental data to aid in the understanding of such phenomena.

An experimental test program in the MIT Wright Brothers Wind Tunnel 7 1/2 X 10 ft. test section, for a few selected values of the available parameters has been run using a tilting duct and a fan-wing model. Forces, moments, power settings and extensive pressure measurements were recorded.

The test models described in Chapter 2 are by no means attempts at obtaining optimum performance since an optimum design would only be such for a specific set of parameters and would be off-design elsewhere. The test models are basically those used in Ref. 13 modified on the basis of past experience and of the present state of the art, and are research models designed to cover a range of disc loadings rather than optimized designs for one desired test configuration.

Particular attention was directed to the following items of interest:

1) Magnitude and direction of the thrust resultant vector, (thrust and horizontal force), and pitching moment for the rotor independently of those acting on the surrounding shroud or wing over a range of V/u and C_T.

2) Magnitude of the momentum drag compared to the total drag of each configuration, the kinetic energy recovery of the system and proportion of mainstream flow velocity passing through the duct.

3) Pressure distributions in the neighborhood of the duct inlet and visual studies of the flow patterns.

Chapter 2 explains the experimental program including the models, and their instrumentation.

Theoretical analyses based on momentum theory are used to correlate the test data. The test results are reviewed and the correlation of experimental data with the theory is discussed in Chapter 3. Finally, conclusions and recommendations will be found in Chapter 4.

Wind tunnel corrections were not applied to the data because it was felt that no satisfactory method is presently available for correcting the fan wake in a constricted section.

II. EXPERIMENTAL PROGRAM

2.1 General Remarks

The experimental program was conducted in two stages with two models having several components in common.

Basic to both the tilting duct and the fan-wing models were the power drive and rotor, the shroud and the instrumentation. The fan-wing model was obtained by locating the tilting duct model in an opening in the wing model which was then attached rigidly to the duct shroud. The models are described in section 2.2; the load measuring and pressure measuring instrumentation system is described in section 2.3. The test program itself is outlined in section 2.4. Experimental difficulties encountered are described in section 2.5.

2.2 Test Models

2.2.1 Tilting Model

The model used the Task variable frequency motor, and the mahogany shroud from Ref. 13 with the addition of a slip ring assembly, new flapping hinges and flapping angle measuring pickup, new blades, a spinner, new velocity rakes, additional inlet pressure points, and a different mounting and load measuring system.

The fan had a two bladed 18-inch diameter rotor with the characteristics listed in Table I; each blade was made of balsa shaped around a tapered 7075 Aluminum alloy spar, covered with .004 in. nylon cloth and finished with several coats of dope. Both blades were very closely matched in weight and C.G. position. The constant area duct was enclosed by a mahogany shroud with a bell mouth inlet. The inlet radius of 0.0833 D_R was larger than the minimum value of 0.06 D_R found necessary to avoid inlet separation in hovering (Ref. 14, 17).

The fan was driven directly by a Task Corp. variable frequency three-phased water cooled electric motor rated at 19 HP at 15000 rpm. Actual operating speeds were limited to 7000 rpm. The motor was mounted by two end steel plates to a steel housing to which were welded the four 0.50 X 1.25 in. supporting steel struts, 90° apart. The struts in turn went through appropriate openings in the duct walls and were brazed to a steel ring inside the exterior shroud contour (Fig. 5). At their shroud ends, the struts were machined to form the various load measuring flexures (Fig. 6). The shroud was mounted by similar flexures directly to the steel ring, which was supported by the balance struts. The fan-motor assembly and the shroud were thus mounted independently of each other. The cooling water hoses, power lines, the tachometer, motor coil thermocouples and shielded signal cables ran from the downstream housing end through a streamlined tubing to the rear wind tunnel balance strut (Fig. 3). A molded fiberglass spinner shielded the blade hub, the flapping pickup and the slip ring assembly.

The exterior contour of the shroud was closed by means of aluminum sheet fairings screwed to the wood.

2.2.2 Fan-Wing Model

The same shroud and fan described in section 2.2.1, without the outer aluminum fairings, were mounted inside an opening in the wing model (Fig. 4). The NACA 0018 airfoil section was chosen to minimize any change in wing moment at all angles of attack and to have no wing lift at zero angle of attack. Any values of lift and moment would then be due to the fan alone. The top and bottom skins of the wing were screwed to the shroud in such a way that all the airloads on the wings were transmitted to the mounting ring through the shroud flexures. The joint between the shroud inlet and the wing top surface was faired, and the inlet shape was made elliptical between the wing top surface and the shroud inner surface (Fig. 9). Characteristics of the wing model are given in Table I. The wing tips were made from balsa blocks shaped as bodies of revolution obtained by rotating half the NACA 0018 profile around a chordline. All power leads, water lines and wires came out of the hub and motor through a faired aluminum tubing to the underside of the wing, and then into the rear balance strut (Fig. 4).

Figures 7 and 8 show the tilting duct model and the fan-wing model mounted in the test section.

2.3 Test Instrumentation

2.3.1 Air Loads Measuring System

The rotor assembly was mounted at four points, 90° apart, to the supporting ring by means of machined beam flexures (Fig. 5, 6). The shroud was mounted to the same support ring also at four points by similar and separate flexures. The bending deflections of selected flexures under load were measured by individual pickups made of a strip of berrylium-copper or aluminum alloy of appropriate thickness (.010 to .060 in. depending upon the range of sensitivity desired for each signal) mounted as a cantilever between the ends of the respective flexure. One end of a pickup was screwed and bonded to one end of a flexure while the other pickup end rested against the other flexure end by means of a teflon bead(later changed to half a 1/2 in. diameter steel ball). Each pickup was instrumented with two or four strain gages; in effect, each pickup served to magnify the flexure bending deflection, without carrying any of the flexure loads. Most of the interactions between pitching moments, thrusts and H loads were eliminated by means of precision ball bearing pivots which allowed shears to be transmitted but not moments (Fig. 6, 12).

Figure 11 shows the location of the various pickups. Those measuring T_R, T_S, H_R, and H_S were instrumented with four strain gages mounted two on each face of the pickup so that all four arms of the resulting bridge were active and exposed to the same temperature environment. The pickups measuring M_R and M_S were instrumented with two gages each located at the front and rear and formed to a complete four-arm bridge in pairs (Fig. 12), such as to cancel deflection signals from thrust loads and to register differential deflections due to pitching moments.

Because of experimental difficulties described in more detail in section 2.5, the pickups were encased in a 1/8 inch thick layer of Silastic RTV 881 silicone rubber for complete insulation from ambient temperature changes during wind tunnel runs.

The pickup bridges were connected into six channels of a Consolidated Model D Carrier Amplifier with 3 kc excitation. Each channel output was used to drive a sensitive galvanometer in a Heiland Model 712C recording oscillograph (Fig. 13).

2.3.2 Power (Torque) Measurement

An attempt was made to determine the power output of the motor at each test condition by measuring the torque on the shaft between the motor and the rotor hub, by means of strain gages. Although very good results were obtained under static conditions, it was not found possible to eliminate completely the errors introduced in the signals by temperature gradients along the shaft with the motor in operation.

Power measurements were obtained by calibrating the motor on a dynamometer at various speeds, while using the same length of power lines as were used in the wind tunnel tests. This precluded obtaining accurate power measurements while operating on the hovering test stand in another building, 250 feet away from the frequency changer control panel. This problem has been discussed in Ref. 13 and is caused by the large inductive reactance in the lines, associated with the low power factors (.5 to .6) at which the motor was operating. Therefore only hovering runs in the wind tunnel are included in this report.

2.3.3 Flapping Angle Measurement

A flexible flapping angle pickup of the same type as those discussed in section 2.3.1 instrumented with four strain gages to form a complete bridge with all arms active and under identical operating conditions, was mounted between the hub center block and a flat on one of the blade root fittings. An identical dummy pickup was mounted on the opposite blade 180° apart, to preserve mass balance of the hub assembly. No amplification was necessary and adequate output was obtained to drive a recording galvanometer directly. Output was linear from -5 to 6° (Fig. 10, 13).

2.3.4 Slip Ring Assembly

The excitation and output leads for the flapping angle pickup (channel 7) and the torque measuring bridge (channel 8) were transferred from the rotating to the fixed system by means of eight coin silver slip rings and three silver graphite brushes per ring. A ninth slip ring with a dead spot produced a timing signal every time the reference blade went through $\psi = 0^o$.

A thin Lucite cylindrical shield in line with the spinner and the motor housing protected the slip ring assembly from slipstream damage. Slip ring noise was negligible in all test results, which result must be credited to the fact that the strain gage bridges were completely on one side of the slip rings.

2.3.5 Pressure Measurements

All measured pressures were recorded by taking Polaroid pictures of two manometer boards (120 tubes) which were later reduced and interpreted. The pressure probes were connected to the manometer boards by 50 ft. long 1/16 in. plastic tubes coming out of the models at the rear balance strut location , and a streamlined fairing was placed around them during the runs.

Inflow velocities

Inflow velocities were measured by 4 rakes, 90° apart at azimuths 45°, 135°, 225°, and 315°, each rake consisting of five total head and three static probes. The probe inlets were internally rounded and located in a plane parallel to and 4 inches downstream of the rotor plane. Each total head probe was located radially such that equal annular disc areas corresponded to each measured velocity. The average inflow through the fan was then taken as the arithmetic mean of all the measured velocities. This value of $\bar{u}$ was used to compute the mean mass flow m.

Inlet pressures

Inlet pressures on both models were measured at five positions, $\psi = 180^{o}$, 225^{o}, 270^{o}, 315^{o} and 360^{o} (Fig. 12). At each location, six pressure points were located axially 0.75 inches apart (stations E, G, H, J). At station F, 4 additional points were located 0.75 inches apart downstream of the rotor plane (Fig. 14, 15).

Wake Survey

Two additional rakes were located perpendicularly to the wing lower surface 4 1/2 inches on one side and 3 3/4 inches on the other side of the fan center line, and 12 inches from the trailing edge of the wing (positions K and L, Fig. 15), to measure the wake profile and observe wake reattachment to the wing underside if any. Each rake had eight total head and two static head probes.

Airfoil pressure distribution

Twenty tube, thin pressure tapes were bonded onto the wing surface and static pressure taps drilled one to each tube at suitable locations on one side of the fan center line (Fig. 15).

2.3.6 Wing Airflow Observation

The upper surface of the wing was marked with a 2 X 2 in. grid, and numerous wool tufts were put on (Fig. 9). Photographs were taken for several representative runs, as well as while the tunnel speed or the rpm were changed. In addition short 16 mm movie runs were taken of steady and transitionary flows for additional observations later.

2.4 Test Program

Tilting Model

The tilting duct model was mounted inverted in the MIT Wright Brothers Wind Tunnel 7 1/2 X 12 ft. elliptical test section (Ref. 9), and by a suitable rear strut linkage was rotated from 0 to 90^o on the Wind Tunnel Balance struts. The model was mounted inverted in order to allow complete rotation with the available rear balance strut travel and to remove the extended rear strut from the vicinity of fan wake (Fig. 7). Tests were run at one blade pitch setting (20^o) of the articulated rotor, at tilt angles of -10, 0, +10, 20, 30, 50, 70 and 90^o and at tunnel velocities 0, 20, 40 mph, and at 3000, 5000, 7000 rpm.

Fan-Wing Model

The fan-wing model was mounted upright in the same test section, and on the same wind tunnel balance struts. Tests were run with the articulated rotor at pitch angles of 10^o, 20^o, and 30^o, at tunnel speeds of 0, 20, 40 and 60 mph, and fan velocities of 3000, 5000 and 7000 rpm. A few runs with the rigid rotor were made at 20^o pitch and 0, 40 and 60 mph wind tunnel speeds.

Height of duct exit from the ground plane was 2.5 fan diameters for both models in hovering position.

Procedures

The tare values of lift, drag and moment were measured for the duct with the fan blades removed, and for the fan-wing with the duct openings covered with shaped aluminum plates.

During the test program, difficulties were encountered in obtaining satisfactory outputs from the strain gage system with the fan in operation, although static calibrations were repeated satisfactorily.

The sources of the erratic outputs were found, but in order to complete the program within the time and funds available, the testing was resumed to obtain total loads and pressure distribution. The complete elimination of the effect of vibrations on the strut supports and amplifier drift on the output signals would have required more time than was then available, and was left for future development.

Results of the flexure readings showed them to be within the range to be expected, but their accuracy and repeatability were questionable and they are therefore not presented in this report.

2.5 Experimental Difficulties

2.5.1 Motor Failures

While calibrating the torque bridge (Channel 8) without rotor, failure of the Task motor shaft was experienced at 9500 rpm. After replacement of the motor shaft and armature and rebuilding of the slip ring assembly, further tests were limited to 7000 rpm.

2.5.2 Torque Bridge (Channel 8)

The torque bridge consisted of two pairs of Baldwin A-7 strain gages mounted 45^{o} to the shaft axis. Erratic output with the motor in operation led to their replacement by two Baldwin ABX-11 bakelite rosettes, then by two temperature compensated Tatnall C6-122-R2c foil rosettes.

In all cases, very good calibrations were obtained with the motor stopped, but drift in the signal was experienced with the motor in operation; this was traced to small temperature gradients along and across the shaft with the gages reading relatively low stress levels. Further corrections involving relocating the gages away from the shaft axis and rebuilding the hub assembly were not attempted so as not to delay further the test program.

Load Flexures

The major difficulties in obtaining repeatable outputs from the load flexures, were temperature effects on the gages, vibrations from the fan operation, and amplifier drift. Temperature effects were minimized by limiting the gage current and suitable insulation of the pickups. A different available amplifier system was used with small improvement. Further work in this direction with development of suitable output filters and amplifier modifications were not pursued for the reasons already stated in 2.5.2.

III. TEST RESULTS AND DISCUSSION

3.1 Inlet Separation and Flow-through Duct

Visual observations of the flow on the wing were made through windows in the ceiling of the wind tunnel test section. All observed flow patterns can be broadly grouped into two categories: before inlet separation occurs and after separation has occurred. These typical flow patterns are shown in Fig. 16a at $V/\bar{u} = .34$ (inlet flow attached) and Fig. 16b at $V/\bar{u} = 2.5$ (inlet flow separated). The difference in flow behavior in and around the duct is striking.

The corresponding pressure distributions are shown in Figs. 17 and 18, and the axial velocity distributions in the duct 4 inches downstream of the fan are shown in Figs. 19a and 19b for the same conditions.

As will be shown later, noticeable changes occur in the fan power when separation occurs.

In all the tests made on the wing, separation consistently occurred for $V/\bar{u}$ of .4 to .6; in this range separation extended gradually.

For values of $V/\bar{u}$ above 1.0 the flow on the inlet shows evidence of skirting around the duct in the direction of the fan rotation, and of outflow on the rear inlet. The locus of the stagnation points on the rear inlet wall is well inside the duct, but its exact location could not be determined accurately.

Some transient flow oscillations were observed behind the fan during transition from one wind tunnel velocity to a higher one. A short 16mm movie shows this occurrence quite clearly.

As can be averred from Fig. 19a, the flow in the duct is very nearly symmetrical with respect to the fore and aft axis as long as inlet separation has not occurred. On the other hand, Fig. 19b shows the asymmetric and turbulent flow distribution when inlet separation has occurred.

No visual flow observations are available for the tilting duct alone because of the manner of its mounting in the tunnel, but it is believed on the basis of available pressure data that conditions similar to those in the fan-wing case prevail.

Extensive data are presented in Tables IV and V and pressure distributions are presented in Tables VI and VII.

3.2 Fan-Wing Tests

The aerodynamic coefficients of the wing (aspect ratio = 1) with the duct opening closed at top and bottom by suitably shaped plates are given in Fig. 20. The plot of C_L vs α is repeated in Fig. 21 with additional values of C_L for various ratios of forward speed to inflow. No change in the lift curve slope occurs with the fan in operation, indicating that the fan lift increment is independent of wing lift due to angle of attack. This result is further verified by Fig. 22 which shows the incremental C_L due to the fan to be independent of angle of attack over the range of α of interest.

Similar results are found for the incremental drag ΔC_D although less pronounced at the lower values of $V/\bar{u}$ (Fig. 23.).

On the other hand the incremental lift achieved by operating the fan depends considerably upon forward flight speed V. For instance Fig. 24 shows the ratio of the measured lift increment ΔL to the fan thrust expected from momentum considerations, i.e., $\rho A\bar{u}^2$. The fan lift would be $\rho A\bar{u}^2 \cos \alpha$ (Eq. 1b). The lift increment reaches a minimum for all angles of attack in the range of $V/\bar{u}$ where inlet separation begins, then increases with forward speed, inlet separation notwithstanding.

Fig. 25 shows the ratio of measured fan shaft power to the expected momentum power. There is a noticeable drop of power with speed before inlet stall occurs, then a peak (for all angles of attack) followed by a power variation that depends directly upon angle of attack. The variation of power with lift increment follows a similar pattern (Fig. 26). These various indications point to some additional mechanisms of lift generation at forward speeds beyond that at which inlet separation occurs, that cannot be explained in terms of momentum alone.

Referring to Figures 1 and 2, in the wind axis system, from momentum considerations:

$$L = m \bar{u} \cos i \tag{1a}$$

(Tilting duct)

or

$$L = m \bar{u} \cos \alpha \tag{1b}$$

(Fan-Wing)

and

$$D = m (V - \bar{u} \sin i) + D_p \tag{2a}$$

(Tilting duct)

or

$$D = m (V + \bar{u} \sin \alpha) + D_p \tag{2b}$$

(Fan-Wing)

Also,

$$\Delta D = D - D_p \tag{2c}$$

These forces are related to those in the body axis system by the relations

$$L = T \cos i + H \sin i \tag{3a}$$

or

$$L = T \cos \alpha - H \sin \alpha \tag{3b}$$

and

$$D = H \cos i - T \sin i \tag{4a}$$

or

$$D = H \cos \alpha + T \sin \alpha \tag{4b}$$

The induced power required to achieve the duct velocity $\bar{u}$ is:

$$(P)_i = \frac{1}{2} m (\bar{u}^2 - \eta V^2) \tag{5}$$

where η is an inlet energy recovery factor.

If all of the free stream energy at the inlet is recovered, $\eta = 1.0$, and the flow is rotated completely into the duct. If no energy recovery occurs, $\eta = 0$, and the fan is pumping air from zero velocity to $\bar{u}$.

As

$$m = \rho A \bar{u} \tag{6}$$

$$(P)_i = \frac{\rho A \bar{u}^3}{2} \qquad (\eta = 0) \tag{7}$$

$$(P)_i = \frac{\rho A \bar{u}}{2} (\bar{u}^2 - \eta V^2) \quad (\eta \neq 0) \tag{8}$$

The induced power required per pound of fan induced lift would be

$$\frac{P}{\Delta L} = \frac{\bar{u}}{2 \cos i} \left[1 - \eta \left(\frac{V}{\bar{u}} \right)^2 \right] \tag{9}$$

(Note: in standard helicopter nomenclature, $\frac{V}{u} = \frac{\mu}{\lambda}$).

The ideal induced power is plotted in Fig. 27 for total recovery ($\eta = 1.0$) and no recovery ($\eta = 0$) (Equations 7 and 8).

By comparison, the ratio of the actual power to the inflow kinetic energy shows trends that confirm Figs. 25 and 26. A definite power decrease occurs with forward speed at all angles of attack but only until inlet separation begins. It is also evident that considerable inlet energy is recovered until inlet separation occurs, after which only for the -10° case does any recovery occur. For all the other cases power increases after inlet separation and more sharply for the higher angles of attack, as may be expected because of the more pronounced separation.

The incremental drag ΔD is defined as the difference between the total drag with fan in operation and that of the same wing without duct, which is herein called "parasite drag". In the case of the wing this term includes profile and induced drags (Eqs. 2a and 2b). The drag increment is essentially the change of momentum of the inflow in the x direction.

From Eqs. (1) and (2)

$$\frac{\Delta D}{\Delta L} = \frac{V - \bar{u} \sin i}{\bar{u} \cos i}$$

$$= \frac{\frac{V}{\bar{u}} - \sin i}{\cos i} \qquad (10a)$$

(tilting duct)

or

$$\frac{\Delta D}{\Delta L} = \frac{\frac{V}{\bar{u}} + \sin \alpha}{\cos \alpha} \qquad (10b)$$

(fan-wing)

For $i = \alpha = 0$

$$\frac{\Delta D}{\Delta L} = \frac{V}{\bar{u}} \qquad (11)$$

In Fig. 28 the measured $\Delta D/\Delta L$ are plotted against $V/\bar{u}$. Comparing the experimental curves with the theory, it is evident that a decrease in drag occurs with increasing forward velocity. This amounts to a decrease in the momentum drag which indicates that the inflow is no longer in the direction of the duct axis but is now slanted rearwards in the duct and at the duct outlet. This affects directly the propulsive power required for forward flight.

The comparative decrease in momentum drag with higher flight speeds is also evident from Fig. 29 which shows a comparison of measured incremental drag with that predicted by Eq. 2c.

The incremental moment ΔC_M depends on both $V/\bar{u}$ and to a smaller extent on angle of attack. Fig. 30 shows a plot of total C_M as a function of $V/\bar{u}$ and Fig. 31 a crossplot of C_M versus angle of attack. The stability derivative C_{M_α} is seen to be essentially constant for the wing with or without fan except at angles of attack greater than 5^o for $V/\bar{u}$ less than 0.8.

The ratio of incremental moment* to increment lift (Fig. 32) is seen to increase with forward speed but at a gradually smaller rate and seemingly decrease at still higher $V/\bar{u}$. This confirms data previously obtained. For instance the same trend is shown in Fig. 36 of Ref. 13 for values of $V/\bar{u}$ up to about 1.2. Additional force and power data are presented in Table III.

3.3 Tilting Duct Tests

The lift induced by the fan in forward flight is compared to the lift expected from momentum theory (Eq. 1) in Fig. 33. A small drop in lift followed by an increase at higher forward flight speeds, similar to Fig. 24 for the fan-wing case, suggests that fan induced circulation on the duct contributes to the lift, in addition to the vertical momentum change.

Figure 34 shows the variation of rate of pitching moment increase** with an increase in lift, and the trend for small tilt angles substantiates the findings of Ref. 13, and that of Fig. 32 for the fan-wing. At higher tilt angles the ducted fan behaves more like a ring wing at large angles of attack.

* i.e.: ΔC_M = the difference in moments with the fan in operation, and with the bare wing, fan covered.

** difference in moments with fan operating and with fan stopped, blades removed.

For instance Figs. 4 and 6 of Ref. 2 show ring wing stall occuring at angles of attack near 20° ($i = 70^{\circ}$). It may be concluded that the stall of the duct acting as a ring wing has a pronounced effect on the pitching moment, and that at high inflow velocities relative to forward speed (low values of $V/\bar{u}$) such stalling is alleviated even for high angles of attack of the ring wing (low values of i).

The variation of momentum drag with $V/\bar{u}$ evidences a similar decrease of drag with forward speed already discussed in the fan-wing case, except for negative values of tilt where a reversal occurs (Fig. 35). This trend is confirmed by Fig. 36.

The actual power compared to the theory (Eq. 7) is plotted in Fig. 37, and shows a strong effect of tilt angle on the power required for forward flight of a wingless ducted fan. Comparing Fig. 37 with Fig. 27 for the same fan without and with a wing, and considering that these curves cover the same range of disc loading and of $V/\bar{u}$ for both models, it appears that comparatively less power is required for the wing-fan at the same angles of attack (NB: $i = -\alpha$) and that the addition of a wing has a favorable effect on the fan power requirements in forward flight (Ref. 18).

3.4 Blade Flapping

Figure 38 shows a plot of typical blade flapping motion in forward flight for $V/\bar{u}$ of .341. As shown in Fig. 16a and Fig. 17 for the same condition, the flow over the leading edge is not yet detached, as it is for instance in Fig. 16b and 18. For the same angle of attack and with $V/\bar{u}$ of .296 the flapping double amplitude increases to 15.5°.

In the case where inlet separation occurred, the flapping record failed repeatedly and the flapping pickup was damaged, indicating that the motion exceeded the expected range of pickup deflection ($-8^{\circ} \leq \beta \leq +8^{\circ}$).

3.5 Comparison of Rigid and Articulated Rotors

Table VIII present a comparison under identical test conditions of the aerodynamic loads measured when the fully articulated hub of the rotor was replaced by a rigid hub, while retaining the same blades.

The effect of rotor articulation is seen not to affect lift, drag and moment significantly except at V = 60 mph where it appears that the rigid rotor maintains 5 per cent more inflow with an increase in pitching moment of about 18% and an increase in lift of 35%. From the discussion of blade flapping amplitude, it can be shown that the blade tip vertical displacement reaches values of 2 to 2 1/2 inches with consequent increases in the tip clearance of as much as .2 inches. It is already known (Ref. 17) that such large tip clearances have a deleterious effect on fan thrust and this accounts for the loss of lift of the articulated rotor under such conditions.

IV. CONCLUSIONS AND RECOMMENDATIONS

4.1 Conclusions

1) A major problem in obtaining optimum performance from a ducted fan is control of inlet separation in forward flight without adversely affecting the lift. This requires a careful theoretical and experimental study of the inlet shape itself as well as of suitable vanes and deflectors.

2) The amplitude of the blade flapping motion in forward flight indicates sizable crossflow. In many cases the measured flapping amplitudes were larger than anticipated.

3) There exists an increase in lift, a decrease in drag and a shaft power increase with forward speed for both the tilting duct and the fan-wing beyond that which could be accounted for by momentum considerations.

4) In the case of the fan wing, the wing lift due to angle of attack is not affected by the fan operation.

5) Similarly, C_{M_α} of the fan-wing is essentially the same as that of the wing alone except at high angles of attack and low forward velocities.

6) The difference in total pitching moments with either an articulated rotor or a rigid rotor is not significant; thus, the major contribution to the pitching moment is from shroud or wing aerodynamic loads and the positioning of the momentum drag line of action at some distance above the center of gravity of the system.

7) The addition of a wing to a ducted fan vehicle reduces to some extent the lifting power requirements in forward flight.

4.2 Recommendations

1) The accurate measurement of individual aerodynamic loads on the fan and shroud is feasible, but additional work is required to eliminate the effects of vibrations and temperature variations on the output from the load measuring pickups.

2) Major emphasis should be placed on the design of inlet shapes

and flow control devices for best results in forward flight.

3) Further studies should consider inclining the duct in the wing in the fore and aft direction as a means of alleviating inlet separation and achieving better inlet energy recovery.

BIBLIOGRAPHY

1. Brogan, E., Casey G., Engel B., and Fay, C., The Vertodyne VTOL Aircraft Study Semi-span Model Tests in Hovering and Forward Flight, Vertol Aircraft Company, Report R-158, March 1960.

2. Fletcher, H. S., Experimental Investigation of Lift, Drag, and Pitching Moment of Five Annular Airfoils, NACA, TN 4117, October 1957.

3. Gill, W. J., et al., Wind Tunnel Tests of Several Ducted Propellers in Non-Axial Flow, Hiller Aircraft Corp., Report No. ARD-224, 1959.

4. Ham, N D. and Moser, H H., Preliminary Investigation of a Ducted Fan in Lifting Flight, Journal A.H.S., Vol. 3, No. 3, July 1958.

5. Helmbold, H. B., Range of Application of Shrouded Propellers, University of Wichita, Engineering Study 189, August 1955.

6. Hickey, D. H., Preliminary Investigation of the Characteristics of a Two-Dimensional Wing and Propeller with the Propeller Plane of Rotation in the Wing-Chord Plane, NACA, RM A57F03, August 1957.

7. Hickey, D. H. and Ellis, D. R., Wind-Tunnel Tests of a Semi-Span Wing with a Fan Rotating in the Plane of the Wing, NASA TN D-88, October 1959.

8. Hubbard, H. H., Sound Measurements for Five Shrouded Propellers at Static Conditions, NACA, TN 2024.

9. Markham, J. R , The MIT Wright Brothers Wind Tunnel and its Operating Equipment, SAE Journal (Transactions) Vol. 49, No. 3, September 1941.

10. Meyerhoff, L. and Finkelstein, A. B., On Theories of the Duct Shape for a Ducted Propeller, Polytechnic Institute of Brooklyn, PIBAL Report 484, 1958.

11. Miller, R. H., Potential VTOL Capabilities of Supersonic Transports, Institute of the Aeronautical Sciences, Paper No. FF-26, January 1060, pp. 12-44.

12. Minnassian, B., Analytical Study of Shrouded Propellers, Longren Aircraft Co., Report LR-501, 1956.

13. Moser, H. H., and Livingston, C. L., Experimental and Analytic Study of the Ducted Fan and Fan-in-Wing in Hovering and Forward Flight, Massachusetts Institute of Technology, ASRL Report No. 79-1, January 1959.

14. Parlett, L. P., Aerodynamic Characteristics of a Small-Scale Shrouded Propeller at Angles of Attack from 0^{o} to 90^{o}, NACA TN 3547, November 1955.

15. Platt, Robert, Jr., Static Tests of a Shrouded and Unshrouded Propeller, NACA, RM L7H25, 1948.

16. Sacks, A. H., and Barnell, J. A., Ducted Propellers - A Critical Review of the State of the Art, Hiller Aircraft Corp., Report ARD-232, 1959.

17. Taylor, R. T., Experimental Investigation of the Effects of Some Shroud Design Variables on the Static Thrust Characteristics of a Small-Scale Shrouded Propeller Submerged in a Wing, NACA TN 1426, January 1958.

18. Templin R. J., Note on the Minimum Power Required for Flight at Low Air-Speeds, National Aeronautical Establishment, Ottawa, Report LR-245, May 1959.

19. Van Niekerk, C. G., Ducted Fan Design Theory, Journal of Applied Mechanics, Vol. 25, No. 3, Septmeber 1958.

BIBLIOGRAPHY (Continued)

20. Wardlaw, R. L. and Templin, R. J., Preliminary Wind Tunnel Tests of a Lifting Fan in a Two-Dimensional Aerofoil, National Aeronautical Establishment, Ottawa, Report LR-207, September 1957.

21. Wardlaw, R. L. and McEachern, N. V., A Wing Submerged Lifting Fan: Wind Tunnel Investigations and Analysis of Transition Performance, National Aeronautical Establishment, Ottawa, LR-243, September 1959.

22. Williams, J., Some British Research on the Basic Aerodynamics of Powered Lift Systems, Journal of the Royal Aeronautical Society, Vol. 64, No. 595, July 1960, pp. 413-419.

23. Theodorsen, T., Theoretical Investigation of Ducted Propeller Aerodynamics, Vols. 1 and 2, August 1960.

TABLE I

Model Dimensions

(Ref. Fig. 3, 4)

Both Models	
Rotor diameter (D_R)	18 in.
Exit diameter (D_R)	18 in.
Inlet radius (r_1)	1.5 in. (=8.33% of D_R)
Hub diameter ($2\ r_h$)	4 in.
Number of blades	2
Blade span ($R-r_h$)	7 in.
Blade chord	2.25 in.
Blade airfoil section	NACA 0012
Effective disc area (A)	1.68 ft.^{2}
Rotor solidity (σ)	.130
Minimum tip clearance	0.10 in.
Hub supporting struts	4
Chord of struts (l)	3 1/8 in.
Tilting Model	
Duct length	6.25 in.
Outer diameter	24 in.
Length of duct downstream of rotor plane	4.25 in.
Base width at duct exit	3 in.
Fan-Wing Model	
Wing span (b)	54.4 in.
Wing chord (c)	52 in.
Aspect ratio (AR)	1
Wing area (S)	18.77 ft.^{2}
Wing airfoil section	NACA 0018
Location of fan axis at	0.30 c
Length of duct downstream of rotor plane	5.0 in.

TABLE II
REDUCED WIND TUNNEL DATA
TILTING DUCT MODEL

ΩR	i	$V_{(mph)}$	$\bar{u}$	m	$V/\bar{u}$	C_L	ΔC_L	C_D	ΔC_D	C_m	(HP)	C_P	C_L^*	C_D^*
236	0	0	42.3	.175	0	-	-	-	-	-	.97	.0102	.084	0
393			67.5	.284	0	-	-	-	-	-	2.47	.0056	.030	0
550			94.3	.397	0	-	-	-	-	-	5.40	.0045	.031	0
236		20	33.4	.140	.878	.261	.261	.224	.125	.027	.86	.0090		
393			61.0	.257	.481	.809	.809	.364	.265	.071	2.10	.0048		
550			83.5	.351	.351	1.700	1.700	.522	.423	.110	4.20	.0035		
236		40	13.9	.059	.422	.098	.101	.113	.061	.008	1.00	.01052		
393			48.5	.204	1.210	.214	.218	.196	.134	.025	2.36	.0054		
550			81.3	.342	.721	.416	.419	.285	.233	.046	5.10	.0042		
236	-10	20	31.4	.132	.934	.287	.287	.284	.100	.031	.90	.0095		
393			57.3	.241	.512	.835	.835	.512	.227	.067	2.15	.0049		
550			84.2	.354	.348	1.618	1.618	.799	.371	.106	4.24	.0035		
393		40	38.4	.161	1.528	.241	.241	.230	.119	.022	2.57	.0058		
550			80.1	.337	.732	.429	.429	.347	.199	.044	5.20	.0043		
236	+10	20	35.4	.149	.823	.287	.287	.211	.107	.027	.85	.0089		
393			61.6	.259	.674	.809	.809	.258	.242	.071	2.06	.0047		
550			68.4	.288	.429	1.644	1.644	.264	.390	.120	4.17	.0034		
236		40	29.1	.122	2.010	.098	.104	.133	.072	.009	.91	.0096		
393			58.5	.246	1.000	.221	.228	.183	.142	.025	2.25	.0051		
550			83.9	.353	.699	.436	.442	.228	.222	.044	5.00	.0041		
236	+20	20	40.2	.196	.730	.287	.287	.174	.062	.025	.89	.0094		
393			62.8	.264	.467	.835	.835	.137	.205	.072	2.03	.0046		
550			84.3	.354	.348	1.644	1.644	-.264	.111	.122	4.20	.0035		
236		40	40.2	.169	1.450	.091	.104	.133	.062	.007	.89	.0094		

(C_m of duct at zero fan rpm = 0)

TABLE II (Continued)

Ω R	i	$V_{(mph)}$	$\bar{u}$	m	$V/\bar{u}$	C_L	ΔC_L	C_D	ΔC_D	C_m	(HP)	C_P	C_L^*	C_D^*
393	+20	40	67.2	.283	.873	.228	.241	.157	.128	.022	2.20	.0050		
550			91.6	.358	.640	.436	.448	.170	.206	.042	4.74	.0039		
236	+30	20	42.9	.180	.684	.313	.313	.095	.031	.023	.75	.0079		
393			63.6	.268	.461	.705	.705	-.116	.042	.066	1.80	.0041		
550			84.4	.355	.348	1.305	1.305	-.535	-.013	.121	4.25	.0035		
236		40	51.6	.217	1.136	.084	.107	.135	.064	.003	.90	.0095		
393			61.3	.258	.957	.228	.250	.135	.126	.020	2.10	.0048		
550			92.1	.887	.637	.429	.452	.114	.197	.004	4.25	.0035		
236	50	20	46.5	.196	.630	.261	.261	-.063	.012	.022	..85	.0089		
393			65.4	.275	.448	.626	.626	-.236	.120	.061	1.97	.0054		
550			85.6	.360	.343	1.096	1.096	-.741	.143	.117	4.17	.0034		
236		40	65.4	.275	.897	.078	.120	.180	.672	.006	.76	.0080		
393			77.4	.326	.758	.176	.218	.094	.104	.018	1.72	.0039		
550			83.6	3.52	.702	.325	.367	.003	.140	.036	3.72	.0031		
236	70	20	43.2	.182	.678	.157	.157	-.023	.031	.016	.86	.0090		
393			66.2	.278	.443	.339	.339	-.404	.046	.048	1.98	.0045		
550			84.8	.357	.346	.600	.600	-1.099	.055	.064	4.17	.0034		
236		40	63.2	.266	.928	.065	.107	.097	.037	.002	.69	.0073		
393			76.8	.323	.764	.117	.159	.027	.045	.011	1.55	.0035		
550			94.7	.398	.619	.195	.237	-.099	.056	.047	3.90	.0034		
236	90	0	33.2	.140	0	-	-	-	0	-	.90	.0095	0	.003
393			56.3	.237	0	-	-	-	0	-	2.04	.0046	0	.026
550			82.8	.349	0	-	-	-	0	-	4.50	.0036	0	.026
236		20	45.7	.139	.640	0	0	-.055	0	.005	.81	.0085		
393			65.7	.276	.446	0	0	-.477	0	.031	1.94	.0043		
550			87.2	.367	.336	0	0	-.590	0	.018	4.13	.0034		
236		40	61.4	.258	.955	-.003	-.003	.072	0	.001	.76	.0080		
393			78.1	.329	.751	-.003	-.003	-.001	0	.003	1.77	.0040		
550			96.2	.405	.610	-.003	-.003	-.135	0	.014	3.75	.0031		

TABLE III
REDUCED WIND TUNNEL DATA
FAN-WING MODEL

ΩR	α	$V_{(mph)}$	$\bar{u}$	m	$V/\bar{u}$	C_L	ΔC_L	C_D	ΔC_D	C_m	ΔC_m	P (shaft hp)	C_P
236	-10	20	41.4	.174	.708	.131	.392	.005	.091	.154	.201	0.85	.0089
393			69.3	.292	.423	.444	.705	.365	.227	.274	.321	1.85	.0042
550			90.5	.381	.324	1.150	1.409	.386	.129	.344	.391	4.05	.0034
236	+10		37.2	.156	.788	.598	.287	.298	.340	.296	.172	0.86	.0090
393			67.2	.283	.434	.992	.731	.491	.615	.435	.316	2.06	.0047
550			92.2	.388	.318	1.828	1.566	.783	1.060	.546	.430	4.10	.0034
236	-10	40	38.8	.163	1.513	-.052	.176	.152	.083	.042	.079	0.84	.0088
393			75.2	.316	.781	.091	.318	.226	.135	.727	.168	2.27	.0052
550			100.6	.423	.583	.240	.468	.285	.168	.193	.236	4.71	.0039
236	+10		20.4	.086	2.877	.312	.026	.111	.099	.077	.029	0.95	.010
393			59.6	.251	.985	.455	.169	.216	.231	.177	.132	2.42	.0055
550			97.1	.409	.605	.643	.358	.316	.368	.250	.208	5.12	.0042
393	-10	60	79.8	.336	1.103	-.029	.203	.083	-.051	.058	.110	2.22	.0050
550			-	-	-	.058	-	.070	-.017	.108	.161	5.03	.0040
393	+10		39.4	.166	2.234	.322	.064	.119	.110	.087	.040	2.42	.0055
550			76.75	.323	1.147	.429	.171	.198	.210	.165	.121	6.20	.0050
236	-5	20	41.2	.173	.711	.235	.365	.758	.199	.184	.204	0.80	.0084
393			70.2	.295	.417	.600	.731	.379	.269	.314	.335	1.95	.0044
550			95.2	.401	.308	1.305	1.436	.477	.305	.399	.419	4.05	.0033
236	+5		39.7	.167	.738	.418	.287	.271	.259	.215	.179	0.85	.0089
393			69.4	.292	.422	.835	.705	.440	.462	.364	.328	2.00	.0045
550			93.5	.393	.313	1.592	1.462	.659	.745	.469	.432	4.08	.0034
236	-5	40	34.3	.144	1.711	.058	.138	.131	.066	.056	.077	0.90	.0095

TABLE III Continued

ΩR	α	$V_{(mph)}$	$\bar{u}$	m	$V/\bar{u}$	C_L	ΔC_L	C_D	ΔC_D	C_m	ΔC_m	P (shaft hp)	C_P
393	-5	40	71.1	.299	.826	.195	.275	.211	.134	.140	.160	2.17	.0049
550			102.8	.433	.571	.351	.431	.278	.186	.214	.235	4.85	.0040
236	+5		26.5	.112	2.215	.188	.039	.104	.069	.081	.053	0.90	.0095
393			64.8	.273	.906	.384	.234	.212	.193	.175	.146	2.22	.0050
550			89.4	.376	.657	.546	.396	.291	.285	.250	.221	4.90	.0040
393	-5	60	68.4	.288	1.287	.061	.154	.140	.079	.002	.095	2.25	.0051
550			100.4	.422	.876	.160	.256	.198	.127	.126	.156	5.17	.0043
393	+5		53.6	.226	1.642	.223	.073	.124	.093	.103	.076	2.53	.0057
550			85.4	.359	1.030	.345	.194	.195	.174	.158	.130	5.93	.0049
236	0	20	40.9	.172	.716	.366	.365	.266	.219	.199	.201	0.85	.0089
393			69.90	.294	.419	.757	.757	.412	.365	.358	.342	2.04	.0046
550			93.10	.392	.315	1.460	1.462	.553	.506	.545	.434	4.10	.0034
236		40	32.2	.135	1.825	.104	.084	.109	.098	.070	.065	0.87	.0092
393			72.30	.304	.812	.299	.280	.208	.160	.157	.156	2.22	.0050
550			97.8	.412	.600	.448	.429	.278	.230	.232	.233	4.88	.0040
393		60	66.4	.279	1.325	.131	.107	.125	.078	.080	.092	2.42	.0055
550			93.5	.393	.941	.255	.232	.193	.147	.138	.152	5.49	.0045

TABLE IV

TILTING DUCT INFLOW VELOCITIE

V_{mph}	40	40	40	40	40	40	40	40	40	40	40	40	40	40
α	90°	90°	70°	70°	50°	50°	30°	30°	30°	20°	20°	20°	10°	10
θ	20°	20°	20°	20°	20°	20°	20°	20°	20°	20°	20°	20°	20°	20
ΩR	393	550	393	550	393	550	236	393	550	236	393	559	235	393
Manometer Tube No.	INFLOW VELOCITIES (ft/s													
9	91.0	93.0	70.5	98.0	78.0	102.	70.5	93.0	117.	70.5	98.0	121.	70.5	103.
11	93.0	102.	70.5	102.	75.5	105.	68.0	94.5	118.	68.0	98.0	124.	65.0	100.
12	87.0	110.	84.5	106.	87.0	108.	70.5	94.5	118.	78.0	102.	123.	46.5	108.
14	73.0	89.0	63.5	82.5	59.5	70.5	53.5	68.0	80.0	38.0	57.0	87.0	18.5	50.0
16	57.0	57.0	53.5	57.0	50.0	50.0	57.0	53.5	63.5	50.0	68.0	68.0	38.0	59.5
1	89.0	110.	87.0	108.	80.0	105.	0	27.0	24.5	18.5	18.5	18.5	18.5	118.
3	91.0	117.	91.0	117.	94.5	120.	B	32.0	82.5	13.0	B	27.0	B	B
4	84.5	108.	84.5	106.	87.0	112.	27.0	70.5	117.	0	33.0	80.0	18.5	0
6	73.0	91.0	73.0	98.0	80.0	98.0	63.5	105.	113.	18.5	94.5	131.	27.0	38.0
8	50.0	53.5	50.0	50.0	59.5	59.5	65.0	57.5	65.0	73.0	75.5	75.5	46.5	70.5
25	87.0	112.	82.5	110.	59.5	87.0	18.5	27.0	27.0	18.5	18.5	27.0	18.5	18.5
27	93.0	117.	91.0	120.	93.0	121.	0	33.0	103.	18.5	0	18.5	B	B
28	87.0	103.	89.0	113.	89.0	115.	18.5	70.5	117.	B	42.5	89.0	27.0	0
30	78.0	87.0	82.5	102.	84.5	105.	84.5	98.0	108.	38.0	102.	120.	33.0	63.5
32	53.5	59.5	59.5	63.5	63.5	65.0	68.0	70.5	78.0	70.5	78.1	80.0	38.0	68.0
17	84.5	110.	89.0	115.	94.5	120.	80.0	103.	130.	80.0	106.5	133.	80.0	112.
19	84.5	107.	82.5	106.	82.0	180.	75.5	94.5	119.	75.5	100.	120.	73.0	103.
20	93.0	118.	94.5	123.	98.0	124.	80.0	105.	133.	78.0	108.	134.	73.0	108.
22	78.0	112.	73.0	75.5	75.5	93.0	70.5	84.5	100.	65.0	94.5	100.	38.0	82.5
24	50.0	50.0	50.0	53.5	57.0	59.5	68.0	70.5	73.0	65.0	73.0	73.0	50.0	73.0

* B indicates Backflow.

2

TABLE IV

TILTING DUCT INFLOW VELOCITIES

0	40	40	40	40	40	40	40	40	40	40	40	40	40	40	40
0°	50°	30°	30°	30°	20°	20°	20°	10°	10°	10°	0	0	0	-10°	-10°
0°	20°	20°	20°	20°	20°	20°	20°	20°	20°	20°	20°	20°	20°	20°	20°
3	550	236	393	550	236	393	559	235	393	550	236	393	550	393	550

INFLOW VELOCITIES (ft/sec)

0	102.	70.5	93.0	117.	70.5	98.0	121.	70.5	103.	113.	59.5	96.5	134.	115.	130.
5	105.	68.0	94.5	118.	68.0	98.0	124.	65.0	100.	133.	46.5	103.	135.	107.	143.
0	108.	70.5	94.5	118.	78.0	102.	123.	46.5	108.	134.	27.0	98.0	139.	65.0	134.
5	70.5	53.5	68.0	80.0	38.0	57.0	87.0	18.5	50.0	89.0	B*	33.0	73.0	B	63.5
0	50.0	57.0	53.5	63.5	50.0	68.0	68.0	38.0	59.5	80.0	33.0	46.5	73.0	27.0	68.0
0	105.	0	27.0	24.5	18.5	18.5	18.5	18.5	118.	18.5	18.5	27.0	18.5	27.0	0
5	120.	B	32.0	82.5	13.0	B	27.0	B	B	B	0	0	0	B	18.5
0	112.	27.0	70.5	117.	0	33.0	80.0	18.5	0	53.5	0	0	27.0	B	18.5
0	98.0	63.5	105.	113.	18.5	94.5	131.	27.0	38.0	131.	0	27.0	42.5	0	80.0
5	59.5	65.0	57.5	65.0	73.0	75.5	75.5	46.5	70.5	87.0	0	63.5	93.0	33	87.0
5	87.0	18.5	27.0	27.0	18.5	18.5	27.0	18.5	18.5	18.5	18.5	18.5	B	27.0	B
0	121.	0	33.0	103.	18.5	0	18.5	B	B	50.0	0	0	0	18.5	0
	115.	18.5	70.5	117.	B	42.5	89.0	27.0	0	63.5	0	B	42.5	B	27.0
	105.	84.5	98.0	108.	38.0	102.	120.	33.0	63.5	121.	0	38.0	103.	B	100.
	65.0	68.0	70.5	78.0	70.5	78.1	80.0	38.0	68.0	65.0	B	63.5	91.0	550.	93.0
	120.	80.0	103.	130.	80.0	106.5	133.	80.0	112.	142.	68.0	112.	142.	112.	142.
	180.	75.5	94.5	119.	75.5	100.	120.	73.0	103.	130.	42.5	103.	131.	100.	115.
	124.	80.0	105.	133.	78.0	108.	134.	73.0	108.	141.	53.5	108.	141.	103.	139.
	93.0	70.5	84.5	100.	65.0	94.5	100.	38.0	82.5	103.	B	73.0	102.	59.5	100.
	59.5	68.0	70.5	73.0	65.0	73.0	73.0	50.0	73.0	82.5	38.0	65.0	87.0	46.5	80.0

w.

TABLE IV (Continued)

TILTING DUCT FLOW VELOCITIES

$V_{(mph)}$	0	0	20	20	20	20	20	20	20	20	20	20	20	20
$\alpha (^{O})$	0	0	0	0	0	-10	-10	-10	+10	+10	+10	+20	+20	+20
$\theta (^{O})$	20	20	20	20	20	20	20	20	20	20	20	20	20	20
ΩR	393	550	236	393	550	236	393	550	236	393	550	236	393	550
Manometer Tube NO.	INFLOW VELOCITIES (ft/sec)													
9	36.0	50.0	26.5	48.5	46.5	33.0	48.5	46.5	30.0	46.5	46.5	30.0	36.0	39.0
11	68.5	87.0	55.5	87.0	104.	50.0	87.0	105.	60.0	85.0	97.0	58.0	80.0	93.0
12	78.0	102.	63.0	90.0	114.	58.0	91.0	115.	63.0	38.0	114.	60.0	85.0	112.
14	74.5	105.	68.0	85.0	106.	54.0	87.0	107.	63.0	82.5	105.	58.0	75.0	104.
16	06.0	87.0	33.0	70.0	71.0	30.0	72.0	73.5	40.0	63.0	71.0	52.0	50.0	68.5
1	68.5	92.5	16.5	13.0	38.0	19.0	0	33.0	18.0	18.0	0	18.0	26.0	74.5
3	75.5	105.	0	13.0	95.0	0	0	82.5	0	26.5	83.5	0	60.0	107.
4	72.0	100.	13.5	63.0	112.	13.0	50.0	117.	0	71.0	91.0	18.0	86.0	106.
6	63.0	87.0	22.5	87.0	98.5	19.0	87.0	104.	33.0	82.5	76.0	58.0	80.0	95.0
8	66.0	33.0	40.5	53.5	50.0	38.0	50.0	57.0	46.5	53.5	0	50.0	40.0	42.5

TABLE IV (Continued)

TILTING DUCT FLOW VELOCITIES

20	20	20	20	20	20	20	20	20	20	20	20	20	20	20
-10	-10	-10	+10	+10	+10	+20	+20	+20	30	30	30	50	50	50
20	20	20	20	20	20	20	20	20	20	20	20	20	20	20
236	393	550	236	393	550	236	393	550	236	393	550	236	393	550

INFLOW VELOCITIES (ft/sec)

33.0	48.5	46.5	30.0	46.5	46.5	30.0	36.0	39.0	26.5	33.0	42.5	26.5	30.0	42.5
50.0	87.0	105.	60.0	85.0	97.0	58.0	80.0	93.0	50.0	71.0	98.5	53.5	98.5	107.
58.0	91.0	115.	63.0	38.0	114.	60.0	85.0	112.	51.7	80.5	109.	56.5	98.5	107.
54.0	87.0	107.	63.0	82.5	105.	58.0	75.0	104.	50.0	76.0	102.	50.0	73.5	100.
30.0	72.0	73.5	40.0	63.0	71.0	52.0	50.0	68.5	33.0	50.0	73.5	33.0	52.1	76.0
19.0	0	33.0	18.0	18.0	0	18.0	26.0	74.5	18.0	63.0	89.0	50.0	71.0	94.5
0	0	82.5	0	26.5	83.5	0	60.0	107.	46.5	80.5	107.	57.0	80.5	109.
13.0	50.0	117.	0	71.0	91.0	18.0	86.0	106.	57.0	78.0	100.	53.5	76.0	100.
19.0	87.0	104.	33.0	82.5	76.0	58.0	80.0	95.0	53.5	86.5	89.0	50.0	65.5	87.0
38.0	50.0	57.0	46.5	53.5	0	50.0	40.0	42.5	42.5	35.5	33.0	38.0	38.0	38.0

TABLE IV (Continued)

TILTING DUCT INFLOW VELOCITIES

V (mph)	20	20	20	20	20	20	0	0	0	40	40	40	40	40	4
α (^{o})	70	70	70	90	90	90	90	90	90	90	90	90	70	70	7
θ (^{o})	20	2020	20	20	20	20	20	20	20	20	20	20	20	20	2
Ω R	236	393	550	236	393	550	236	393	550	236	393	550	236	393	55

INFLOW VELOCITIES (ft/sec)

Manometer Tube No.															
9	26.5	33.0	42.5	33.0	35.5	42.5	13.0	13.0	36.0	57.0	57.0	57.0	53.5	53.5	553
11	50.0	76.0	103.	53.5	67.0	104.	33.0	61.5	91.0	68.5	87.0	107.	68.5	88.0	112
12	50 .0	100.	108.	53.5	72.5	110.	46.5	79.0	109.	66.0	91.0	117.	66.0	89.0	115
14	50.0	74.5	102.	50.0	76.0	104.	42.5	76.0	104.	64.5	87.0	110.	63.0	82.5	109
16.	38.0	57.0	78.0	42.6	60.0	85.0	35.0	59.0	81.5	57.0	72.0	91.0	53.5	63.0	81.
1	50.0	73.5	98.5	53.5	77.0	102.	40.0	68.5	97.0	68.5	89.0	110.	71.0	87.0	113
3	50.0	78.0	109.	53.5	82.5	110.	46.5	78.0	109.	66.0	93.0	121.	71.0	91.0	114
4	48.5	93.5	98.5	50.0	76.0	102.	42.5	71.0	100.	63.0	85.0	110.	68.5	85.0	107
6	42.5	63.0	82.5	425.	63.0	85.0	33.0	57.0	82.5	53.5	71.0	93.0	63.0	76.0	91.5
8	26.5	33.0	26.5	26.5	26.5	26.5	0	0	18.0	50.0	50.0	44.5	53.5	53.5	52.0

TABLE IV (Continued)

TILTING DUCT INFLOW VELOCITIES

0	0	0	40	40	40	40	40	40	40	40	40	40	40	40
90	90	90	90	90	90	70	70	70	50	50	50	30	30	30
20	20	20	20	20	20	20	20	20	20	20	20	20	20	20
236	393	550	236	393	550	236	393	550	236	393	550	236	393	550

INFLOW VELOCITIES (ft/sec)

13.0	13.0	36.0	57.0	57.0	57.0	53.5	53.5	553.	46.5	46.5	46.5	57.0	52.0	64.0
33.0	61.5	91.0	68.5	87.0	107.	68.5	88.0	112.	69.7	89.0	114.	74.5	98.5	118.
46.5	79.0	109.	66.0	91.0	117.	66.0	89.0	115.	69.7	89.0	115.	74.5	98.5	121.
42.5	76.0	104.	64.5	87.0	110.	63.0	82.5	109.	65.5	87.0	109.	73.5	96.5	118.
35.0	59.0	81.5	57.0	72.0	91.0	53.5	63.0	81.5	50.0	57.0	68.5	71.0	76.0	78.0
40.0	68.5	97.0	68.5	89.0	110.	71.0	87.0	113.	57.0	82.5	98.0	18.0	19.0	33.0
46.5	78.0	109.	66.0	93.0	121.	71.0	91.0	114.	73.6	93.0	117.	0	26.5	73.5
42.5	71.0	100.	63.0	85.0	110.	68.5	85.0	107.	82.5	87.0	110.	13.0	37.0	118.
33.0	57.0	82.5	53.5	71.0	93.0	63.0	76.0	91.5	73.5	80.5	98.5	58.5	33.0	11.7
0	0	18.0	50.0	50.0	44.5	53.5	53.5	52.0	68.5	63.0	63.0	76.0	76.0	76.0

TABLE IV (Continued)

TILTING DUCT INFLOW VELOCITIES

$V_{(mph)}$	40	40	40	40	40	40	40	40	40	40	40
$\alpha\,(^{\circ})$	20	20	20	10	10	10	0	0	0	-10	-10
$\theta\,(^{\circ})$	20	20	20	20	20	20	20	20	20	20	20
ΩR	236	236	550	236	393	550	236	393	550	393	550
Manometer Tube No.	INFLOW VELOCITIES										
9	56.5	68.5	73.5	33.0	53.5	80.5	26.5	42.5	73.5	33.0	68.5
11	73.5	195.	127.	68.5	107.	141.	40.0	94.5	143.	104.	136.
12	68.5	105.	124.	63.0	105.	139.	26.5	105.	144.	96.5	136.
14	76.0	100.	126.	50.0	107.	131.	18.0	91.0	138.	63.0	142.
16	46.5	85.0	112.	00	63.0	117.	0	33.0	109.	0	104.
1	19.0	18.0	18.0	26.5	26.5	18.0	18.0	0	0	26.5	0
3	0	0	26.5	0	0	0	0	0	18.0	0	18.0
4	0	18.0	89.0	0	0	0	0	0	0	0	18.0
6	0	91.0	132.	0	46.5	123.	0	26.5	98.5	18.0	78.0
8	73.5	80.5	87.0	59.0	76.0	89.0	0	26.5	89.0	42.5	87.0

TABLE V

FAN-WING INFLOW VELOCITIES

V(mph)	0	0	0	0	0	0	0	0	0	20	20	20	20	20	[illegible]
α (°)	-10	-10	-10	0	0	0	+10	+10	+10	-10	-10	-10	-5	-5	[illegible]
θ (°)	20	20	20	20	20	20	20	20	20	20	20	20	20	20	[illegible]
ΩR	236	393	550	236	393	550	236	393	550	236	393	550	236	393	[illegible]
Manometer Tube No.									INFLOW VELOCITIES (ft/sec)						
9	38.0	70.5	93.0	42.5	70.5	96.5	38.0	68.0	98.0	53.5	82.5	105.	53.5	82.5	19[illegible]
11	46.5	78.0	103.	46.5	78.0	108.	46.5	75.5	106.	57.0	87.0	115.	57.0	87.0	11[illegible]
12	42.5	75.5	102.	46.5	78.0	106.	42.5	75.5	103.	59.5	87.0	108.	63.5	87.0	10[illegible]
14	38.0	65.0	87.0	38.0	65.0	89.0	33.0	63.5	89.0	33.0	70.5	82.5	33.0	75.5	82[illegible]
16	18.5	33.0	38.0	18.5	27.0	42.5	0	27.0	46.5	27.0	46.5	46.5	18.5	46.5	46[illegible]
1	33.0	63.5	87.0	38.0	63.5	87.0	38.0	65.0	93.0	33.0	27.0	89.0	33.0	27.0	87[illegible]
3	46.5	78.0	102.	46.5	78.0	105.	42.5	78.0	105.	27.0	50.0	112.	27.0	46.5	11[illegible]
4	46.5	75.5	100.	46.5	78.0	106.	42.5	78.0	105.	0	78.0	105.	0	73.0	10[illegible]
6															
8	18.5	33.0	42.5	18.5	33.0	46.5	18.5	33.0	42.5	27.0	42.5	42.5	33.0	46.5	46[illegible]
25															
27															
28															
30															
32															
17	42.5	68.0	94.5	46.5	73.0	98.0	42.5	73.0	98.0	59.5	89.0	121.	39.5	89.0	120
19	42.5	73.0	96.5	42.5	73.8	98.0	42.5	70.5	98.0	57.0	82.5	110.	57.0	82.5	108
20	46.5	75.5	103.	46.5	78.0	106.	46.5	78.0	106.	63.5	89.0	50.0	59.5	89.0	118

TABLE V

FAN-WING INFLOW VELOCITIES

0	0	0	20	20	20	20	20	20	20	20	20	20	20	20
+10	+10	+10	-10	-10	-10	-5	-5	-5	0	0	0	+5	+5	+5
20	20	20	20	20	20	20	20	20	20	20	20	20	20	20
236	393	550	236	393	550	236	393	550	236	393	550	236	393	550

INFLOW VELOCITIES (ft/sec)

38.0	68.0	98.0	53.5	82.5	105.	53.5	82.5	195.	57.0	84.5c	106.	50.0	82.5	105.
46.5	75.5	106.	57.0	87.0	115.	57.0	87.0	113.	59.5	89.0	115.	57.0	84.5	113.
42.5	75.5	103.	59.5	87.0	108.	63.5	87.0	106.	63.5	87.0	106.	59.5	84.5	106.
33.0	63.5	89.0	33.0	70.5	82.5	33.0	75.5	82.5	33.0	73.0	80.0	27.0	73.0	82.5
0	27.0	46.5	27.0	46.5	46.5	18.5	46.5	46.5	18.5	46.5	42.5	18.5	46.5	42.5
38.0	65.0	93.0	33.0	27.0	89.0	33.0	27.0	87.0	27.0	27.0	80.0	27.0	65.0	78.0
42.5	78.0	105.	27.0	50.0	112.	27.0	46.5	110.	27.0	42.5	106.	27.0	33.0	106.
42.5	78.0	105.	0	78.0	105.	0	73.0	103.	0	68.0	103.	0	63.5	103.

18.5	33.0	42.5	27.0	42.5	42.5	33.0	46.5	46.5	33.0	46.5	38.0	38.0	42.5	46.5

42.5	73.0	98.0	59.5	89.0	121.	39.5	89.0	120.	59.5	89.0	117.	59.5	87.0	117.
42.5	70.5	98.0	57.0	82.5	110.	57.0	82.5	108.	53.5	82.5	105.	53.5	80.0	105.
46.5	78.0	106.	63.5	89.0	50.0	59.5	89.0	118.	59.5	91.0	117.	59.5	89.0	117.

TABLE V (Continued)

FAN-WING INFLOW VELOCITIES

$V_{(mph)}$	0	0	20	20	40	40	60	60	0	0	20	20
$\alpha\,(^{o})$	0	0	0	0	0	0	0	0	0	0	0	0
$\theta\,(^{o})$	30	30	30	30	30	30	30	30	10	10	10	10
ΩR	393	472	393	472	393	472	393	472	393	550	393	550
Manometer Tube No.	INFLOW VELOCITIES (ft/sec											
9	80.0	102.	106.	125.	94.5	108.	113.	133.	46.5	68.0	63.5	78.0
11	98.0	123.	110.	131.	118.	114.	98.0	133.	50.0	68.0	63.5	78.0
12	100.	123.	105.	125.	113.	137.	53.5	91.0	50.0	65.0	57.0	73.0
14	91.0	108.	87.0	102.	70.5	117.	0	33.0	38.0	50.0	38.0	59.5
16	50.05	63.5	46.5	50.0	46.5	63.5	42.5	38.0	18.5	18.5	18.5	46.5
1	18.5	91.0	68.0	63.5	38.0	38.0	46.5	50.0	42.5	59.5	27.0	27.0
3	94.5	115.	103.	103.	33.0	33.0	27.0	33.0	46.5	68.0	27.0	57.0
4	100.	121.	103.	120.	27.0	59.5	27.0	0	46.5	65.0	18.5	80.0
6												
8	50.0	59.5	50.0	59.5	70.5	84.5	53.5	50.0	19.5	27.0	33.0	27.0
25	0	94.5	93.0	93.0	46.5	46.5	38.0	46.5	46.5	63.5	33.0	33.0
27	98.0	117.	106.	118.	46.5	50.0	38.0	50.0	53.5	68.0	38.0	57.0
28	102.	125.	105.	127.	33.0	73.0	0	0	46.5	68.0	42.5	65.0
30	89.0	108.	100.	117.	70.5	117.	33.0	46.5	38.0	53.5	46.5	57.0
32	53.5	89.0	59.5	70.5	78.0	93.0	42.5	82.5	0	18.5	33.0	33.0
17	87.0	102.	106.	134.	113.	131.	127.	137.	50.0	68.0	65.0	80.0
19	98.0	123.	103.	125.	128.	147.	133.	158.	46.5	63.5	57.0	68.0
20	105.	125.	113.	138.	115.	135.	121.	137.	50.0	82.5	68.0	84.5
22	89.0	103.	89.0	106.	98.0	112.	98.0	113.	33.0	50.00	46.5	59.5
24	42.5	57.0	46.5	46.5	33.0	50.0	B	18.5	18.5	81.5	18.5	18.5

* B indicates Backflow.

TABLE V (Continued)

FAN-WING INFLOW VELOCITIES

20	40	40	60	60	0	0	20	20	40	40	60	60
0	0	0	0	0	0	0	0	0	0	0	0	0
30	30	30	30	30	10	10	10	10	10	10	10	10
472	393	472	393	472	393	550	393	550	393	550	393	550

INFLOW VELOCITIES (ft/sec)

125.	94.5	108.	113.	133.	46.5	68.0	63.5	78.0	70.5	96.5	82.5	106.
131.	118.	114.	98.0	133.	50.0	68.0	63.5	78.0	70.5	98.0	46.5	105.
125.	113.	137.	53.5	91.0	50.0	65.0	57.0	73.0	57.0	96.5	33.0	68.0
102.	70.5	117.	0	33.0	38.0	50.0	38.0	59.5	0	42.5	0	B*
50.0	46.5	63.5	42.5	38.0	18.5	18.5	18.5	46.5	0	27.0	38.0	18.5
63.5	38.0	38.0	46.5	50.0	42.5	59.5	27.0	27.0	33.0	46.5	33.0	50.0
103.	33.0	33.0	27.0	33.0	46.5	68.0	27.0	57.0	33.0	38.0	0	53.5
120.	27.0	59.5	27.0	0	46.5	65.0	18.5	80.0	18.5	0	0	27.0

59.5	70.5	84.5	53.5	50.0	19.5	27.0	33.0	27.0	0	46.5	46.5	42.5
93.0	46.5	46.5	38.0	46.5	46.5	63.5	33.0	33.0	38.0	42.5	18.5	46.5
118.	46.5	50.0	38.0	50.0	53.5	68.0	38.0	57.0	38.0	42.5	0	18.5
127.	33.0	73.0	0	0	46.5	68.0	42.5	65.0	27.0	0	0	18.5
117.	70.5	117.	33.0	46.5	38.0	53.5	46.5	57.0	0	46.5	0	0
70.5	78.0	93.0	42.5	82.5	0	18.5	33.0	33.0	0	57.0	33.0	0
134.	113.	131.	127.	137.	50.0	68.0	65.0	80.0	53.5	102.	65.0	118.
125.	128.	147.	133.	158.	46.5	63.5	57.0	68.0	53.5	87.0	0	78.0
138.	115.	135.	121.	137.	50.0	82.5	68.0	84.5	75.5	100.	57.0	110.
106.	98.0	112.	98.0	113.	33.0	50.00	46.5	5915	33.0	63.5	0	33.0
46.5	33.0	50.0	B	18.5	18.5	81.5	18.5	18.5	. B	38.0	B	B

w.

TABLE V (Continued)

FAN-WING INFLOW VELOCITI

$V_{(mph)}$	40	40	40	40	40	40	40	60	60	60	60	
α (°)	+10	+10	+10	+15	+15	+20	+20	-10	-5	-5	0	
θ (°)	20	20	20	20	20	20	20	20	20	20	20	
ΩR	236	393	550	393	550	393	550	393	393	550	393	5
Manometer Tube No.	INFLOW VELOCITIES (ft/											
9	27.0	75.5	125.	80.0	121.	82.5	120.	102.	100.	130.	89.0	11
11	0	89.0	131.	84.5	130.	84.5	131.	106.	91.0	143.	63.5	13
12	18.5	75.5	128.	63.5	130.	59.5	133.	105.	63.5	151.	46.5	13
14	0	18.5	84.5	0	84.5	0	89.0	38.0	50.0	75.5	0	53.
16	27.0	18.5	68.0	18.5	65.0	0	59.5	42.5	38.0	59.5	46.5	50.
1	27.0	50.0	59.5	50.0	59.5	53.5	59.5	57.0	53.5	70.5	46.5	68.
3	18.5	46.5	59.5	50.0	59.5	53.5	59.5	53.5	75.5	63.5	42.5	63.
4	18.5	0	42.5	0	33.0	18.5	33.0	18.5	0	0	0	
6												
8	38.0	46.5	84.5	18.5	82.5	18.5	80.0	73.0	33.0	91.0	42.5	84.
25												
27												
28												
30												
32												
17	33.0	100.	131.	100.	130.	98.0	128.	112.	110.	144.	105.	141.
19	18.5	93.0	120.	91.0	120.	91.0	120.	137.	98.0	131.	80.0	130.
20	18.5	102.	131.	100.	131.	100.	133.	113.	108.	144.	102.	143.
22												
24												

TABLE V (Continued)

FAN-WING INFLOW VELOCITIES

40	40	40	40	60	60	60	60	60	60	60	60	60
+15	+15	+20	+20	-10	-5	-5	0	0	+5	+5	+10	+10
20	20	20	20	20	20	20	20	20	20	20	20	20
393	550	393	550	393	393	550	393	550	393	550	393	550

INFLOW VELOCITIES (ft/sec)

80.0	121.	82.5	120.	102.	100.	130.	89.0	113.	82.5	113.	65.0	118.
84.5	130.	84.5	131.	106.	91.0	143.	63.5	137.	42.5	128.	0	117.
63.5	130.	59.5	133.	105.	63.5	151.	46.5	139.	42.5	110.	27.0	75.5
0	84.5	0	89.0	38.0	50.0	75.5	0	53.5	0	27.0	0	0
18.5	65.0	0	59.5	42.5	38.0	59.5	46.5	50.0	46.5	27.0	38.0	33.0
50.0	59.5	53.5	59.5	57.0	53.5	70.5	46.5	68.0	50.0	68.0	38.0	70.5
50.0	59.5	53.5	59.5	53.5	75.5	63.5	42.5	63.5	46.5	63.5	33.0	65.0
0	33.0	18.5	33.0	18.5	0	0	0	0	18.5	0	27.0	0
18.5	82.5	18.5	80.0	73.0	33.0	91.0	42.5	84.5	50.0	65.0	57.0	33.0
100.	130.	98.0	128.	112.	110.	144.	105.	141.	100.	141.	63.5	137.
91.0	120.	91.0	120.	137.	98.0	131.	80.0	130.	73.0	137.	53.5	131.
100.	131.	100.	133.	113.	108.	144.	102.	143.	91.0	146.	70.5	141.

TABLE V (Continued)

FAN-WING INFLOW VELOCITIES

V(mph)	20	20	20	20	20	20	20	40	40	40	40	40	40	
α (°)	+10	+10	+10	+15	+15	+20	+20	-10	-10	-10	-5	-5	-5	
θ (°)	20	20	20	20	20	20	20	20	20	20	20	20	20	
ΩR	236	393	550	393	550	393	550	236	393	550	236	393	550	
Manometer Tube No.								INFLOW VELOCITIES (ft/sec)						
9	46.5	84.5	105.	84.5	89.0	82.5	104.	57.0	98.0	125.	57.0	93.0	125.	4
11	57.0	89.0	113.	91.0	115.	87.0	113.	59.5	103.	128.	46.5	100.	128.	1
12	59.5	87.0	106.	89.0	108.	84.5	106.	50.0	106.	127.	33.0	105.	125.	2
14	18.5	73.0	82.5	78.0	82.5	73.0	82.5	0	59.5	113.	0	57.0	143.	
16	0	50.0	42.5	50.0	42.5	50.0	42.5	27.0	46.5	70.5	18.5	42.5	73.0	2
1	27.0	27.0	63.5	18.5	59.5	27.0	46.5	33.0	53.5	53.5	27.0	53.5	57.0	3
3	27.0	27.0	103.	27.0	102.	27.0	94.5	33.0	46.5	465.	18.5	50.0	50.0	2
4	0	63.5	105.	63.5	110.	59.5	110.	18.5	18.5	84.5	0	0	78.0	1
6														
8	38.0	46.5	42.5	50.0	42.5	46.5	42.5	27.0	28.0	73.0	18.5	59.5	78.0	3
25														
27														
28														
30														
32														
17	59.5	89.0	118.	89.0	118.	87.0	117.	70.5	103.	133.	70.5	100.	133.	x59
19	53.5	82.5	106.	82.5	106.	80.0	105.	63.5	96.5	120.	53.5	93.0	120.	42
20	59.5	91.0	118.	91.0	118.	87.0	118.	27.0	103.	133.	68.0	100.	133.	53
22														
24														

2

TABLE V (Continued)

FAN-WING INFLOW VELOCITIES

20	20	20	40	40	40	40	40	40	40	40	40	40	40	40
15	+20	+20	-10	-10	-10	-5	-5	-5	0^{o}	0^{o}	0^{o}	+5	+5	+5
20	20	20	20	20	20	20	20	20	20	20	20	20	20	20
50	393	550	236	393	550	236	393	550	236	393	550	236	339	550

INFLOW VELOCITIES (ft/sec)

.0	82.5	104.	57.0	98.0	125.	57.0	93.0	125.	46.5	93.0	125.	33.0	82.5	121.
5.	87.0	113.	59.5	103.	128.	46.5	100.	128.	18.5	98.0	128.	0	94.5	127.
8.	84.5	106.	50.0	106.	127.	33.0	105.	125.	27.0	105.	125.	18.5	94.5	123.
.5	73.0	82.5	0	59.5	113.	0	57.0	143.	0	46.5	98.0	0	38.0	87.0
.5	50.0	42.5	27.0	46.5	70.5	18.5	42.5	73.0	27.0	38.0	68.0	27.0	27.0	63.5
.5	27.0	46.5	33.0	53.5	53.5	27.0	53.5	57.0	33.0	50.0	57.0	27.0	50.0	59.5
2.	27.0	94.5	33.0	46.5	-465.	18.5	50.0	50.0	27.0	46.5	50.0	18.5	46.5	57.0
0.	59.5	110.	18.5	18.5	84.5	0	0	78.0	18.5	0	53.5	18.5	0	46.5
.5	46.5	42.5	27.0	28.0	73.0	18.5	59.5	78.0	33.0	27.0	82.5	46.5	59.5	84.5
8.	87.0	117.	70.5	103.	133.	70.5	100.	133.	x59.5	98.0	533.	53.5	96.5	130.
6.	80.0	105.	63.5	96.5	120.	53.5	93.0	120.	42.5	93.0	120.	33.0	91.0	117.
8.	87.0	118.	27.0	103.	133.	68.0	100.	133.	53.5	100.	133.	42.5	98.0	57.0

1

TABLE VI
TILTING DUCT INLET PRESSURE DISTRIBUTION

V(mph)	40	40	40	40	40	40	40	40	40	40	40	40	40	
α(°)	90	90	70	70	50	50	30	30	20	20	20	10	10	
θ(°)	20	20	20	20	20	20	20	20	20	20	20	20	20	
ΩR	393	550	393	550	393	550	236	393	550	236	393	550	236	3
Manometer Tube No.	**PRESSURE DISTRIBUTION IN INCHES OF ALCOHOL**													
33	0	+.3	+0.5	+0.3	-0.8	-1.6	-1.2	-2.7	-4.7	-1.8	-3.5	-5.4	-3.2	-4
34	+0.5	+0.4	-0.5	-1.3	-2.8	-4.6	-2.0	-4.4	-7.6	-1.9	-4.5	-7.6	-1.7	-4
35	-0.4	-0.4	-3.0	-4.9	-5.8	-9.1	-1.9	-4.8	-10.	-1.8	-4.2	-1.8	-1.9	-3
36	-2.4	-4.6	-5.4	-8.5	-6.0	-10.	-2.0	-4.9	-8.8	-1.9	-4.1	-7.3	-2.0	-3
37	-2.3	-4.0	-4.1	-5.5	-5.9	-8.1	-2.6	-5.6	-8.4	-2.2	-5.1	-8.7	-2.0	-4
38	-1.3	-1.8	-2.2	-3.3	-3.4	-4.3	-1.0	-1.8	-3.7	-0.8	-1.2	-2.1	-0.8	-0
39	-2.5	-4.7	-4.5	-7.4	-5.6	-9.7	-1.8	-4.1	-8.1	-1.7	-3.6	-6.1	-1.8	-3
40	0	0	0	+0.1	0	+0.1	-0.5	-0.5	-0.4	-0.5	-0.4	-0.4	-0.6	-0.
41	-0.5	-0.1	+0.9	+0.4	+0.2	-0.2	-0.5	-1.1	-2.1	-0.9	-1.8	-2.9	-1.6	-2.
42	-1.5	-1.4	-2.0	-2.8	-3.1	-3.8	11.1	-1.7	-3.3	-0.8	-1.1	-1.9	-0.7	-0.
43	+0.4	+0.4	+0.1	-0.4	-1.4	-2.4	-1.3	-2.7	-4.9	-1.6	-3.2	-5.3	-1.7	-3.
44	-0.1	-0.1	-1.7	-3.3	-3.9	-6.3	1.8	-4.3	0	-1.6	-3.6	-7.0	-1.6	-3.
45	-0.8	-0.8	-1.3	-1.4	-1.6	-2.0	-1.1	-1.4	-1.8	-0.8	-0.9	-0.9	-0.8	-0.
46	-0.8	-0.7	-1.1	-1.2	-1.3	-1.5	-1.1	-1.0	-1.0	-0.8	-0.7	-0.4	-0.8	-0.
47	-0.9	-0.7	-1.1	-1.1	-1.2	01.3	-1.0	-1.9	-0.7	-0.8	-0.6	-0.3	-0.8	-0.
48	-0.9	-0.8	-1.0	-1.1	-1.0	-1.1	-1.0	-1.8	-0.6	-0.8	-0.6	-0.3	-0.7	-0.
49	+0.3	+0.4	+0.3	+0.4	+0.3	+0.5	-0.1	-0.1	0	-0.2	0	0	-0.2	-0.
50	+0.4	+0.4	+0.4	+0.5	+0.4	+0.6	-0.1	0	+0.1	-0.1	0	-0.1	-0.1	-0.
51	0	0	0	+0.1	-0.1	+0.1	-0.6	-0.5	-0.5	-0.4	-0.6	-0.5	-0.4	-0.
52	-2.3	-4.5	-0.4	-4.6	-2.6	-5.0	-0.9	-2.3	-4.9	-0.9	-2.2	-4.4	-0.9	-1.
53	-1.9	-3.3	-1.9	-3.5	-2.1	-3.6	-0.7	-2.6	-2.9	-0.8	-1.7	-2.7	-0.8	-1.
54	-0.9	-0.9	-1.0	-1.1	-1.0	-1.5	-0.4	-0.4	-0.8	-0.6	-0.5	-0.4	-0.5	-0.
55	-0.5	0	-1.6	-1.0	-1.1	-1.3	-1.0	-1.5	-1.8	-1.2	-1.5	-1.7	-1.7	-1.

2

TABLE VI

TILTING DUCT INLET PRESSURE DISTRIBUTION

40	40	40	40	40	40	40	40	40	40	40	40	40	40	40
50	30	30	20	20	20	10	10	10	0	0	0	-10	-10	-10
20	20	20	20	20	20	20	20	20	20	20	20	20	20	20
550	236	393	550	236	393	550	236	393	550	236	393	550	393	550

PRESSURE DISTRIBUTION IN INCHES OF ALCOHOL

-1.6	-1.2	-2.7	-4.7	-1.8	-3.5	-5.4	-3.2	-4.3	-7.0	-1.9	-5.1	-8.4	-5.7	-9.9
-4.6	-2.0	-4.4	-7.6	-1.9	-4.5	-7.6	-1.7	-4.4	-8.5	-1.4	-4.7	-9.3	-9.7	-10.
-9.1	-1.9	-4.8	-10.	-1.8	-4.2	-1.8	-1.9	-3.9	-7.0	-1.2	-3.2	-7.0	-2.9	-6.4
-10.	-2.0	-4.9	-8.8	-1.9	-4.1	-7.3	-2.0	-3.5	-6.3	-1.6	-3.2	-5.4	-3.3	-5.9
-8.1	-2.6	-5.6	-8.4	-2.2	-5.1	-8.7	-2.0	-4.2	-7.2	-1.2	03.6	-7.0	-3.7	-7.6
-4.3	-1.0	-1.8	-3.7	-0.8	-1.2	-2.1	-0.8	-0.7	-1.6	-0.4	-2.8	-1.0	0	-0.7
-9.7	-1.8	-4.1	-8.1	-1.7	-3.6	-6.1	-1.8	-3.3	-5.6	-1.8	-0.4	-5.0	-3.0	-4.6
+0.1	-0.5	-0.5	-0.4	-0.5	-0.4	-0.4	-0.6	-0.4	-0.4	-0.6	-3.4	-0.4	-1.2	00.8
-0.2	-0.5	-1.1	-2.1	-0.9	-1.8	-2.9	-1.6	-2.7	-4.3	-1.5	-0.3	-5.6	-3.7	-7.0
-3.8	11.1	-1.7	-3.3	-0.8	-1.1	-1.9	-0.7	-0.7	-1.3	-0.3	-3.6	-0.7	+0.1	-0.5
-2.4	-1.3	-2.7	-4.9	-1.6	-3.2	-5.3	-1.7	-3.5	-6.1	-12.	-1.5	-6.8	-3.2	-7.5
-6.3	1.8	-4.3	0	-1.6	-3.6	-7.0	-1.6	-3.2	-6.6	-1.3	-0.2	-6.5	-2.0	-6.4
-2.0	-1.1	-1.4	-1.8	-0.8	-0.9	-0.9	-0.8	-0.5	-0.4	-0.4	-0.1	-0.1	+0.1	+0.1
-1.5	-1.1	-1.0	-1.0	-0.8	-0.7	-0.4	-0.8	-0.4	0	-0.8	-0.1	+0.2	+0.1	+0.3
01.3	-1.0	-1.9	-0.7	-0.8	-0.6	-0.3	-0.8	-0.3	+0.1	-0.5	-0.1	+0.3	+0.1	+0.4
-1.1	-1.0	-1.8	-0.6	-0.8	-0.6	-0.3	-0.7	-0.3	+0.1	-0.5	-0.1	+0.5	0	+0.3
+0.5	-0.1	-0.1	0	-0.2	0	0	-0.2	-0.1	0	-0.3	-0.1	-0.1	-0.8	-0.5
+0.6	-0.1	0	+0.1	-0.1	0	-0.1	-0.1	-0.1	0	-0.2	Q	0	-0.9	-0.5
+0.1	-0.6	-0.5	-0.5	-0.4	-0.6	-0.5	-0.4	-0.6	-0.5	-0.4	-0.6	-0.5	-0.4	-0.9
-5.0	-0.9	-2.3	-4.9	-0.9	-2.2	-4.4	-0.9	-1.9	-4.3	-2.4	-3.7	-4.4	-4.4	-3.2
-3.6	-0.7	-2.6	-2.9	-0.8	-1.7	-2.7	-0.8	-1.6	-3.4	0	-0.5	-3.8	+4.9	-3.9
-1.5	-0.4	-0.4	-0.8	-0.6	-0.5	-0.4	-0.5	-0.5	-0.6	+0.2	-0.1	-0.6	+0.7	-0.5
-1.3	-1.0	-1.5	-1.8	-1.2	-1.5	-1.7	-1.7	-1.6	-0.5	-1.2	-1.6	-1.1	0	-0.7

TABLE VI (Continued)

TILTING DUCT INLET PRESSURE DISTRIBUTION

$V_{(mph)}$	40	40	40	40	40	40	40	40	40	40	40	40	40
α (°)	90	90	70	70	50	50	30	30	30	20	20	20	10
θ (°)	20	20	20	20	20	20	20	20	20	20	20	20	20
Ω R	393	550	393	550	393	550	236	393	550	550	236	393	550
Manometer Tube No.	PRESSURE DISTRIBUTION IN INCHES OF ALCOHOL												
56	+0.5	+0.4	+0.1	+0.4	-0.1	+0.2	-0.9	-0.7	-0.4	-1.2	-0.9	-0.5	-1.5
57	-0.3	-1.3	+0.4	0	+0.5	+0.4	0	+0.3	+0.4	-0.3	+0.1	+0.3	-0.6
58	-1.4	-3.6	-0.8	-1.6	-0.6	-1.0	-0.1	-0.3	-0.8	-0.2	-0.3	-0.6	-0.1
59	-2.0	-3.4	-1.1	-2.1	-0.7	-1.6	+0.3	-0.2	-0.9	+0.3	-0.1	-0.6	+0.2
60	-1.4	-1.4	-1.0	-0.5	-0.7	-1.3	+0.3	+0.3	+0.4	-0.6	+0.9	+1.0	+0.9
61	0	+0.2	-1.4	-0.9	-1.2	-1.1	-0.9	-1.1	-1.1	-0.8	-1.0	-1.0	-1.1
62	+0.4	+0.3	0	+0.4	-0.4	0	-1.0	-0.9	-0.6	-0.9	-1.0	-0.8	-1.4
63	-0.5	-1.6	+0.5	+0.1	+0.6	+0.6	+0.2	+0.2	+0.6	-0.5	+0.1	+0.4	-0.9
64	-2.3	-4.4	-0.5	-1.9	+0.3	-0.6	+0.6	+0.6	+0.2	-0.5	+0.6	+0.4	+0.4
65	-1.9	-3.4	-0.7	-1.8	-0.2	-0.9	+0.5	+0.2	-0.4	-0.6	+0.3	0	+0.6
66	-0.9	-1.0	0	+0.4	+0.1	-0.9	+0.5	+0.8	+0.8	-0.6	+0.5	-1.5	+1.1

TABLE VI (Continued)

TILTING DUCT INLET PRESSURE DISTRIBUTION

40	40	40	40	40	40	40	40	40	40	40	40	40	40	40
50	30	30	30	20	20	20	10	10	10	0	0	0	-10	-10
20	20	20	20	20	20	20	20	20	20	20	20	20	20	20
550	236	393	550	550	236	393	550	236	393	550	236	393	550	393

PRESSURE DISTRIBUTION IN INCHES OF ALCOHOL

+0.2	-0.9	-0.7	-0.4	-1.2	-0.9	-0.5	-1.5	-0.9	-0.5	-1.1	-1.1	-0.4	-0.8	-0.2
+0.4	0	+0.3	+0.4	-0.3	+0.1	+0.3	-0.6	0	+0.2	-0.5	-0.2	+0.1	-0.3	+0.1
-1.0	-0.1	-0.3	-0.8	-0.2	-0.3	-0.6	-0.1	-0.3	-0.7	-0.3	-0.4	-0.7	-0.5	-0.9
-1.6	+0.3	-0.2	-0.9	+0.3	-0.1	-0.6	+0.2	-0.7	+0.1	-0.2	-0.7	+0.1	+0.1	-0.6
-1.3	+0.3	+0.3	+0.4	-0.6	+0.9	+1.0	+0.9	+1.3	+1.3	+0.6	+1.7	+1.5	+2.4	+1.7
-1.1	-0.9	-1.1	-1.1	-0.8	-1.0	-1.0	-1.1	-0.9	-0.9	-1.2	-0.9	-0.9	-2.5	-1.0
0	-1.0	-0.9	-0.6	-0.9	-1.0	-0.8	-1.4	-1.1	-0.7	-1.4	-1.0	-0.8	-2.2	-0.9
+0.6	+0.2	+0.2	+0.6	-0.5	+0.1	+0.4	-0.9	-0.2	+0.4	-0.9	-0.4	-0.3	-0.8	+0.3
-0.6	+0.6	+0.6	+0.2	-0.5	+0.6	+0.4	+0.4	+0.6	+0.4	+0.4	+0.6	+0.5	+0.4	+0.6
-0.9	+0.5	+0.2	-0.4	-0.6	+0.3	0	+0.6	+0.4	-0.1	+0.5	+0.3	0	+0.2	-0.1
-0.9	+0.5	+0.8	+0.8	-0.6	+0.5	-1.5	+1.1	+0.6	+1.4	+1.2	+1.3	+1.4	+2.4	+2.2

TABLE VII

FAN-WING PRESSURE DISTRIBU

$V_{(mph)}$	0	0	20	20	40	40	60	60	0	0	20	
α (°)	0	0	0	0	0	0	0	0	0	0	0	
θ (°)	30	30	30	30	30	30	30	30	10	10	10	
ΩR	393	472	393	472	393	472	393	472	393	550	393	
Manometer Tube No.	PRESSURE DISTRIBUTION IN INCHES OF A											
34	-1.5	-2.3	-6.3	0	-4.0	-6.5	-2.4	-4.7	-0.3	-0.7	-1.8	-
35	-2.9	-4.3	-9.3		-3.4	-6.1	02.5	-4.2	-0.7	-1.5	-1.7	-
36	-4.2	-6.1	-7.9	-9.4	-4.1	-6.0	-3.9	-6.2	-1.1	-2.3	-1.4	-
37	-3.5	-4.9	-7.7	-8.9	-3.9	-6.2	-1.4	-3.5	-0.9	-1.7	-1.8	-
38	-1.8	-2.8	-4.9	-5.8	-0.8	-1.9	-0.2	-0.9	-0.7	-1.2	+0.2	-
39	-3.6	-5.5	-7.1	-8.9	-2.3	-3.6	-3.5	-4.3	-1.0	-2.1	-0.9	-
40	-3.6	-5.0	-5.1	-6.2	-0.8	-2.6	+1.3	-0.8	-0.8	-26.	-0.9	-
41												
42	-1.5	-2.4	-3.0	-3.6	+0.1	-0.8	+1.7	+0.8	-0.3	-0.6	+0.2	-
43	-0.1	-0.2	-0.2	-0.2	+0.5	+0.3	0	-0.1	0	0	+0.1	+
44	-2.1	-3.2	-5.6	-6.0	-1.5	-3.3	-1.6	-2.6	-0.6	-0.2	-1.2	-
45	-0.5	-0.8	-1.6	-1.7	+0.6	-0.1	+0.8	+0.8	0	0	+0.3	
46	-0.1	-0.1	-0.8	-0.8	+0.9	+0.4	+0.5	+1.0	+0.1	+0.1	+0.4	+
47	-0.1	-0.1	-0.3	-0.5	+1.0	+0.6	+0.3	+0.9	+0.1	+0.1	+0.4	+
48	0	-0.1	00.2	-0.3	+1.1	+0.9	+0.2	+0.8	+0.1	+0.1	+0.4	+
49												
50	-0.1	-0.1			+1.3		-0.1				+0.3	+
51	-0.9	-1.2	-0.9	-1.1	+1.9	+1.1	+4.7	+4.6	-0.2	-0.2	+0.3	+
42	-2.9	-4.3	-3.2	-4.4	-0.5	-2.0	+1.0	+1.0	-0.7	-1.3	-0.3	-
53	-3.3	-5.1	04.7	-6.5	-1.4	-1.9	-5.4	-5.3	-0.9	-2.0	-0.5	-
54	-2.3	-3.6	-3.0	-4.2	-0.3	-1.2	-1.9	-1.5	-0.6	-1.2	-0.3	-
55												

1

TABLE VII

FAN-WING PRESSURE DISTRIBUTION

20	20	40	40	60	60	0	0	20	20	40	40	60	60
0	0	0	0	0	0	0	0	0	0	0	0	0	0
30	30	30	30	30	30	10	10	10	10	10	10	10	10
93	472	393	472	393	472	393	550	393	550	393	550	393	550

PRESSURE DISTRIBUTION IN INCHES OF ALCOHOL

.3	0	-4.0	-6.5	-2.4	-4.7	-0.3	-0.7	-1.8	-3.2	-1.1	-3.2	-1.6	-2.9
.3		-3.4	-6.1	02.5	-4.2	-0.7	-1.5	-1.7	-3.8	-1.0	-2.9	-1.3	-2.7
.9	-9.4	-4.1	-6.0	-3.9	-6.2	-1.1	-2.3	-1.4	-3.0	-1.1	-2.9	-1.3	-2.8
.7	-8.9	-3.9	-6.2	-1.4	-3.5	-0.9	-1.7	-1.8	-3.1	-1.1	-3.6	-1.4	-2.9
.9	-5.8	-0.8	-1.9	-0.2	-0.9	-0.7	-1.2	+0.2	-1.2	+0.7	+0.9	0	+0.7
.1	-8.9	-2.3	-3.6	-3.5	-4.3	-1.0	-2.1	-0.9	-2.6	-0.8	+1.2	-1.3	-2.4
.1	-6.2	-0.8	-2.6	+1.3	-0.8	-0.8	-26.	-0.9	-1.9	-1.0	+0.8	+0.3	-1.5
.0	-3.6	+0.1	-0.8	+1.7	+0.8	-0.3	-0.6	+0.2	-0.7	+0.7	+1.0	+0.5	+0.9
.2	-0.2	+0.5	+0.3	0	-0.1	0	0	+0.1	+0.1	+0.3	+0.3	0	0
.6	-6.0	-1.5	-3.3	-1.6	-2.6	-0.6	-0.2	-1.2	-2.4	-0.7	-2.5	-0.9	-2.0
.6	-1.7	+0.6	-0.1	+0.8	+0.8	0	0	+0.3	0	+0.7	+0.9	+0.4	+0.8
.8	-0.8	+0.9	+0.4	+0.5	+1.0	+0.1	+0.1	+0.4	+0.2	+0.7	+0.9	c+0.3	+0.8
.3	-0.5	+1.0	+0.6	+0.3	+0.9	+0.1	+0.1	+0.4	+0.3	+0.7	+0.9	+0.3	+0.8
.2	-0.3	+1.1	+0.9	+0.2	+0.8	+0.1	+0.1	+0.4	+0.3	+0.7	+0.9	+0.3	+0.8
		+1.3		-0.1				+0.3	+0.4	+0.3		+0.4	+0.4
.9	-1.1	+1.9	+1.1	+4.7	+4.6	-0.2	-0.2	+0.3	+0.1	+0.3	+1.1	+1.0	+1.1
.2	-4.4	-0.5	-2.0	+1.0	+1.0	-0.7	-1.3	-0.3	-0.9	-0.4	-0.4	+0.7	-0.5
.7	-6.5	-1.4	-1.9	-5.4	-5.3	-0.9	-2.0	-0.5	-1.5	-0.2	-1.0	-0.7	-0.9
.0	-4.2	-0.3	-1.2	-1.9	-1.5	-0.6	-1.2	-0.3	-0.9	0	-0.4	-0.4	-0.4

TABLE VII (Continued)

FAN-WING PRESSURE DISTRIBUTION

$V_{(mph)}$	0	0	20	20	40	40	60	60	0	0	20	20	40	40	60	60
α (°)	0	0	0	0	0	0	0	0	0	0	0	0	0	0	0	0
θ (°)	30	30	30	30	30	30	30	30	10	10	10	10	10	10	10	10
Ω R	393	472	393	472	393	472	393	472	393	550	393	550	393	550	393	550
Manometer Tube No.	PRESSURE DISTRIBUTION IN INCHES OF ALCOHOL															
56	-0.2	-0.1	-0.2	-0.1	+0.6	+0.4	+0.2	+0.1	+0.1	+0.1	+0.1	+0.1	+0.4	+0.4	+0.2	+0.1
57	-2.0	-1.3	-0.6	-0.1	+0.7	+0.6	+0.2	+0.2	-0.3	-0.5	+0.2	+0.2	+0.6	+0.7	+0.6	+0.5
58	-3.4	-2.2	-1.5	-2.5	+0.6	+0.1	+0.7	+0.6	+0.4	+0.9	+0.1	-0.1	+0.6	+0.6	+0.9	+0.9
59	-2.0	-1.3	-0.4	-0.7	+2.6	+1.6	+3.0	+4.3	-0.3	-0.5	+0.6	+0.6	+2.2	+2.1	+2.6	+4.2
60	-4.6	-3.3	-2.7	-3.9	+0.8	-0.3	+1.7	+1.8	-0.8	-1.5	+0.1	-0.4	+0.7	+0.6	+1.5	+1.2
61																
62	+1.1	+1.1	-3.1	+3.2	+2.5			+3.5								
63	-3.5	-2.3	-0.5	-1.1	+1.4	+1.5	+1.0	+1.3	-0.4	-0.9	+0.4	+0.5	+0.5	+0.9	+0.5	+0.3
64	-5.5	-3.7	-1.9	-3.3	+1.3	+1.0	+2.0	+1.9	-0.8	-1.8	+0.4	-0.5	+1.3	+1.4	+2.4	+2.1
65	-4.5	-3.1	-2.0	-3.0	+1.2	-0.1	+2.4	+1.9	-0.6	-1.2	+0.3	0	+1.4	+1.2	+2.6	+2.4
66	-2.2	-1.3	+0.1	+0.1	+0.1	+2.5	+1.6	+3.6	+3.4	-0.1	-0.1	+1.0	+2.0	+2.2	+2.6	+4.6

TABLE VII (Continued)

FAN-WING PRESSURE DISTRIBUTION

V (mph)	0	40	60	20	0	20	40	60	0	40	60
α (°)	0	0	0	0	0	0	0	0	0	0	0
θ (°)	30	30	30	30	10	10	10	10	20	20	20
ΩR	393	393	393	393	393	393	393	393	393	393	393
Manometer Tube No.	PRESSURE DISTRIBUTION IN INCHES OF ALCOHOL										
33											
34	-1.3	-4.3	-2.4	-5.5	-0.2	-2.6	-1.3	-1.2	-0.8	-3.7	-2.1
35	-3.0	-4.0	-2.6	-8.5	-0.5	-2.7	-0.7	-0.4	-1.9	-3.6	-1.6
36	-4.5	-4.7	-4.2	-8.7	-0.9	-2.4	-0.7	-0.5	-2.9	-3.3	-2.4
37	-3.3	-3.6	-1.7	-8.3	-0.7	-2.7	-1.0	-0.8	-2.2	-4.3	-2.3
38	-1.7	-1.6	-0.7	-4.4	-0.6	+0.3	+0.8	+0.7	-1.3	-1.1	+0.1
39	-4.2	-3.2	-4.4	-6.8	-0.9	-2.9	-0.6	-0.8	-2.7	-1.7	-1.9
40	-3.2	-1.4	+1.1	-5.2	-0.8	-2.0	-1.0	0.9	-2.1	-2.3	-0.9
41											
42	-1.5	-1.2	+1.0	-2.0	-0.4	+0.2	+0.9	1.1	-1.2	-0.1	+2.0
43	0	-0.6	-0.8	-0/3	0	+0.1	+0.5	0.6	0	+0.3	+0.7
44	-2.3	-2.4	-2.2	-5.2	-0.4	-1.1	-0.6	-0.4	-1.3	-1.5	-0.7
45	-1.5	-0.6	+0.3	-1.6	0	+0.3	+0.8	1.0	0	+0.8	1.9
46	-0.1	-0.2	-0.1	-0.9	0	+0.3	+0.8	0.9	0	+0.9	1.8
47	0	0	-0.3	-0.6	0	+0.2	+0.8	0.8	0	+1.0	1.7
48	0	-0.1	-0.3	-0.4	0	+0.3	+0.8	0.8	0	+1.1	1.6
49											
50											
51	-0.8	+0.8	+4.3	-1.1	-0.1	+0.3	+1.0	1.7	-1.8	+0.6	2.9
52	-2.8	-1.6	+0.7	-3.4	-0.6	-0.3	-0.3	1.2	-2.3	-0.6	-0.8
53	-3.5	-2.3	-6.1	-4.8	-0.8	-0.5	0	0	-1.3	-0.4	-1.7
54	-2.2	-1.2	-3.6	-3.0	-0.5	-0.2	+0.3	0.1	-1.3	-0.2	-0.1
55											
56	-1.5	-0.1	-2.0	-0.5	-0.4	+0.3	+0.5	0.2	-1.0	+0.5	+0.3
57	-1.3	-0.2	-0.3	-0.8	-0.3	+0.2	+0.8	1.2	0.9	+0.7	+1.1
58	-2.2	-0.4	+0.1	-1.7	-0.4	+0.2	+0.8	1.5	-1.3	+0.7	+1.4

TABLE VII (Continued)

FAN-WING PRESSURE DISTRIBUTION

$V_{(mph)}$	0	40	60	20	0	20	40	60	0	40	60
$\alpha(^{\circ})$	0	0	0	0	0	0	0	0	0	0	0
$\theta(^{\circ})$	30	30	30	30	10	10	10	10	20	20	20
ΩR	393	393	393	393	393	393	393	393	393	393	393
Manometer Tube No.	PRESSURE DISTRIBUTION IN INCHES OF ALCOHOL										
59	-1.1	+1.0	+2.5	-0.8	-0.3	+0.7	+2.4	3.2	-1.1	+1.3	+2.9
60	-3.0	-0.2	+1.1	-2.8	-0.8	+0.1	+0.8	2.0	-2.1	+0.7	+2.1
61											
62	-0.2	-0.6	-0.4	-0.7	0	+0.3	+0.6				
63	-2.2	+0.6	+0.5	-0.6	-0.4	+0.4	+0.7	1.1	-1.3	+1.2	+1.2
64	-3.8	+0.5	-0.5	-2.2	-0.9	+0.4	+1.5	3.0	-2.6	+1.5	+2.9
65	-3.1	0	-0.8	-2.2	-0.7	+0.3	+1.5	3.1	-1.9	+1.2	+3.2
66	-1.2	+0.9	-2.9	-0.1	-0.2	+0.7	+1.9	3.2	-1.1	+1.9	+4.0
67											
68	0	0	0	0	0	0	0	0	0	0	0
69	0	-0.2	-0.1	0	0	+0.2	+0.7	0.2	0	+0.7	+1.2
70	0	-0.2	-0.1	0	0	+0.2	+0.7	1.2	0	+0.7	+1.2
71	-0.5	-3.3	-3.1	-3.0	-0.1	-1.5	-2.0	-0.3	0	-1.4	-2.0
72	-0.3	-2.6	-2.7	-2.2	0	-1.1	-1.4	-2.3	-0.2	-2.5	-3.1
73	0	-2.0	-2.3	-1.4	0	-0.9	-1.1	-1.8	0	-1.9	-2.6
74	0	-1.6	-1.9	-1.1	0	-0.8	-0.9	-1.5	0	-1.6	-2.2
75	0	-1.2	-1.1	-0.9	0	-0.6	-0.5	-0.6	0	-1.1	-1.2
76	-0.1	+0.7	+1.0	+0.3	0	+0.1	+0.5	+0.5	0	+0.7	+0.9
77	-0.1	+0.3	+0.2	+0.1	0	-0.1	+0.2	0	0	+0.4	+0.3
78	-0.1	+0.3	+0.2	+0.2	0	-0.1	+0.1	-0.1	0	+0.3	+0.2
79	0	+0.1	0	0	0	-0.1	0	-0.1	0	+0.1	0
80	-0.1	+0.3	0	+0.2	0	0	+0.1	-0.4	0	+0.2	+0.1
81	-0.9	-0.3	-1.6	-0.2	-0.2	-0.2	-0.8	-2.1	0	-0.6	-2.1
82	-0.2	-0.1	-0.4	+0.2	0	-0.1	-0.2	-0.6	0	-0.2	-0.6
83	0	-0.3	-0.6	0	0	-0.1	-0.2	-0.5	0	-0.3	-0.7
84	0	-0.5	-0.6	-0.1	0	-0.2	-0.2	-0.2	0	+0.4	-0.6
85	-0.4	-1.6	-1.3	-1.5	0	-1.0	-1.2	-1.6	0	-1.5	-1.7

TABLE VII (Continued)

FAN-WING PRESSURE DISTRIBUTION

V(mph)	0	40	60	20	0	20	40	60	0	40	60
$\alpha(^{o})$	0	0	0	0	0	0	0	0	0	0	0
$\theta(^{o})$	30	30	30	30	+10	10	10	10	10	20	20
ΩR	393	393	393	393	393	393	393	393	393	393	393
Manometer Tube No.	PRESSURE DISTRIBUTION IN INCHES OF ALCOHOL										
86	-0.4	-2.3	-2.0	-2.0	-0.1	-1.0	-1.4	-2.1	0	-2.1	-2.7
87	-0.2	-1.6	-1.8	-1.1	-0.1	-0.7	-1.0	-1.6	0	-1.5	-2.1
88	-0.1	-1.6	-2.1	-1.0	0	-0.7	-1.0	-1.8	0	-1.5	-2.3
89	-0.1	-1.6	-1.6	-1.2	0	-0.7	-0.9	01.4	0	-1.3	-1.8
90	0	-1.1	-1.0	-1.0	0	-0.6	-0.5	-0.7	0	-1.0	-1.1
91	0	-0.4	+0.6	+0.6	0	0	+0.3	+0.3	0	+0.5	+0.7
92	0	-0.1	-0.2	-0.2	0	-0.1	-0.1	-0.4	0	+0.1	0
93	0	-0.1	-0.4	-0.1	0	-0.2	-0.1	-0.5	0	0	-0.3
94	0	-0.2	0	0	0	-0.1	0	-0.5	0	+0.1	-0.1
95	0	-0.2	0	0	0	-0.1	+0.1	-0.5	0	+0.2	0
96	0	-1.9	-1.6	-0.8	0	-0.5	-0.6	-1.2	0	-0.8	-0.4
97	0	-0.9	-1.4	-0.5	0	-0.5	-0.6	-1.2	0	-0.7	-1.3
98	0	-0.8	-1.3	-0.4	0	-0.5	-0.5	-1.2	0	-0.7	-1.2
99	0	-0.7	-1.0	-0.2	0	-0.4	-0.5	-0.6	0	-0.7	-1.1
100	0	-0.6	-0.9	-0.2	-0.1	-0.4	-0.4	-0.8	0	-0.6	-1.0
101	0	-0.6	-0.9	-0.2	0	-0.4	-0.4	-0.5	0	-0.6	-1.0
102	0	-0.6	-0.9	-0.2	0	-0.4	-0.4	-0.5	0	-0.6	-1.9
103	0	-0.6	-0.9	-0.2	0	-0.4	-0.4	-0.5	0	-0.6	-1.0
104	0	-0.8	-0.9	-0.5	0	-0.5	-0.4	-0.6	0	-0.8	-1.0
105	0	-1.0	-1.4	-0.5	0	-0.5	-0.6	-1.1	0	-0.9	-1.5
106	0	-0.9	-1.5	-0.5	0	-0.4	-0.6	-1.1	0	-0.9	-1.5
107	0	-1.0	-1.5	-0.6	0	-0.5	-0.7	-1.5	0	-1.0	-1.6
108	0	-1.0	-1.5	-0.6	0	-0.5	-0.7	-1.5	0	-1.0	-1.6
109	0	-0.7	-1.1	-0.6	0	-0.4	-0.5	-1.0	0	-0.7	-1.1
110	0	-0.3	-0.6	-0.1	0	-0.2	-0.2	-0.7	0	-0.4	-0.8
111	0	-0.3	-0.6	-0.1	0	-0.2	-0.2	-0.5	0	-0.4	-0.6

TABLE VII (Continued)

FAN-WING PRESSURE DISTRIBUTION

$V_{(mph)}$	0	40	60	20	0	20	40	60	0	40	60
$\alpha (^{o})$	0	0	0	0	0	0	0	0	0	0	0
$\theta (^{o})$	30	30	30	30	10	10	10	10	20	20	20
ΩR	393	393	393	393	393	393	393	393	393	393	393
Manometer Tube No.	PRESSURE DISTRIBUTION IN INCHES OF ALCOHOL										
112	0	-0.3	-0.6	-0.1	0	-0.2	-0.2	-0.4	0	-0.4	-0.6
113	0	-0.3	-0.4	-0.1	0	-0.2	-0.1	-0.1	0	-0.4	-0.6
114	0	+0.1	+0.1	0	0	-0.1	+0.1	+0.1	0	+0.1	+0.1
115	0	+0.3	+0.1	+0.1	0	-0.1	+0.1	-0.2	0	+0.2	+0.1
116	0	+0.1	-0.2	0	0	-0.1	-0.1	-0.5	0	+0.1	-02.
117	0	0	-0.4	0	0	-0.1	-0.1	-0.8	0	0	-0.5
118	0	0	-0.4	-0.1	0	-0.1	00.1	-0.7	0	0	-0.4
119	0	-0.3	-0.5	-0.5	0	-0.2	-0.1	-0.5	0	-0.2	-0.4
120	0	-0.7	-0.8	-0.8	0	-0.4	-0.3	-0.7	0	-0.6	-0.9
121	0	0	B	18.5	0	0	0	B	0	0	0
122											
123	0	0	B	18.5	0	0	0	B	0	0	0
124	0	0	0	18.5	0	0	0	B	0	0	0
125	0	0	0	0	0	0	0	B	0	0	0
126	0	0	0	0	0	0	0	B	0	0	0
127											
128	0	0	0	18.5	0	0	0	B	0	0	0
129	0	0	0	18.5	0	0	0	B	0	0	0
130	0	0	0	18.5	0	0	0	B	0	0	0
131	0	-0.5	-0.9	-0.2	-0.1	+0.1	+0.5	0.7	0	+0.4	+0.8
132	0	-0.9	-1.3	-0.4	0	0	+0.2	0.2	0	0	+0.2
133	0	-0.9	-1.1	-0.2	0	0	+0.2	-.7	0	0	+0.3

TABLE VIII

COMPARISON OF RIGID AND ARTICULATED ROTORS

Fan-Wing

$\alpha = 0^{o}$ $\theta = 20^{o}$ N = 5000 rpm

same blades

RIGID ROTOR

V mph	$\bar{u}$ (ft/sec)	$V/\bar{u}$	L (lb)	D (lb)	M (ft. lb)
0	63.3	0	14.5	0	0
40	63.0	.93	23.5	16.5	53.6
60	58.4	1.51	30.5	24.6	72.8

ARTICULATED ROTOR

0	68.9	0	15.5	0	1.6
40	66.3	.885	23.0	16.0	53.0
60	55.5	1.58	22.5	21.5	61.4

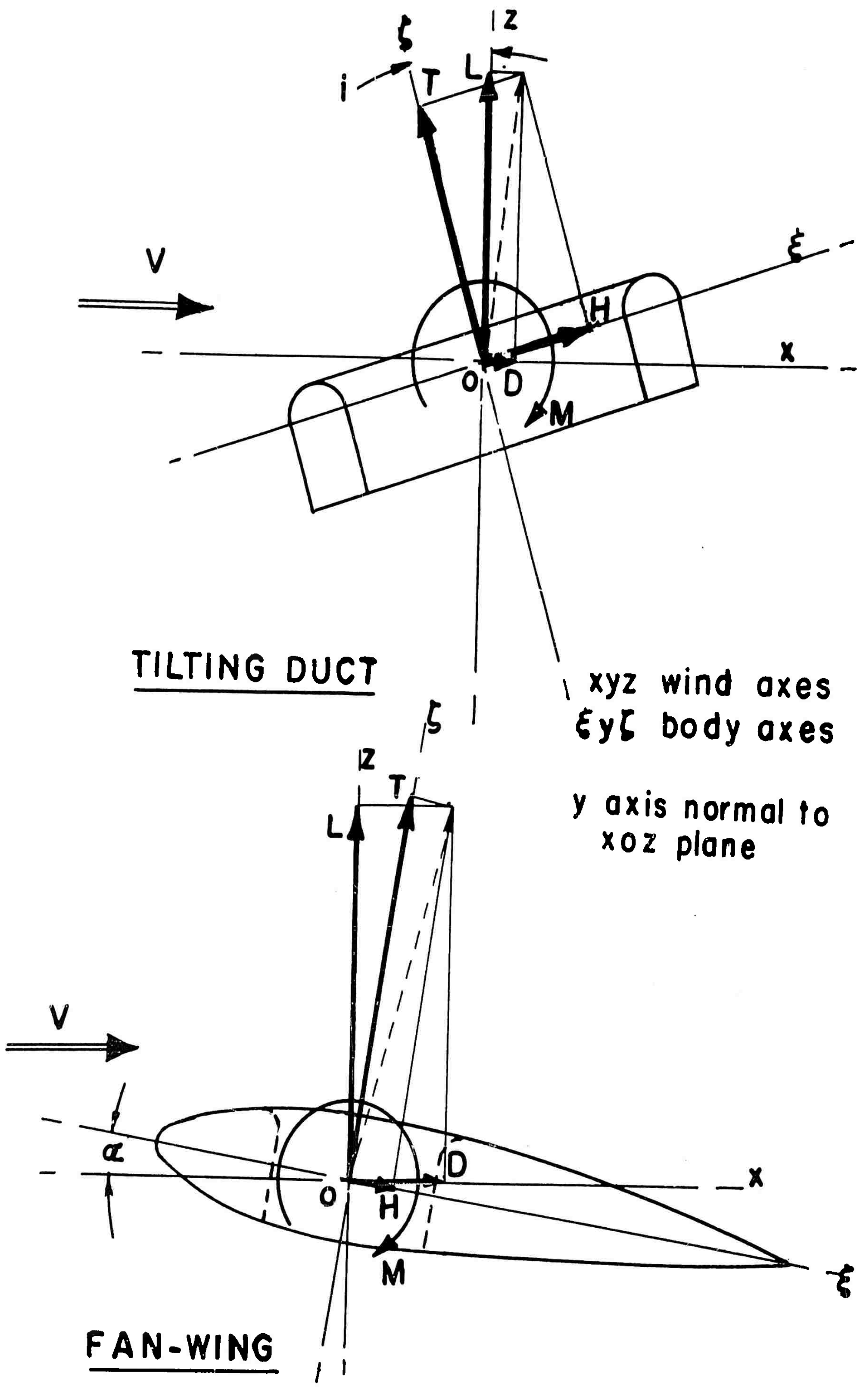

FIG. I AXES & FORCES

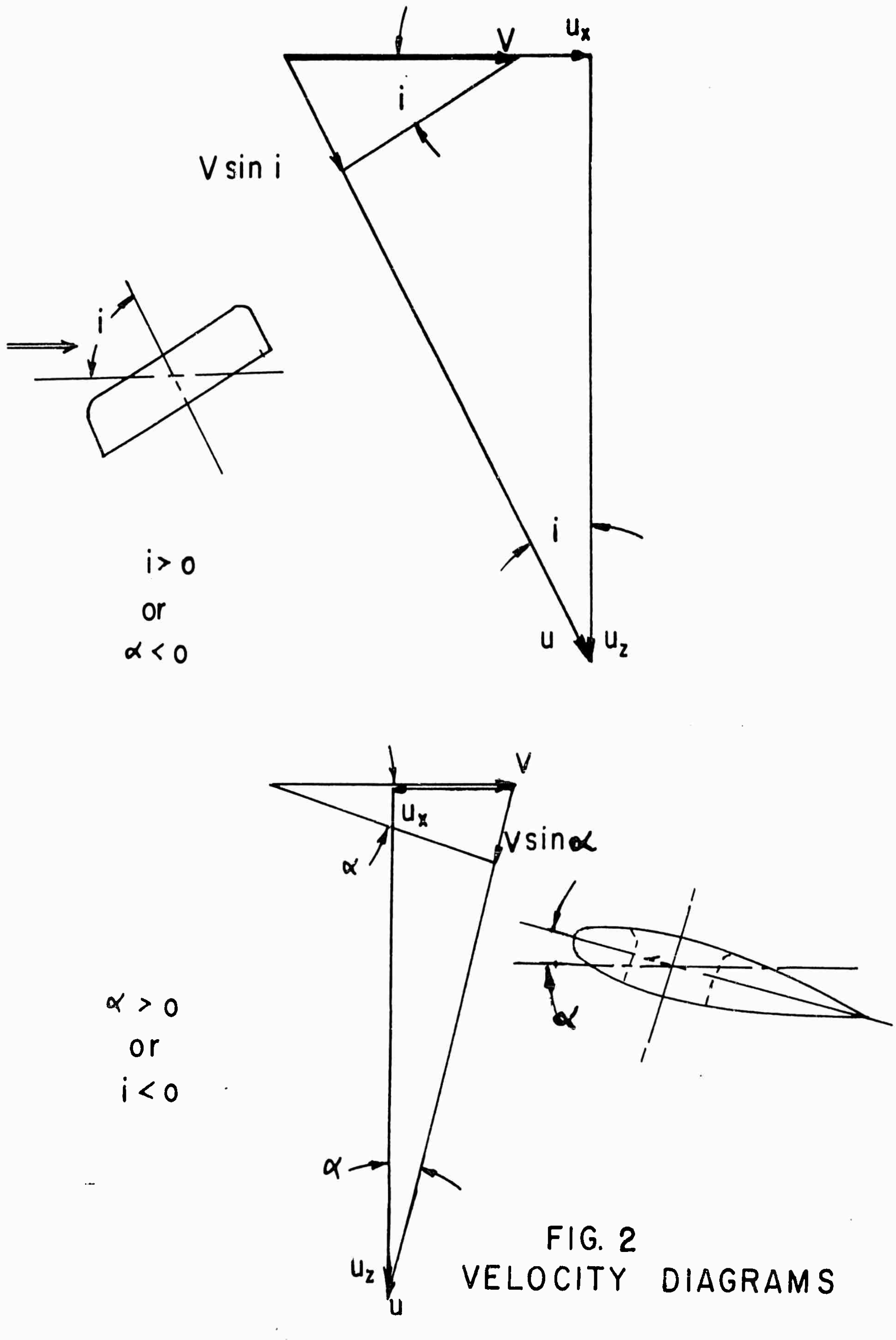

FIG. 2
VELOCITY DIAGRAMS

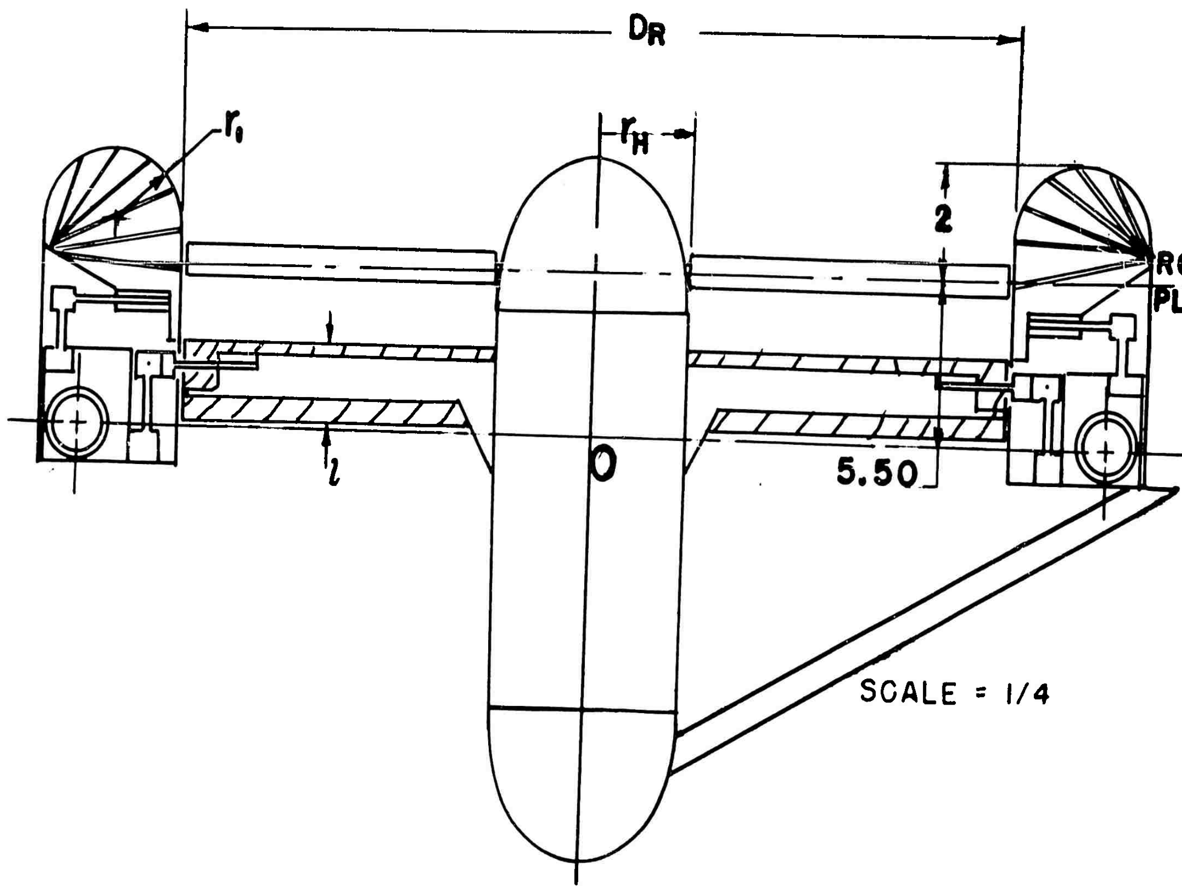

FIGURE 3 TILT MODEL GEOMETRY

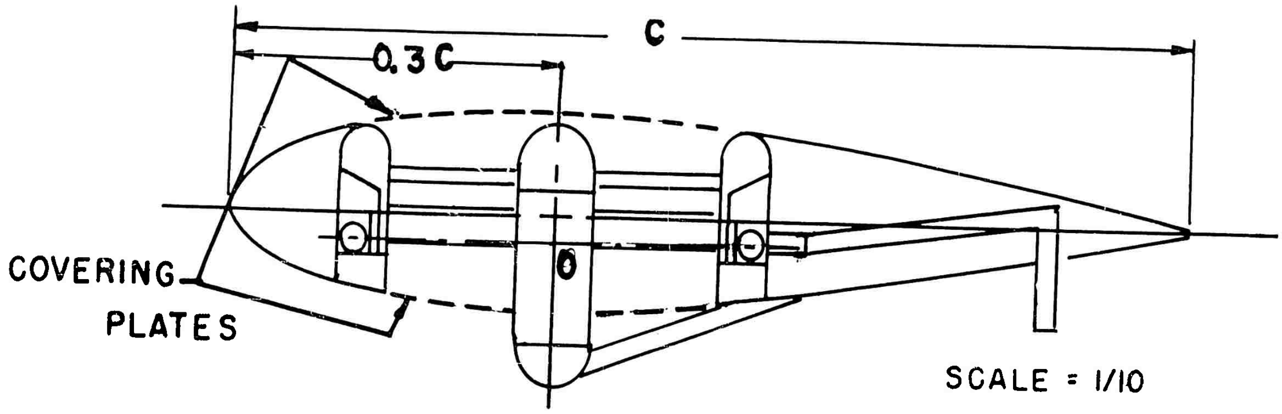

FIGURE 4 FAN-WING MODEL GEOMETRY

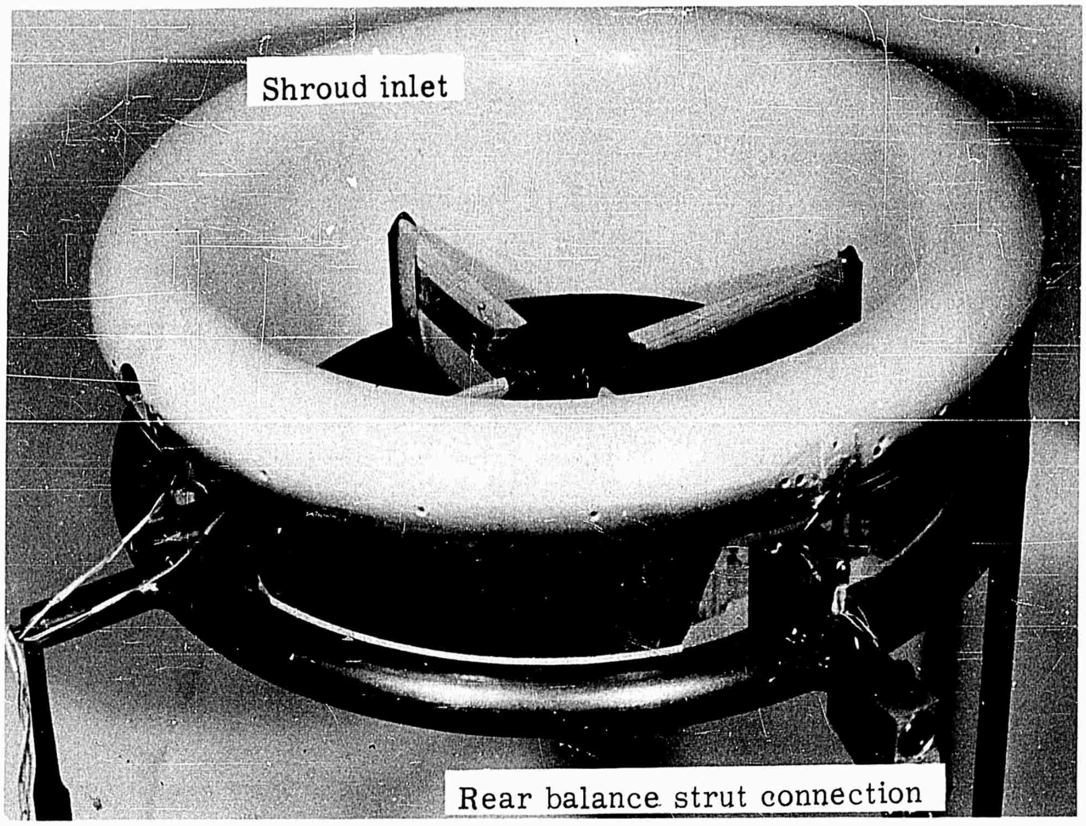

Fig. 5. Independent shroud and rotor suspension.

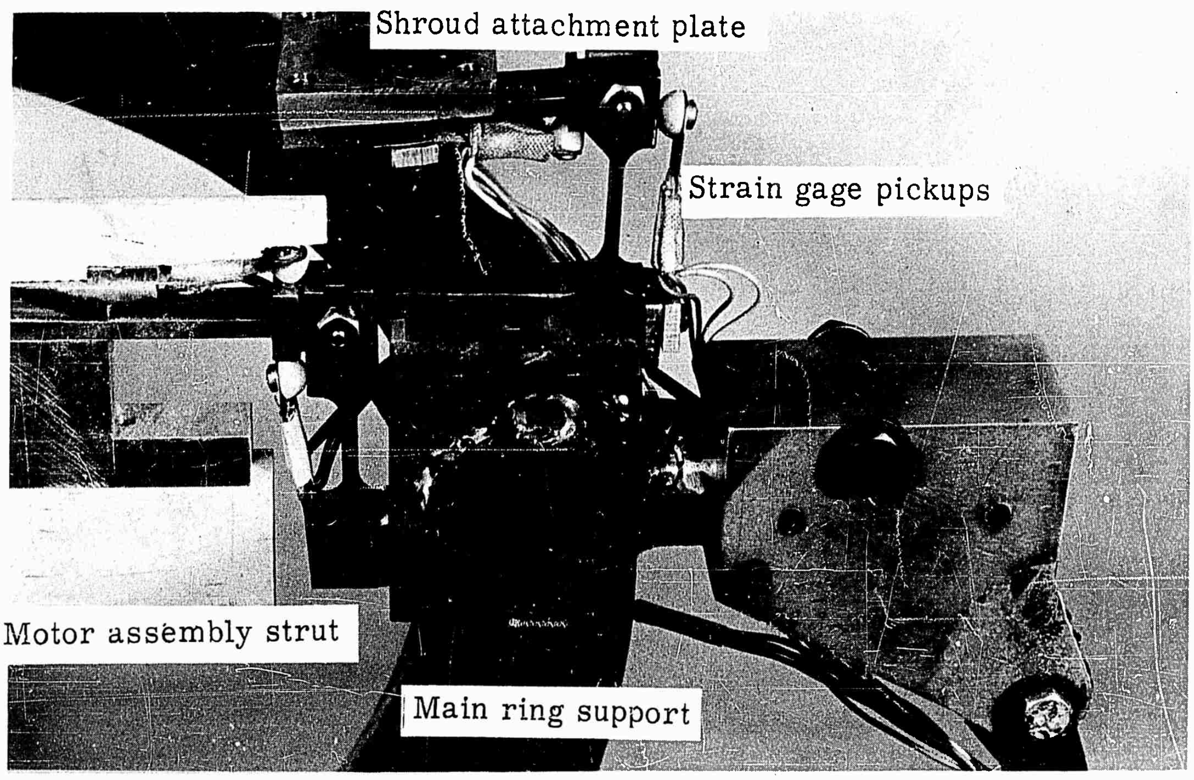

Fig. 6. Detail of rear flexures and pickups.

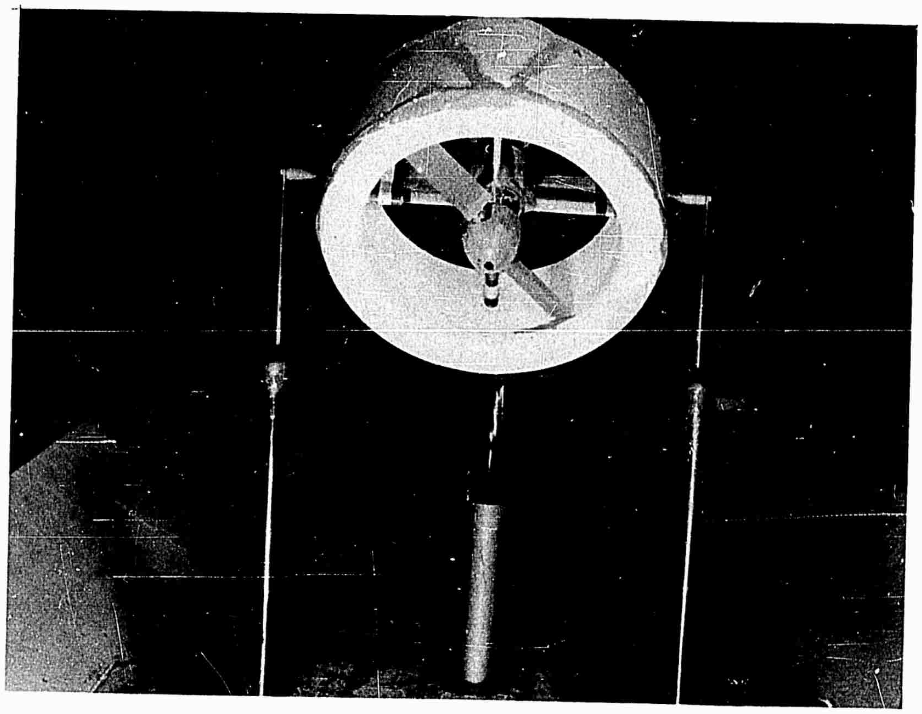

Fig. 7. Tilting model in wind tunnel.

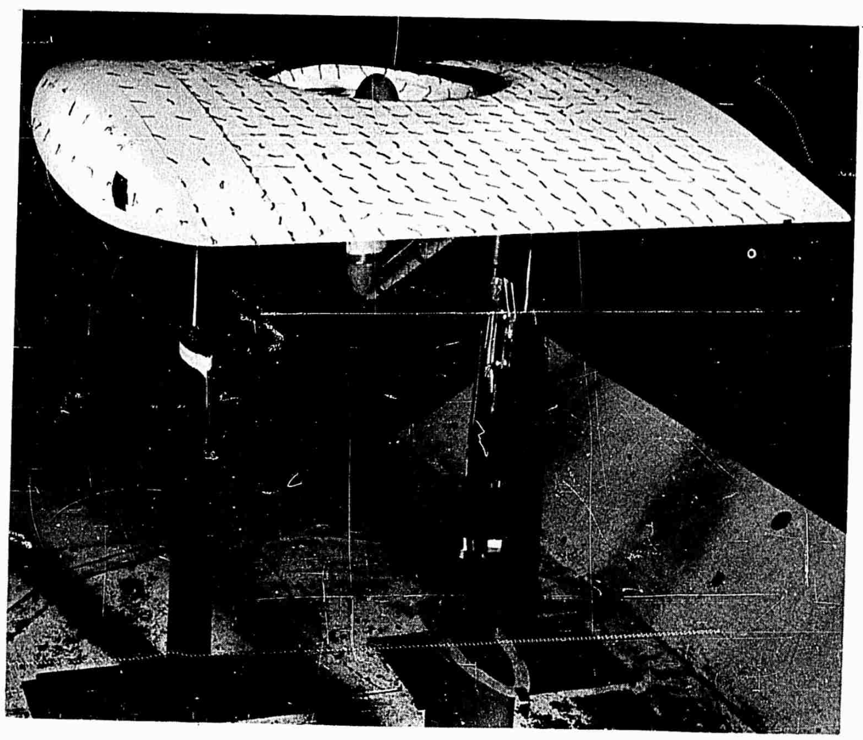

Fig. 8. Fan-wing model in wind tunnel.
Rear strut fairing removed.

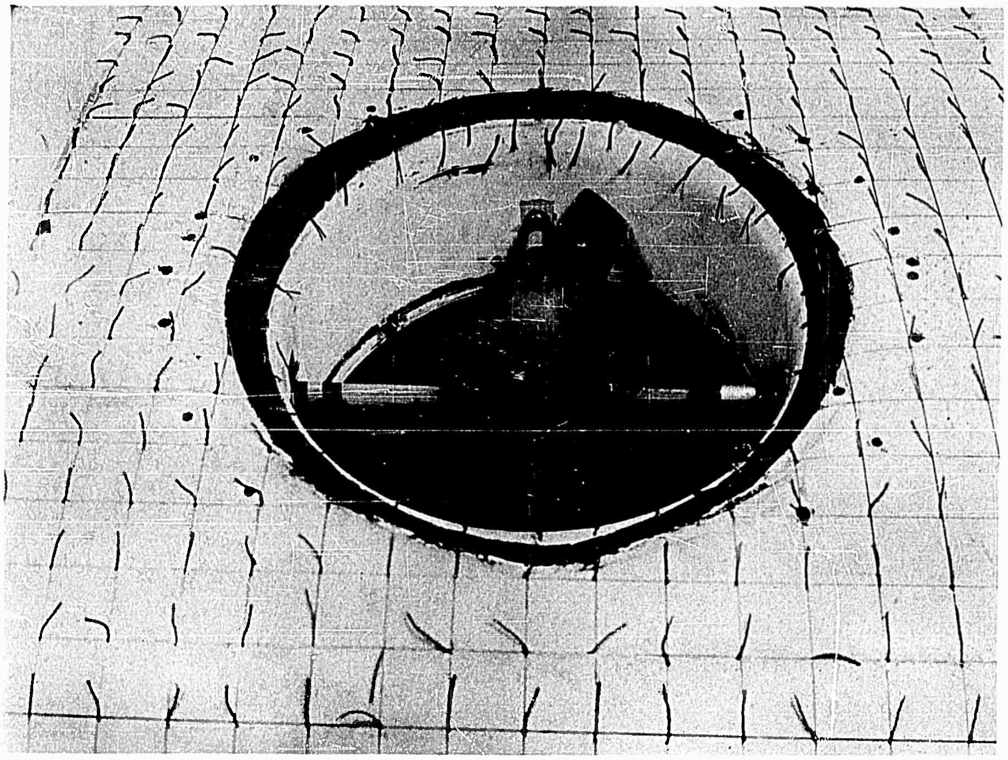

Fig. 9. Detail of fan installation in wing.

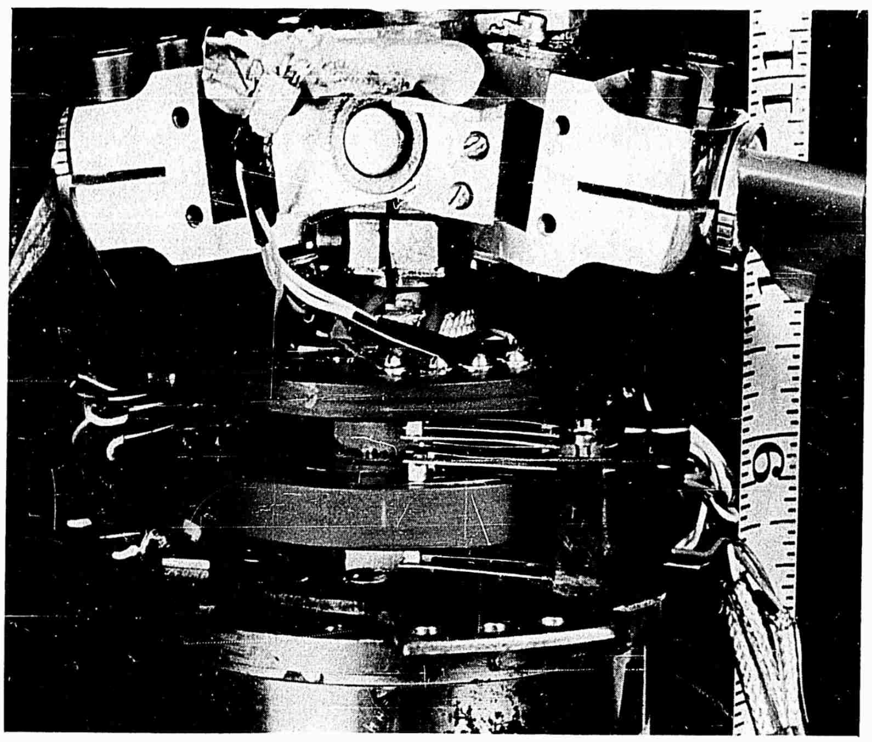

Fig. 10. Detail of hub and slip ring assembly.

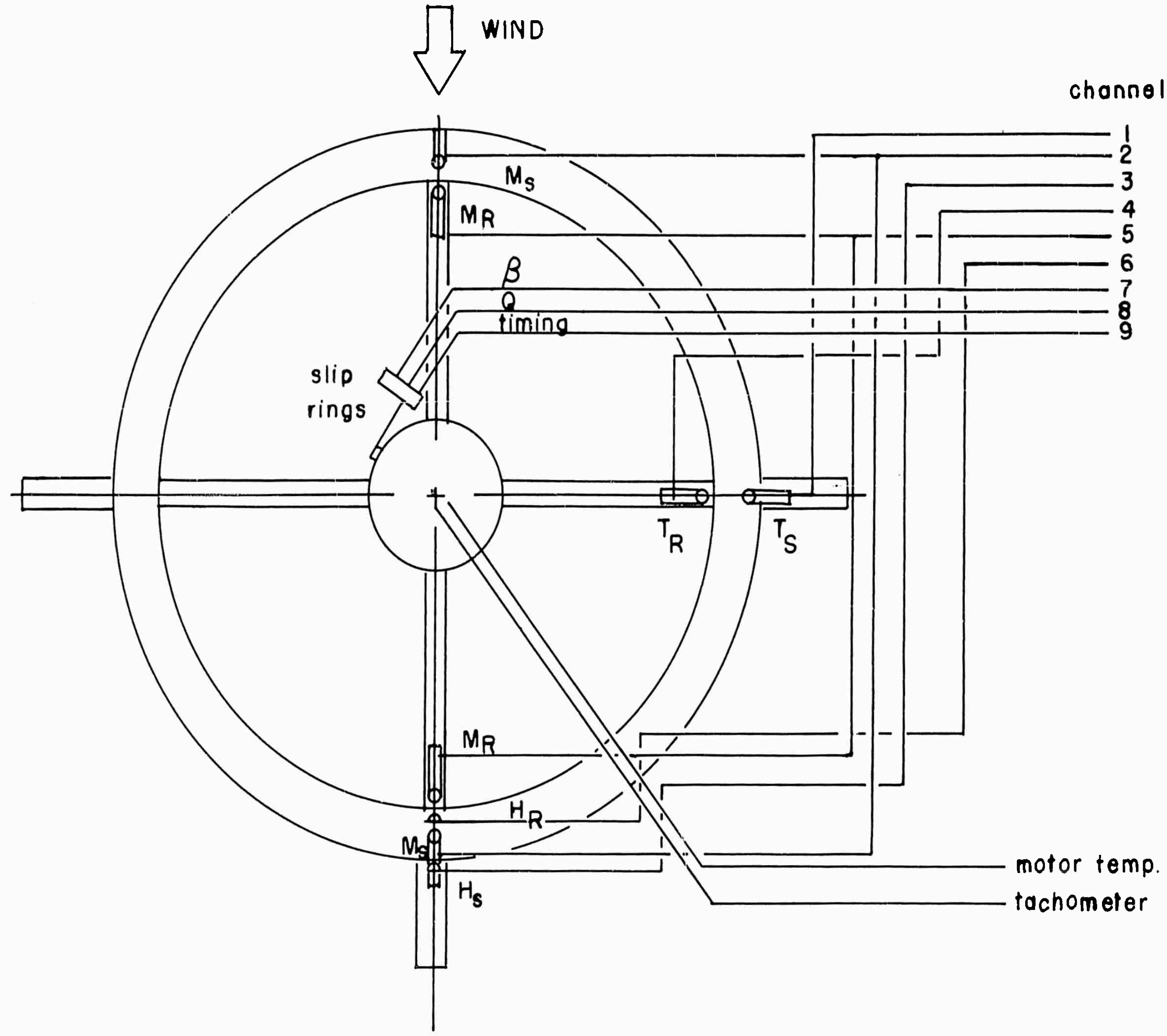

FIGURE 11 INSTRUMENTATION SCHEMATIC

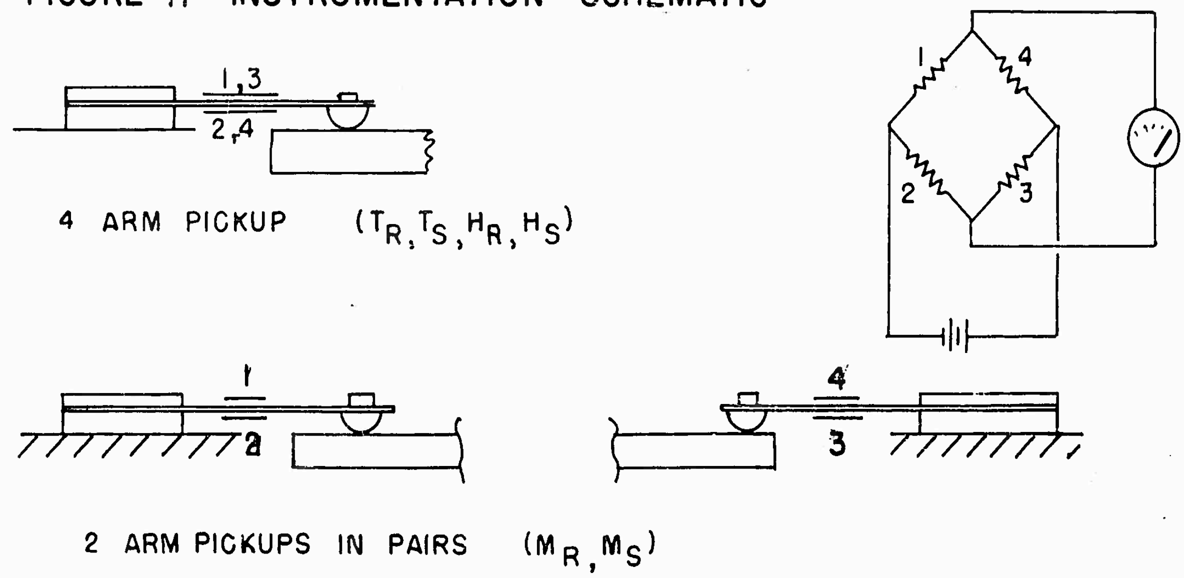

FIGURE 12 DETAIL OF PICKUP INSTRUMENTATION

FIGURE 13 CIRCUIT SCHEMATIC

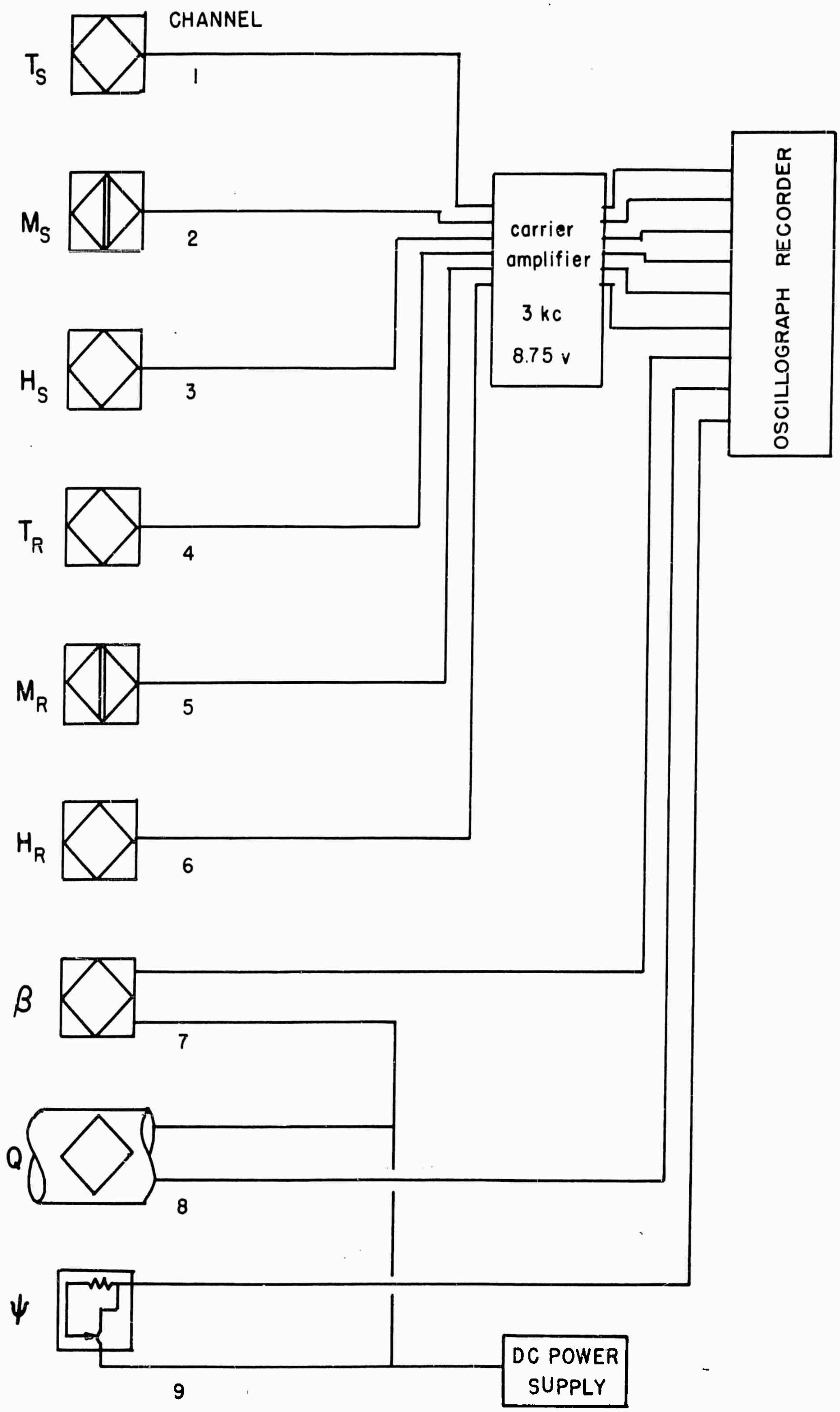

FIGURE 14 SHROUD INLET PRESSURE LOCATIONS

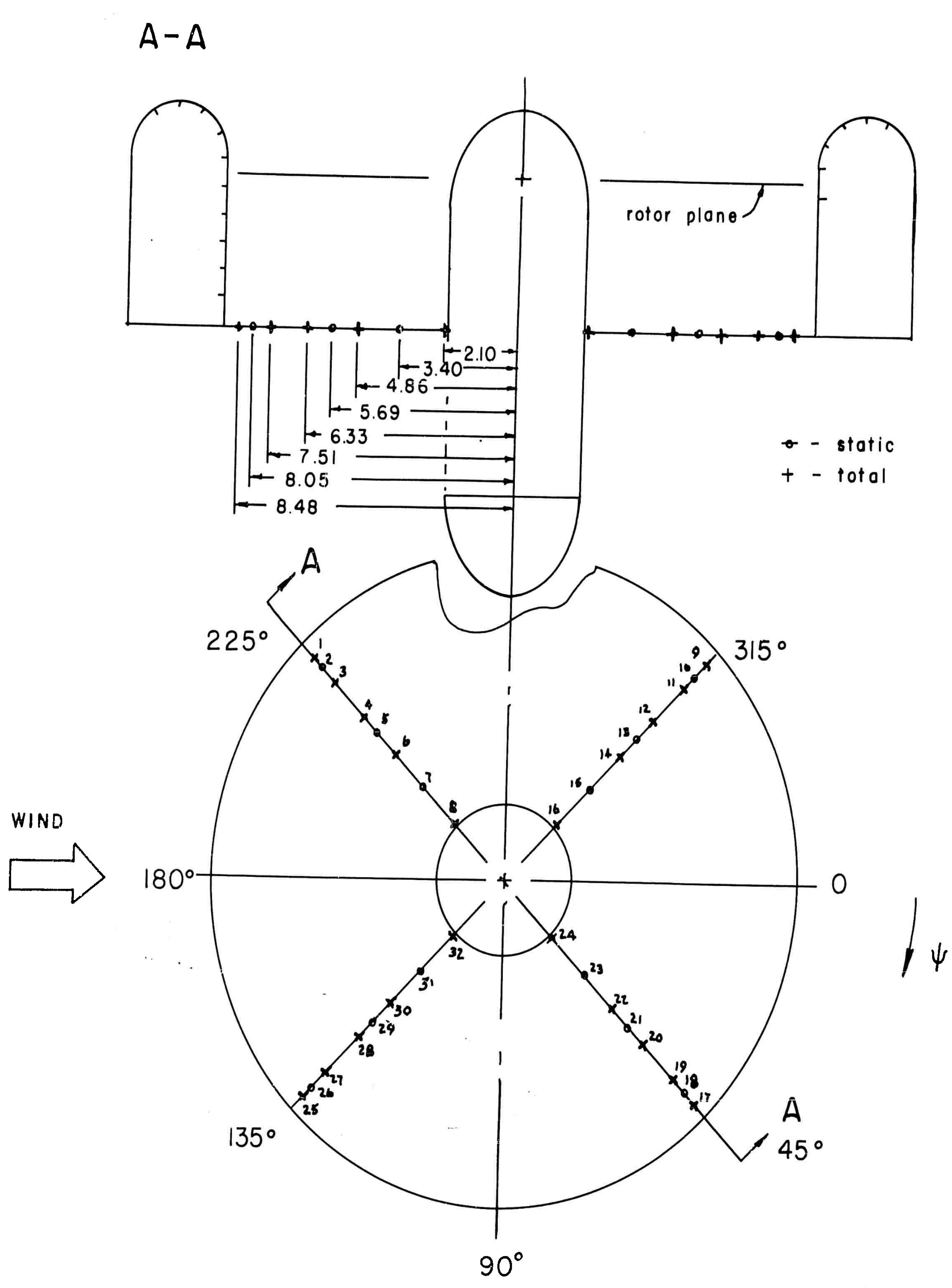

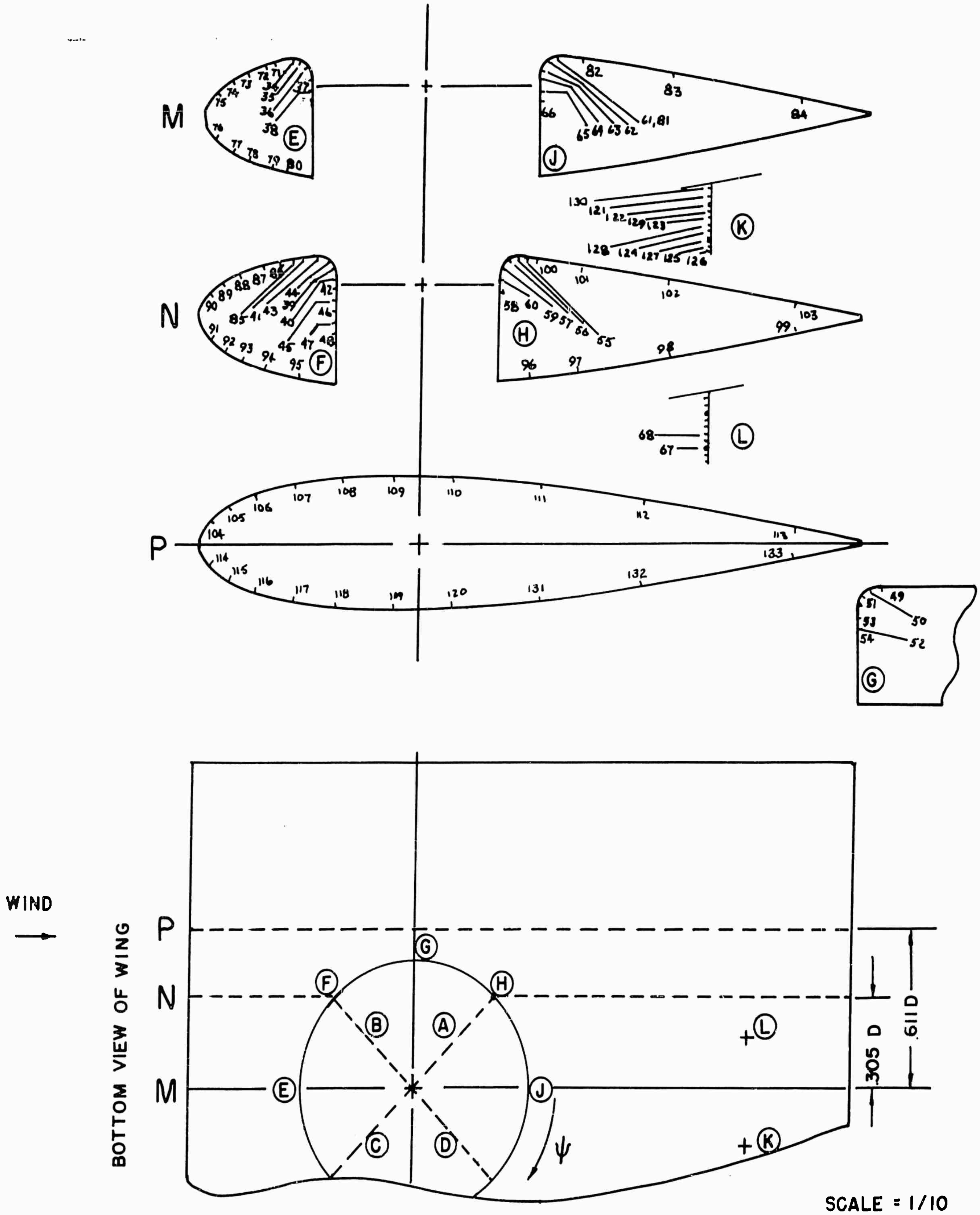

FIGURE 15 PRESSURE TAP LOCATIONS ON WING

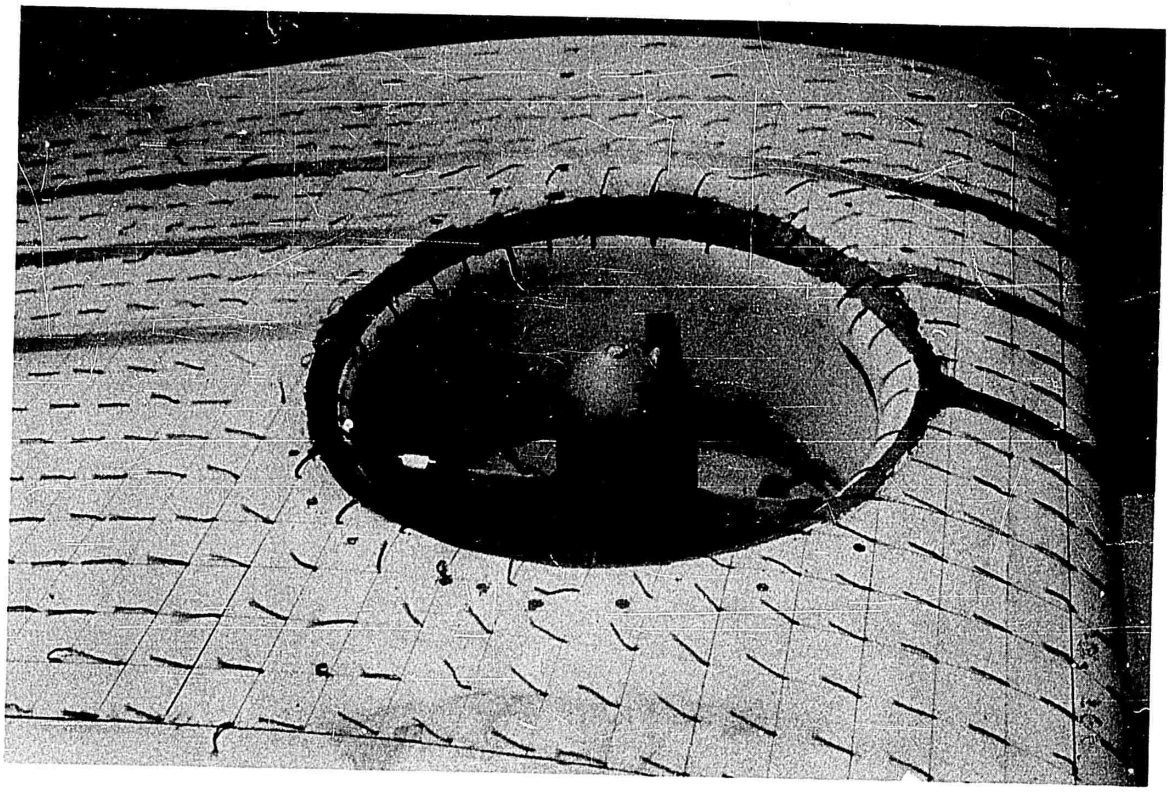

Fig. 16a. Flow around duct; $V/\bar{u} = .341$.

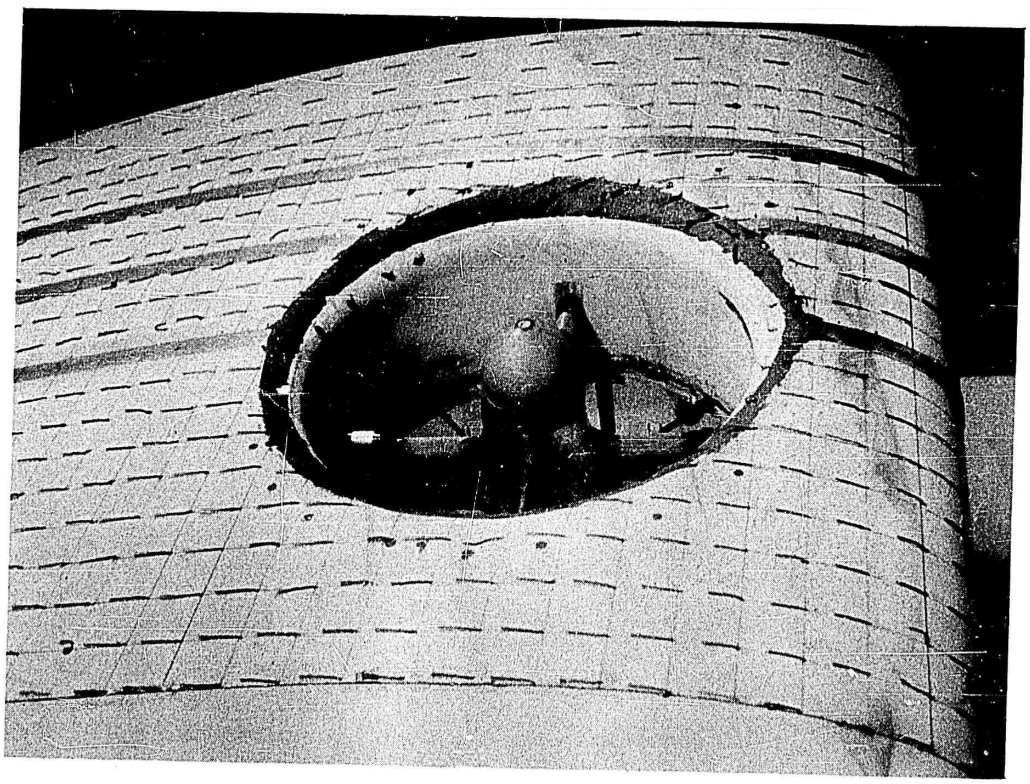

Fig. 16b. Flow around duct; $V/\bar{u} = 2.51$.

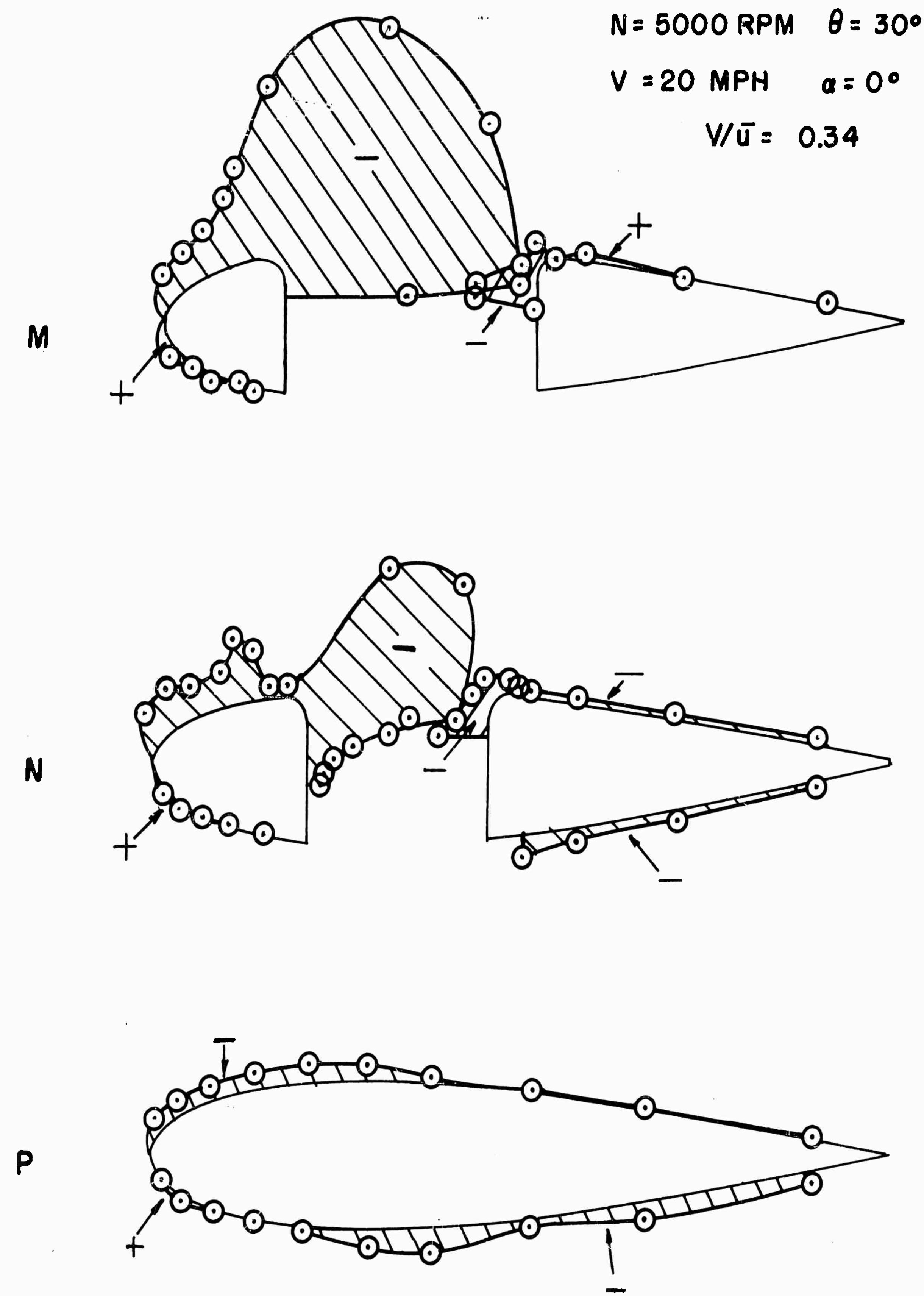

FIGURE 17 FAN-WING PRESSURE DISTRIBUTION

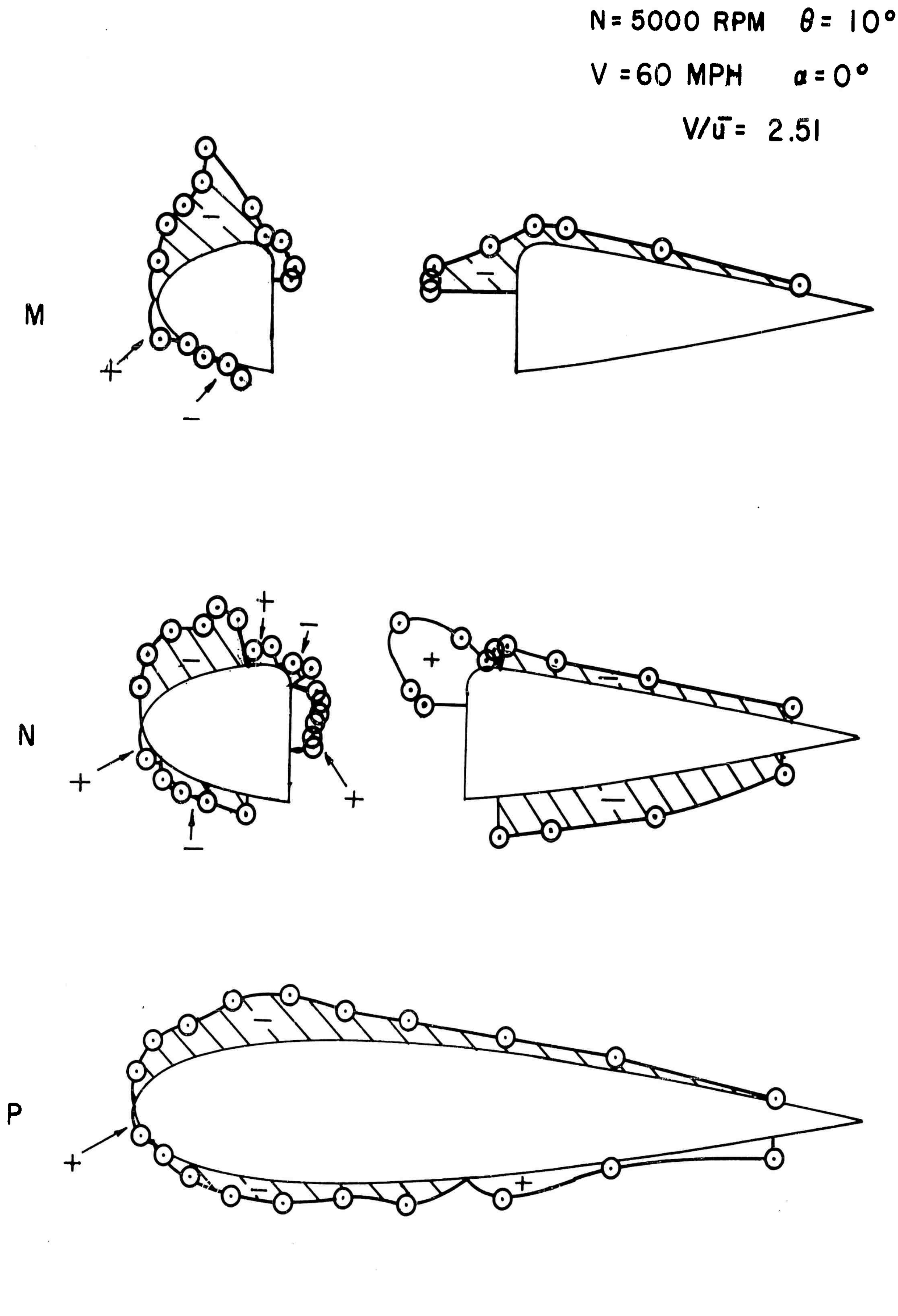

FIGURE 18 FAN — WING PRESSURE DISTRIBUTION

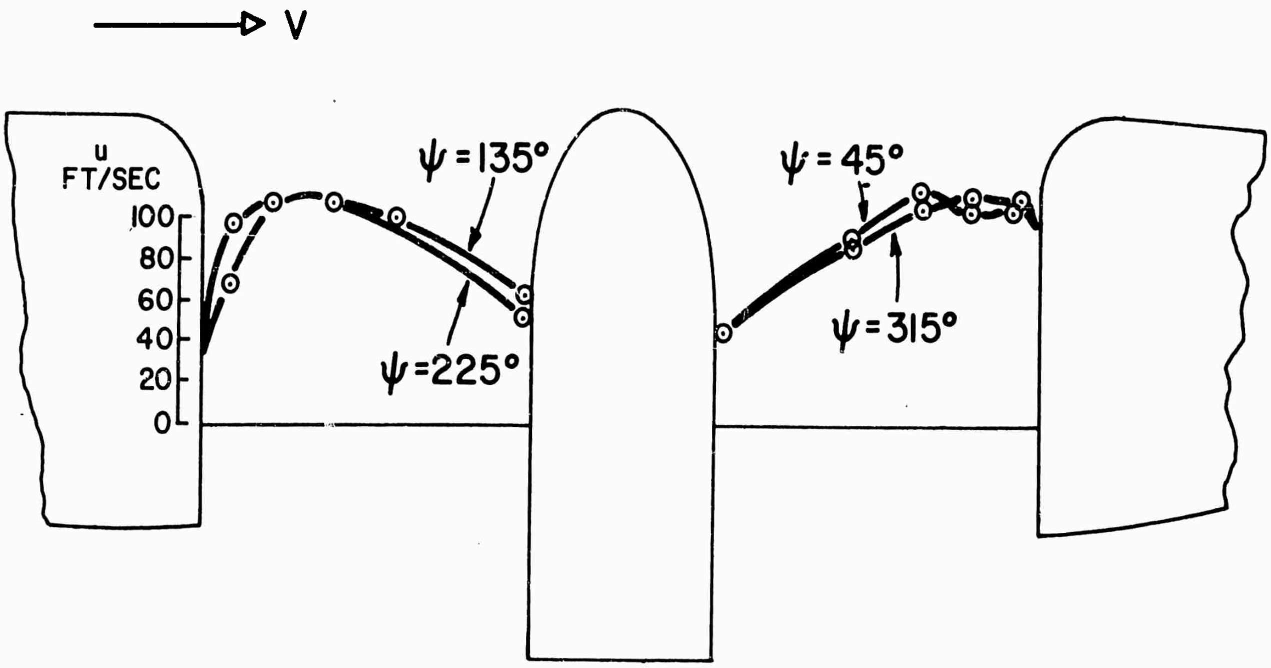

FIGURE 19 a FAN-WING, DUCT VELOCITY DISTRIBUTION
N=5000 RPM $\theta=30°$ V=20 MPH $\alpha=0°$
$V/\bar{u}=0.34$

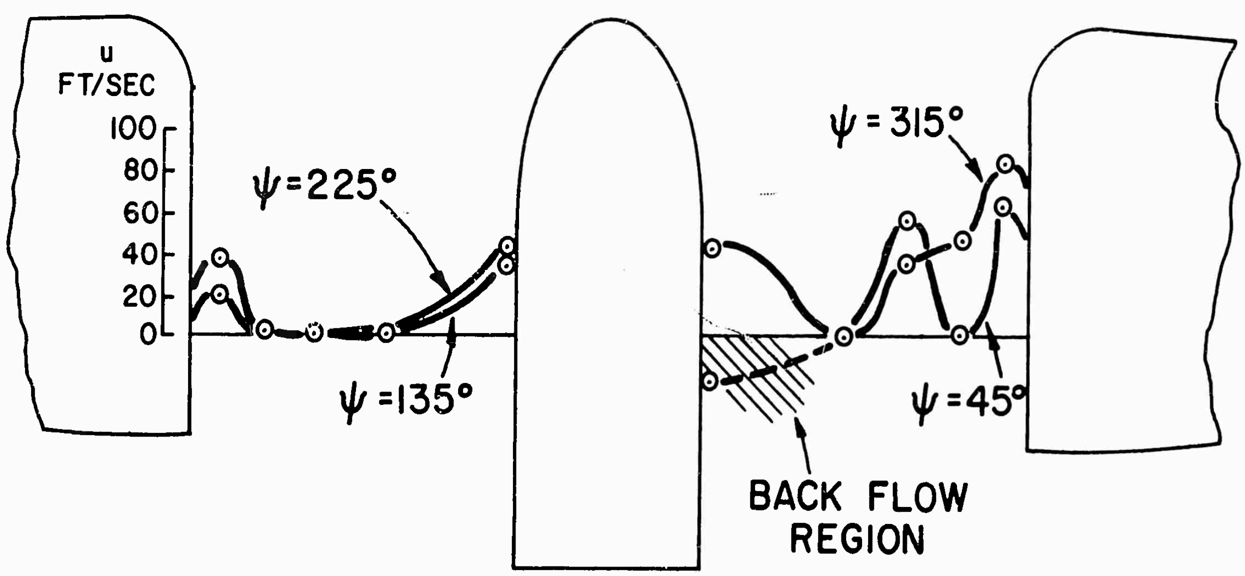

FIGURE 19 b FAN-WING DUCT VELOCITY DISTRIBUTION
N=5000 RPM $\theta=10°$ V=60 MPH $\alpha=0°$
$V/\bar{u}=2.51$

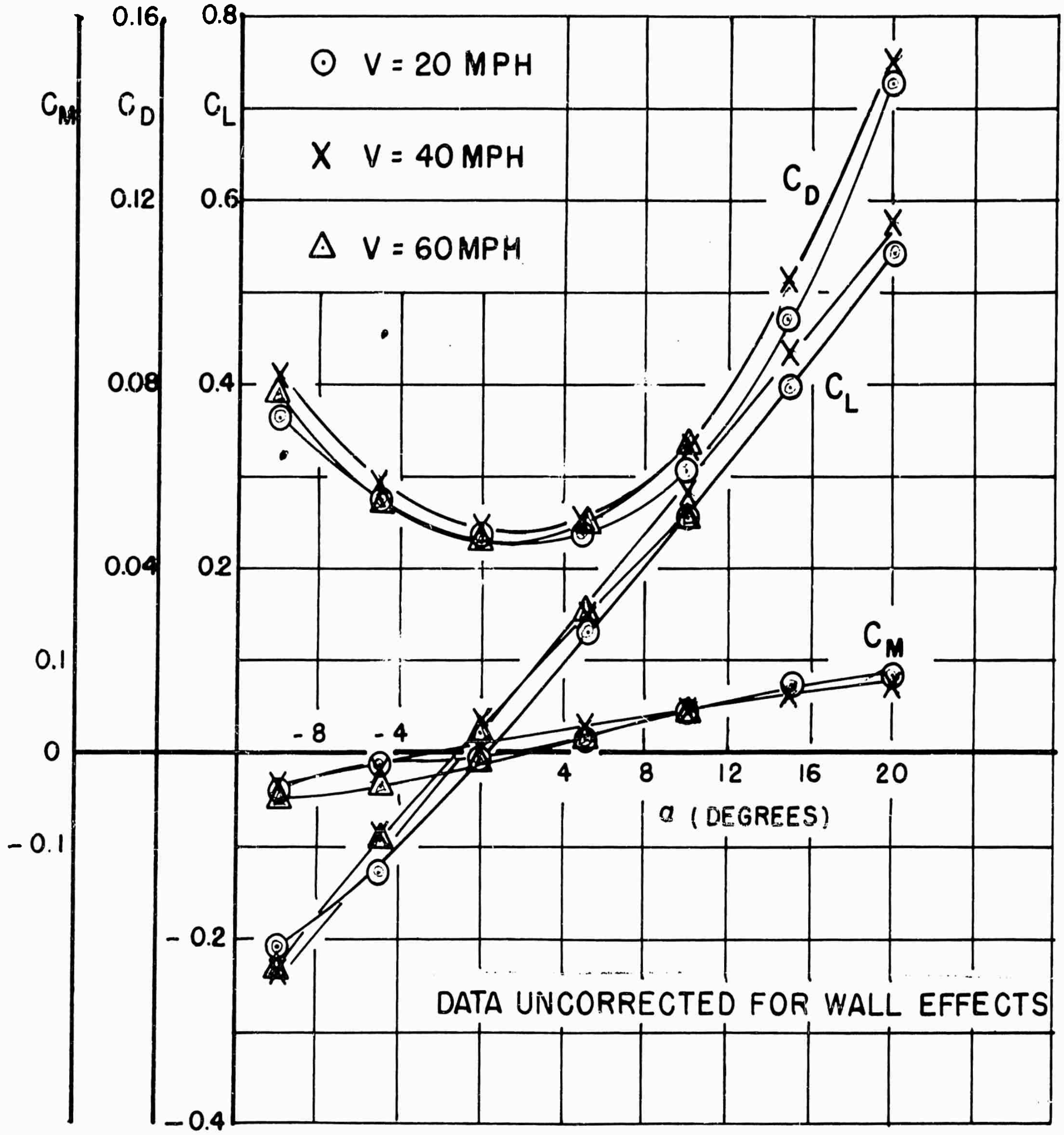

FIGURE 20. WING TARE DATA

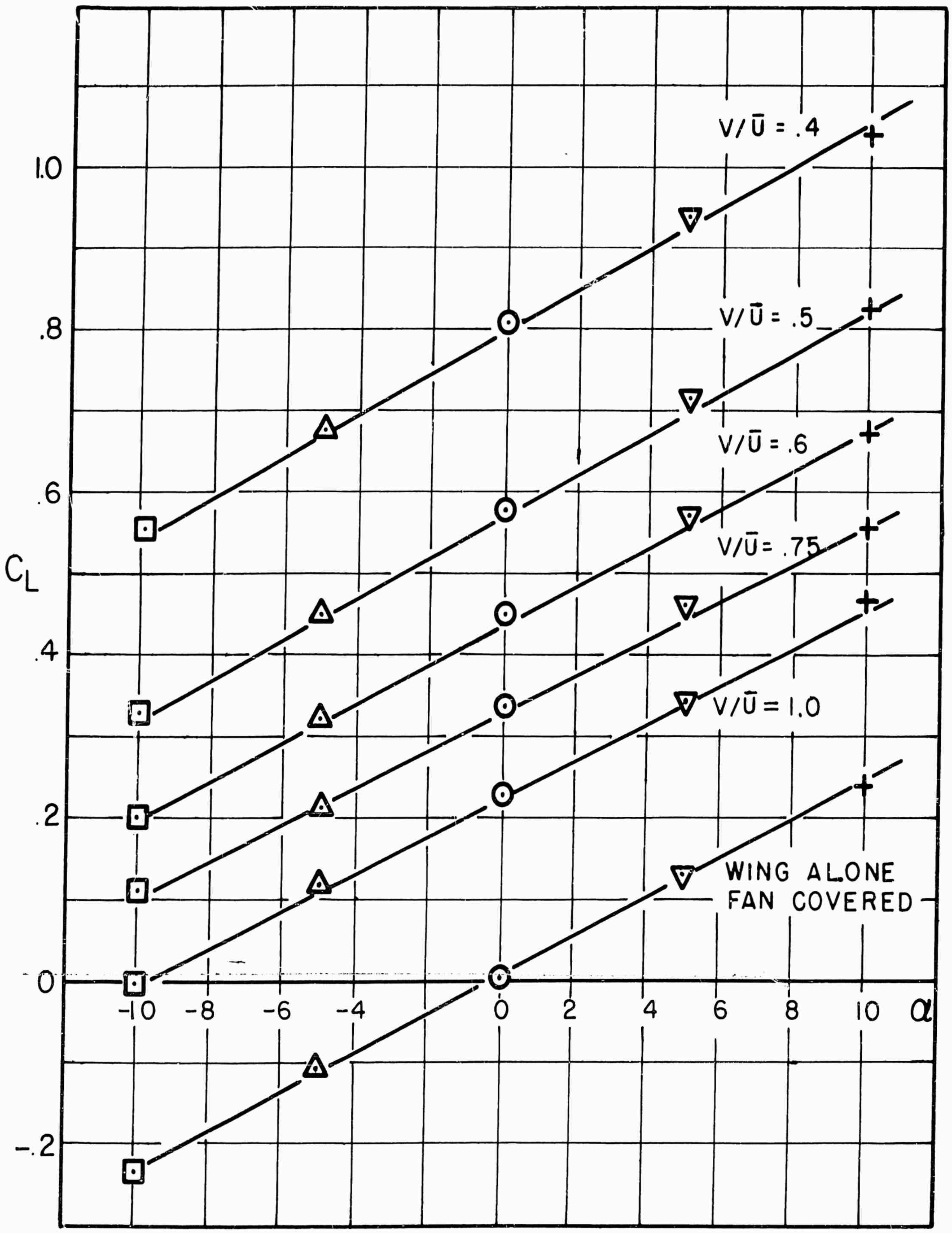

FIGURE 21 FAN-WING LIFT CURVE SLOPE.

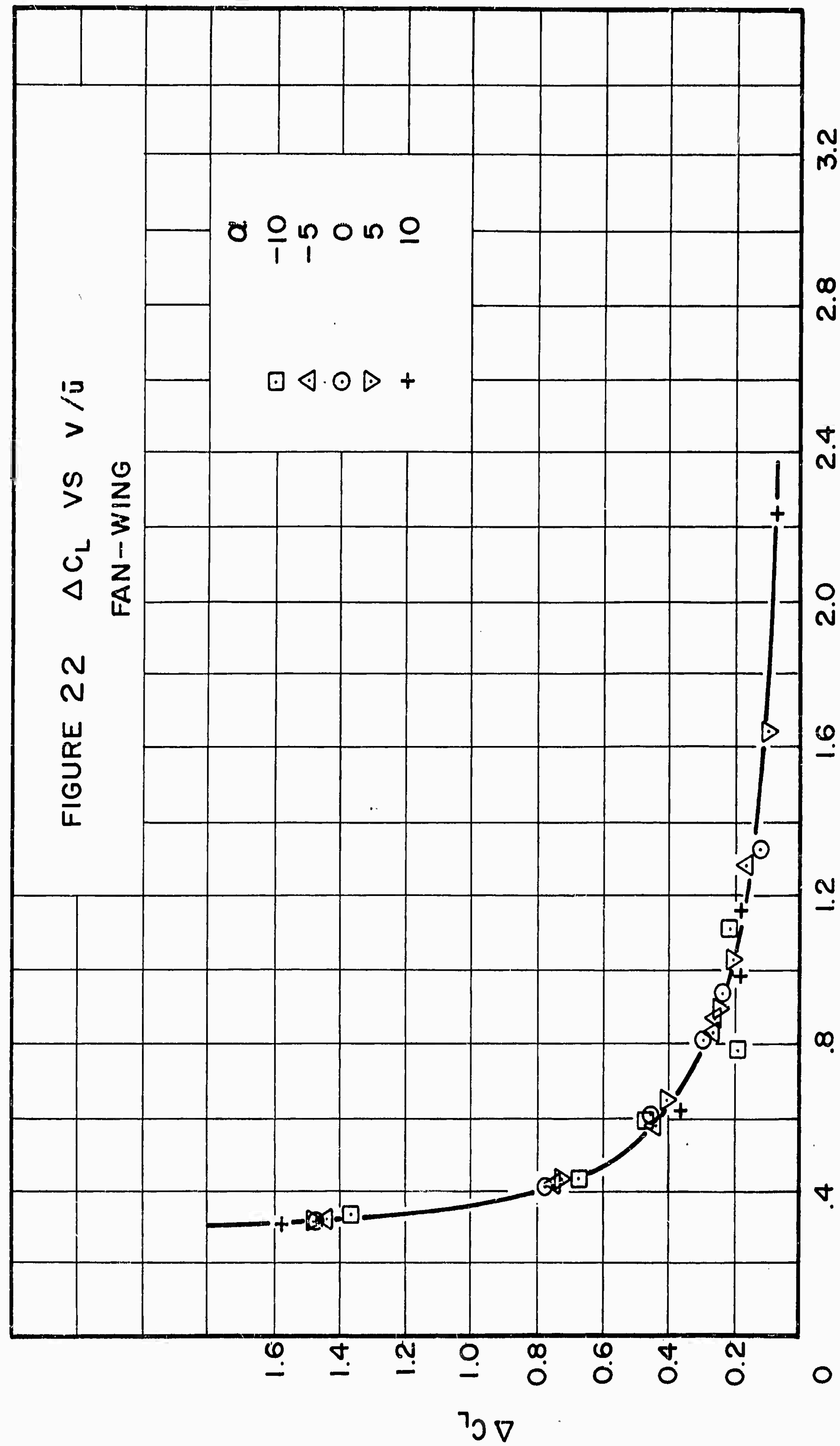
FIGURE 22 ΔC_L VS V/ū
FAN-WING
α
-10
-5
0
5
10
ΔC_L
1.6
1.4
1.2
1.0
0.8
0.6
0.4
0.2
0
.4
.8
1.2
1.6
2.0
2.4
2.8
3.2
V/ū

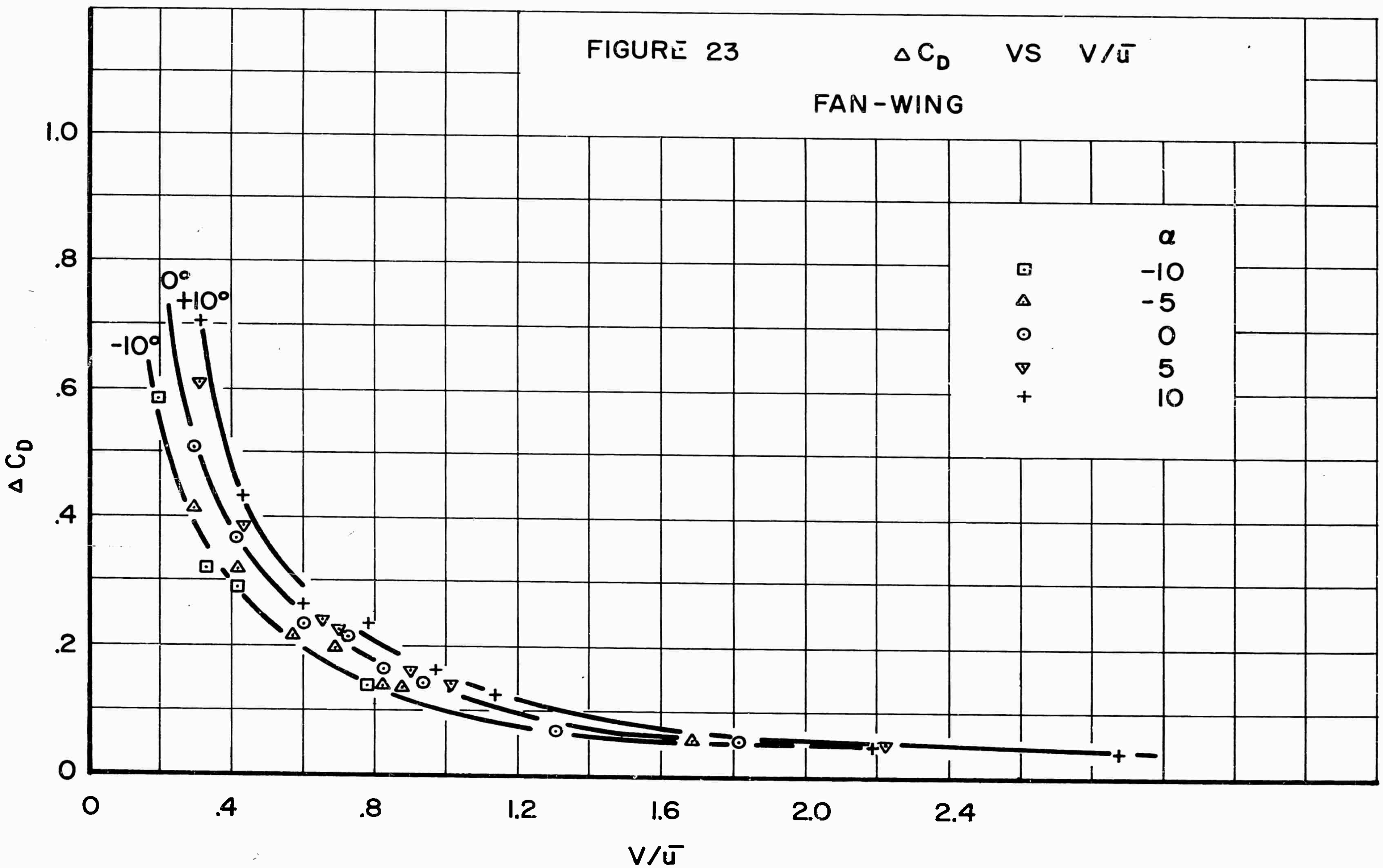

FIGURE 23 ΔC_D VS $V/\bar{u}$

FAN-WING

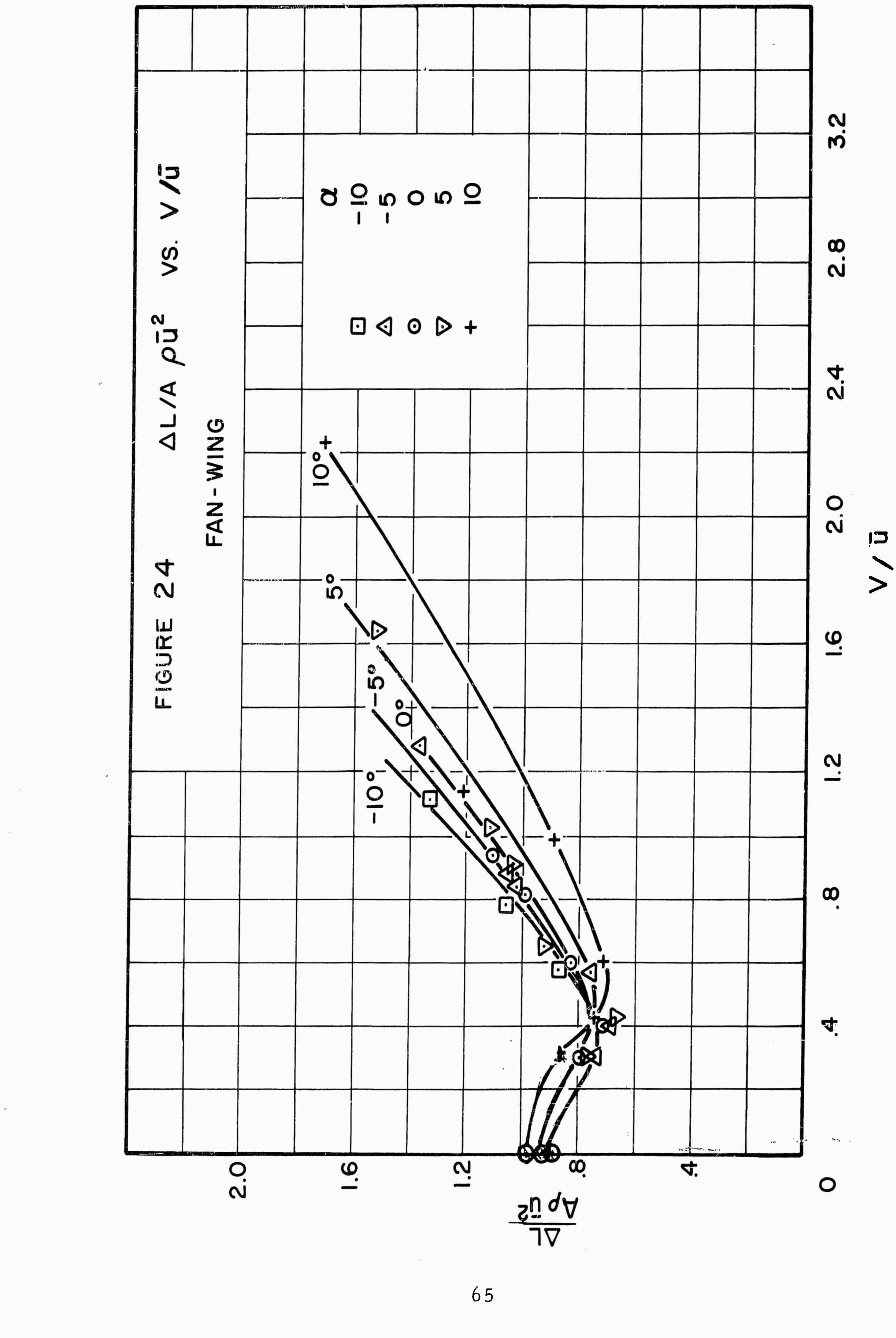

FIGURE 24
ΔL/A ρū² VS. V/ū
FAN-WING
α
-10
-5
0
5
10
10°
5°
-5°
0°
-10°
0
.4
.8
1.2
1.6
2.0
2.4
2.8
3.2
V/ū
ΔL/Δρū²

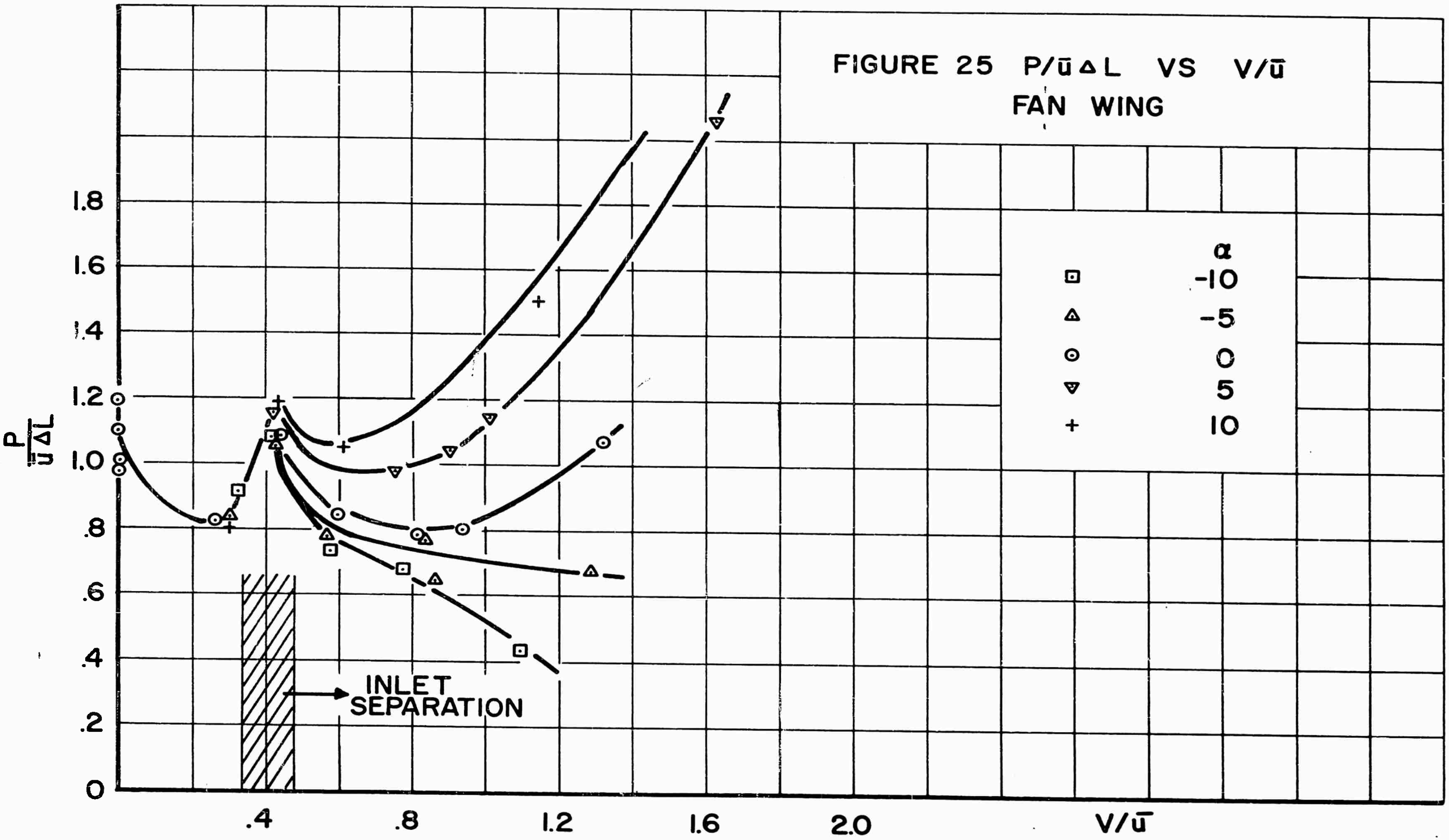

FIGURE 25 $P/\bar{u}\Delta L$ VS $V/\bar{u}$
FAN WING

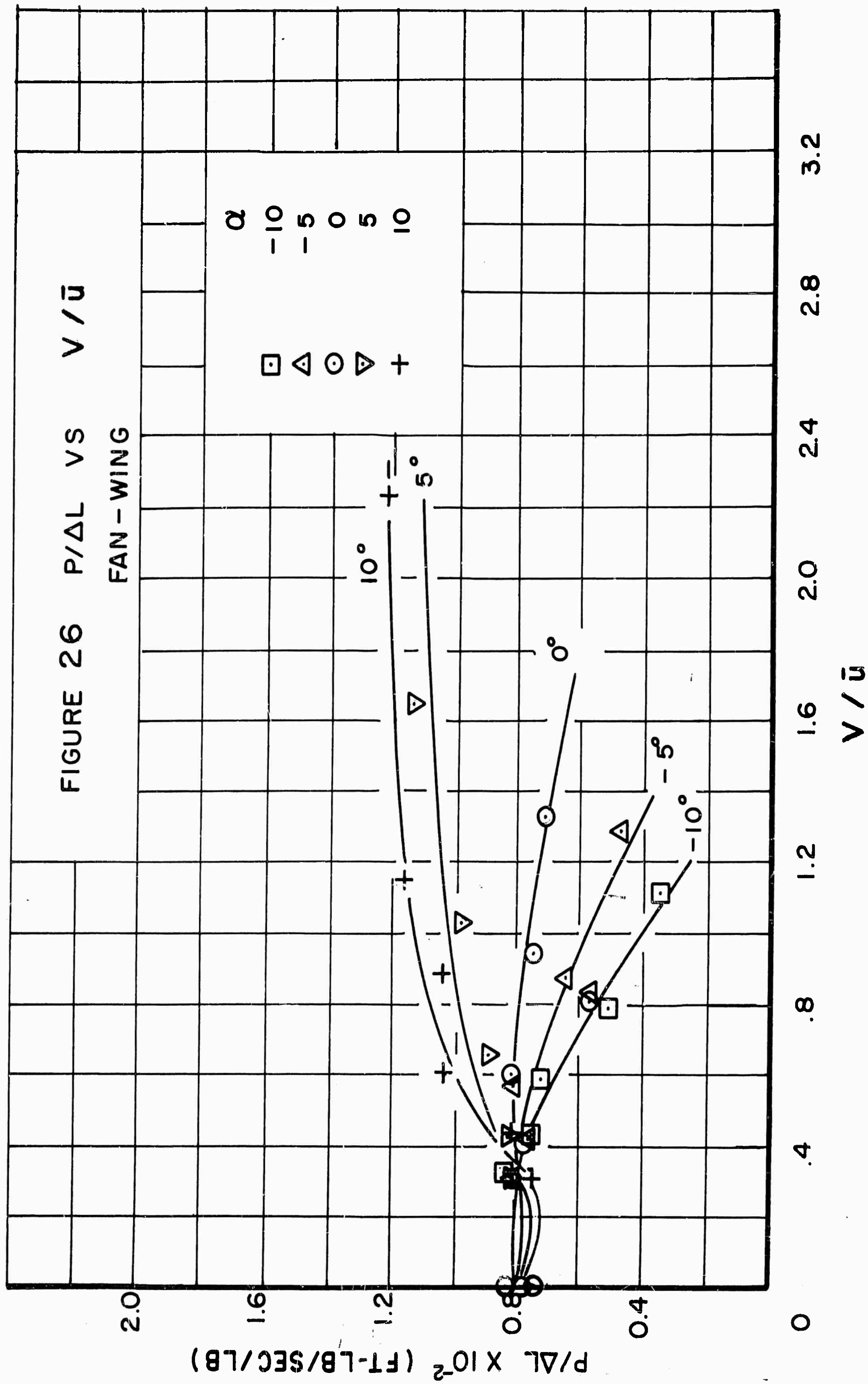

FIGURE 26 P/ΔL VS V/ū
FAN-WING
α
-10
-5
0
5
10
10°
5°
0°
-5°
-10°
0
.4
.8
1.2
1.6
2.0
2.4
2.8
3.2
V/ū
0.4
0.8
1.2
1.6
2.0
P/ΔL X 10^-2 (FT-LB/SEC/LB)

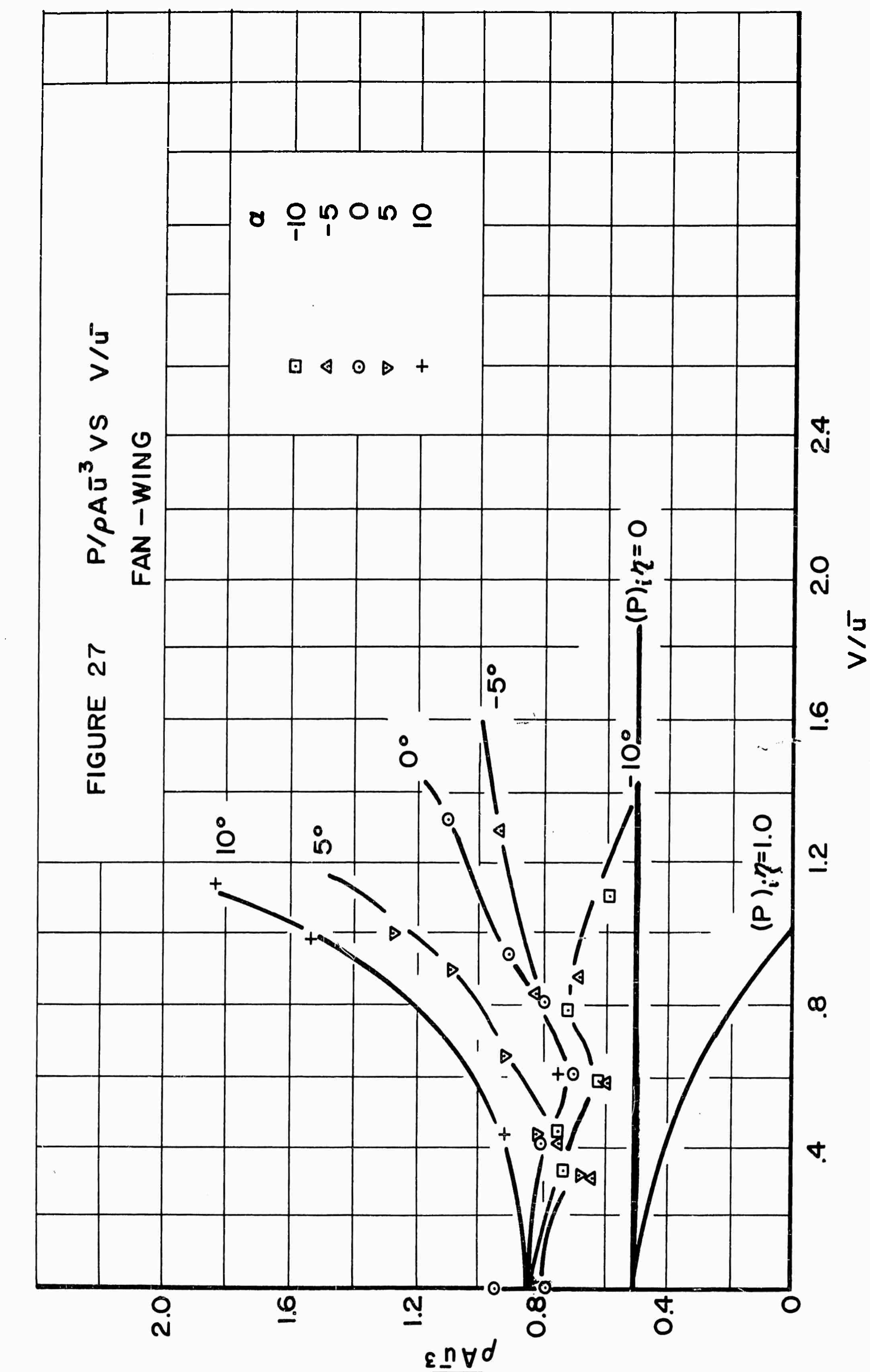

FIGURE 27 $P/\rho A\bar{u}^3$ VS $V/\bar{u}$

FAN-WING

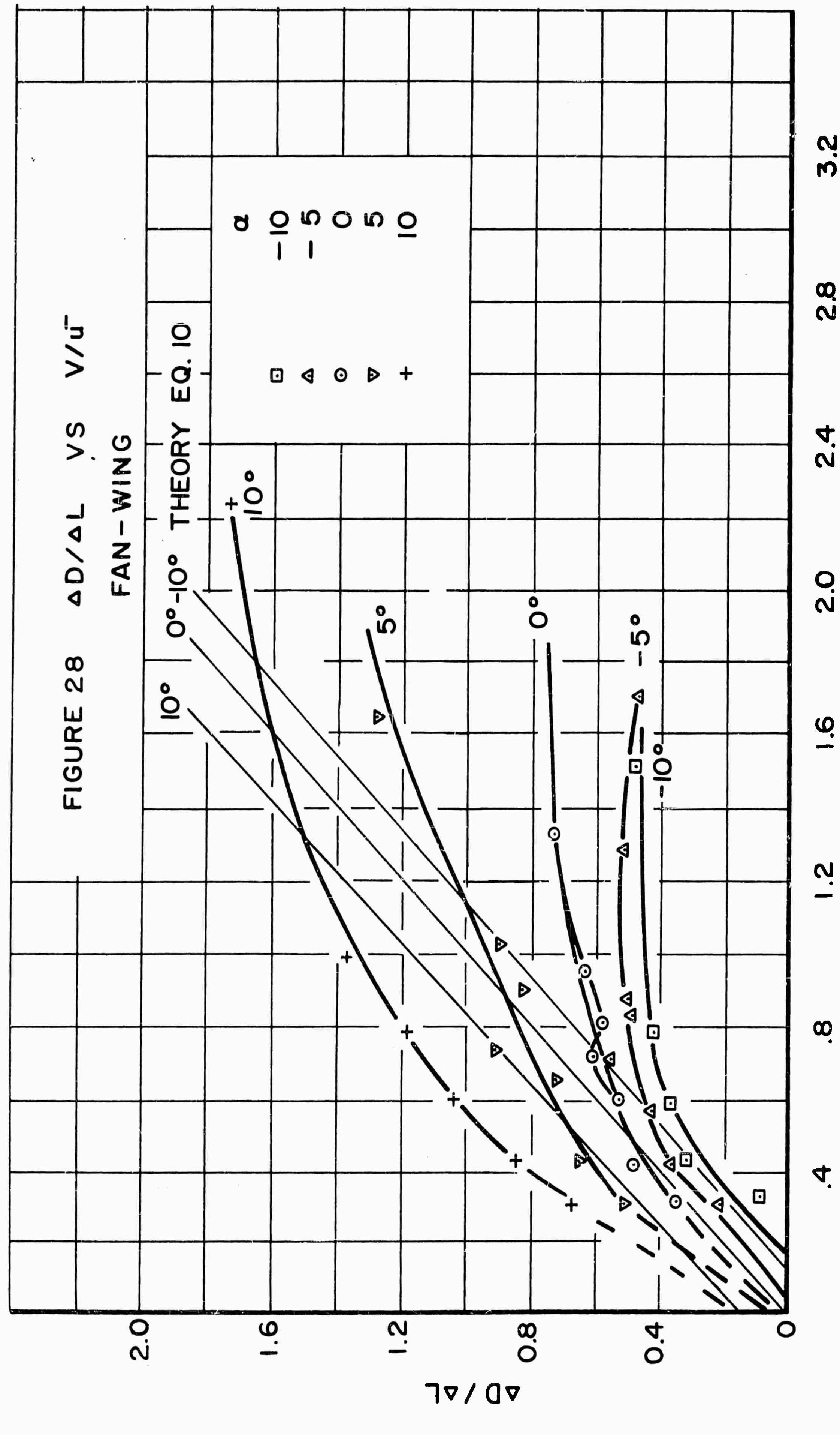
FIGURE 28 ΔD/ΔL VS V/u'
FAN-WING
0°-10° THEORY EQ. 10
10°
5°
0°
-5°
-10°
α
□ -10
△ -5
⊙ 0
▷ 5
+ 10
ΔD/ΔL
V/u'
0
0.4
0.8
1.2
1.6
2.0
.4
.8
1.2
1.6
2.0
2.4
2.8
3.2

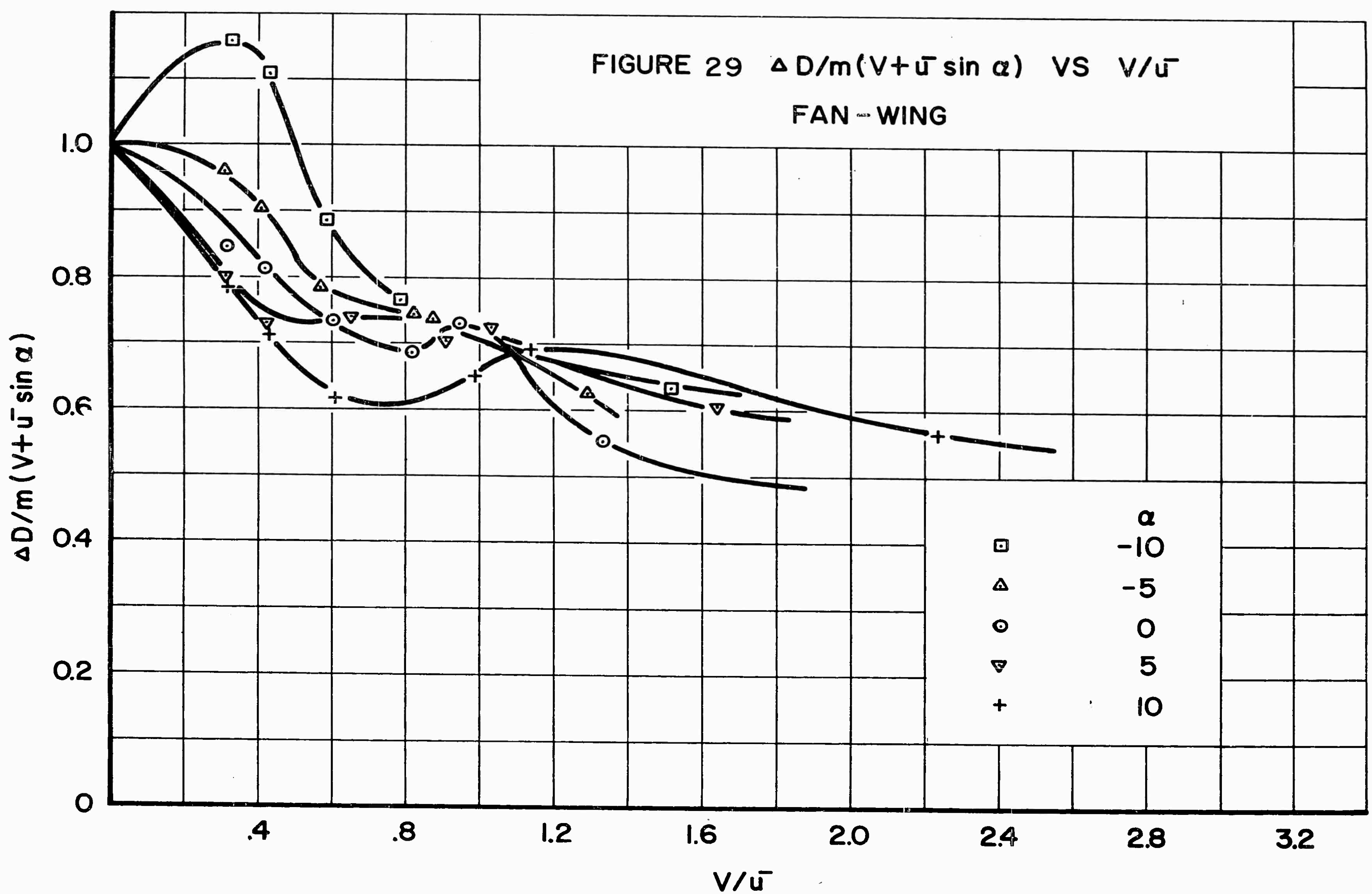

FIGURE 29 ΔD/m(V+ū sin α) VS V/ū
FAN - WING
1.0
0.8
0.6
0.4
0.2
0
.4
.8
1.2
1.6
2.0
2.4
2.8
3.2
V/ū
ΔD/m (V+ū sin α)
α
-10
-5
0
5
10

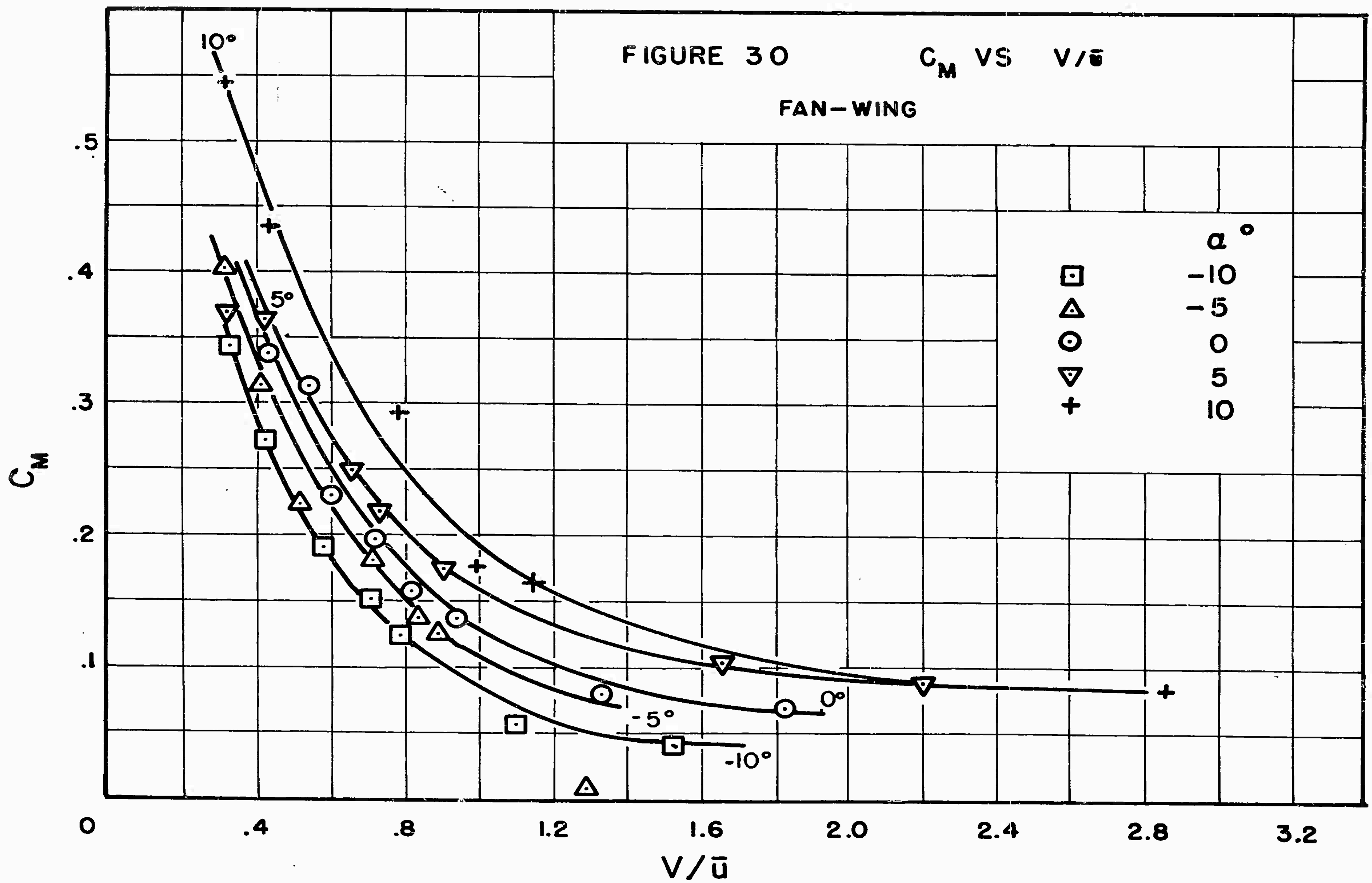
FIGURE 30
C_M VS V/ū
FAN—WING
α°
−10
−5
0
5
10
10°
5°
0°
-5°
-10°
C_M
.5
.4
.3
.2
.1
0
.4
.8
1.2
1.6
2.0
2.4
2.8
3.2
V/ū

FIG. 31 FAN WING C_M VS α

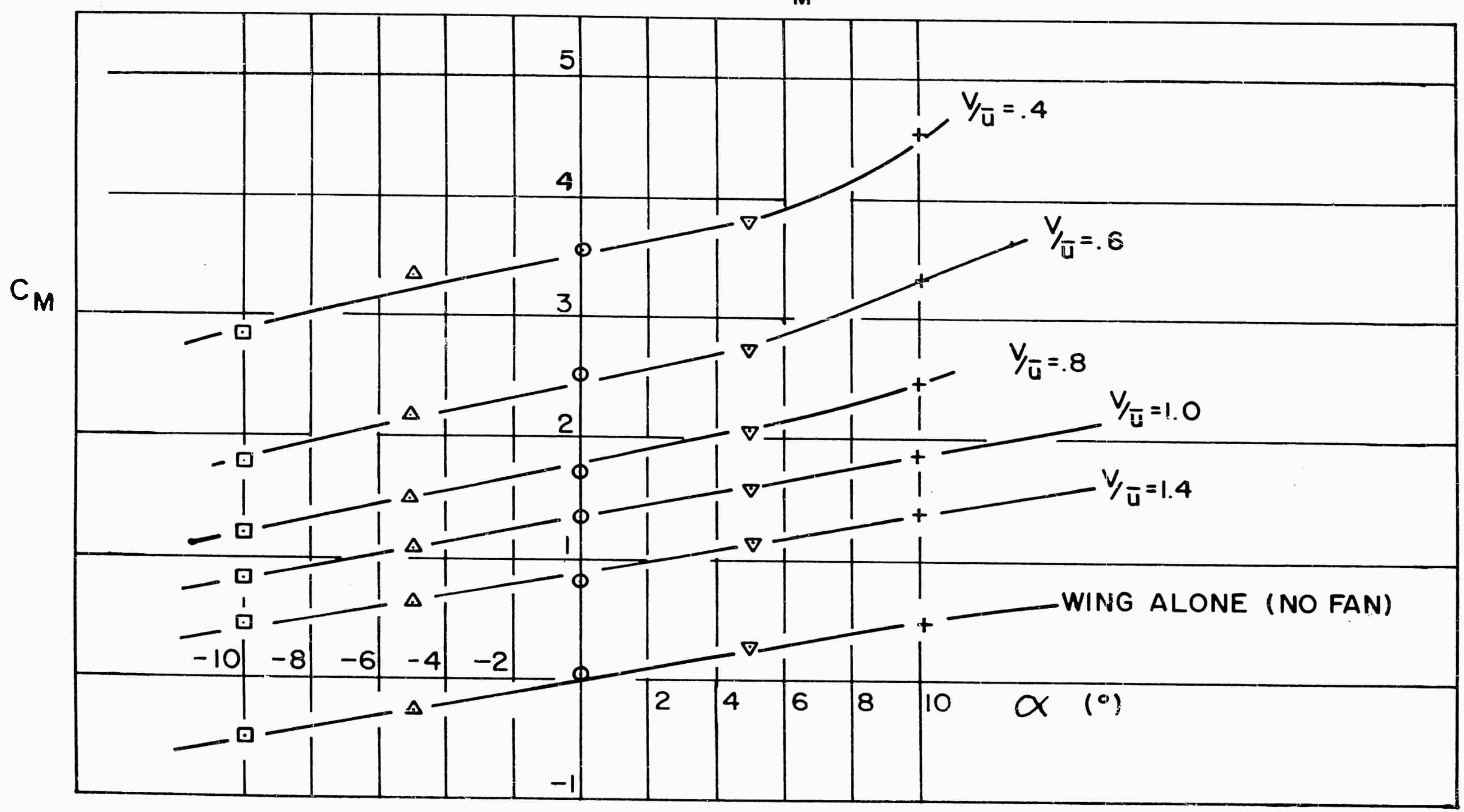

FIGURE 32 $\Delta C_M / \Delta C_L$ VS $V/\bar{u}$

FAN-WING

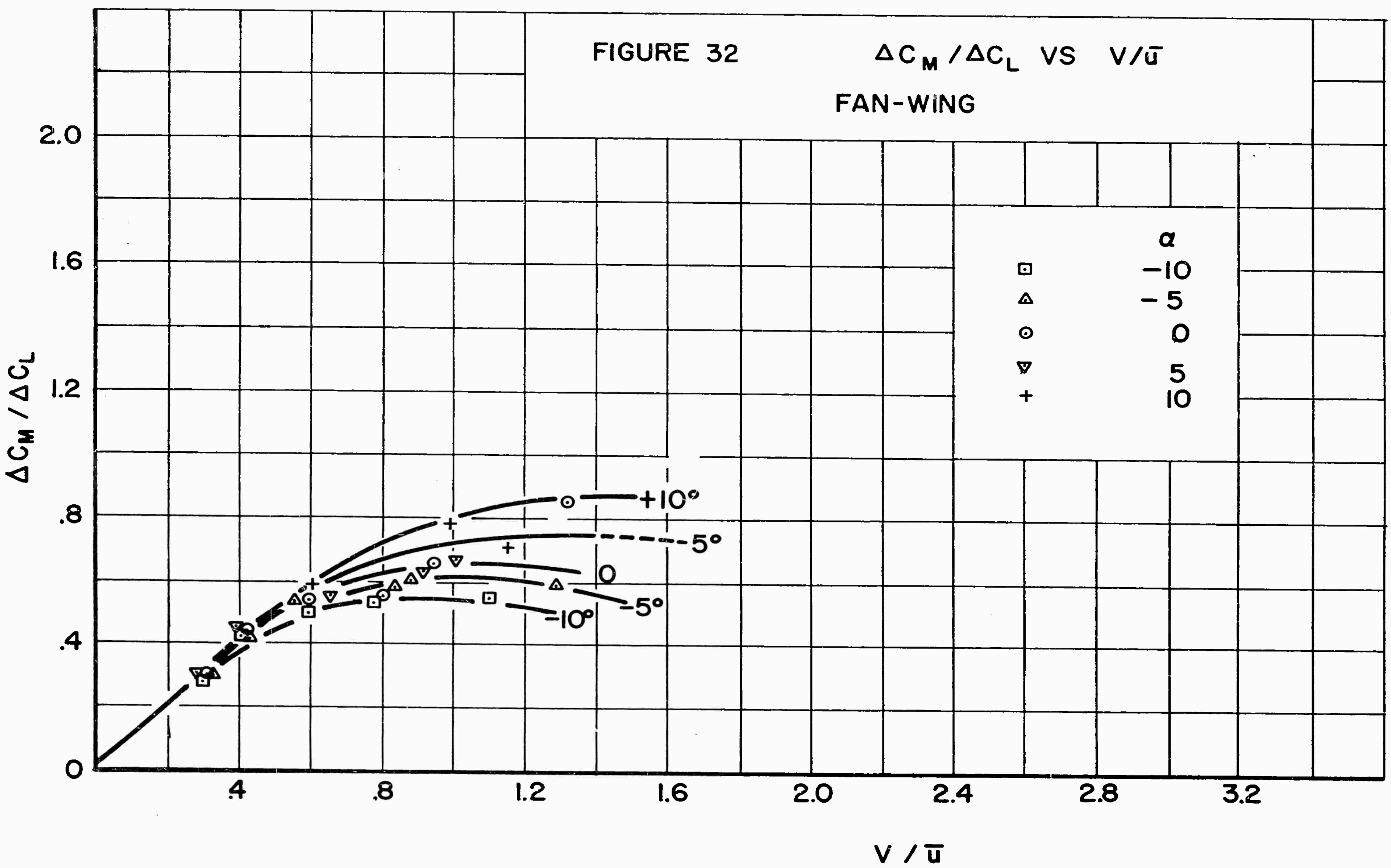

TILTING DUCT

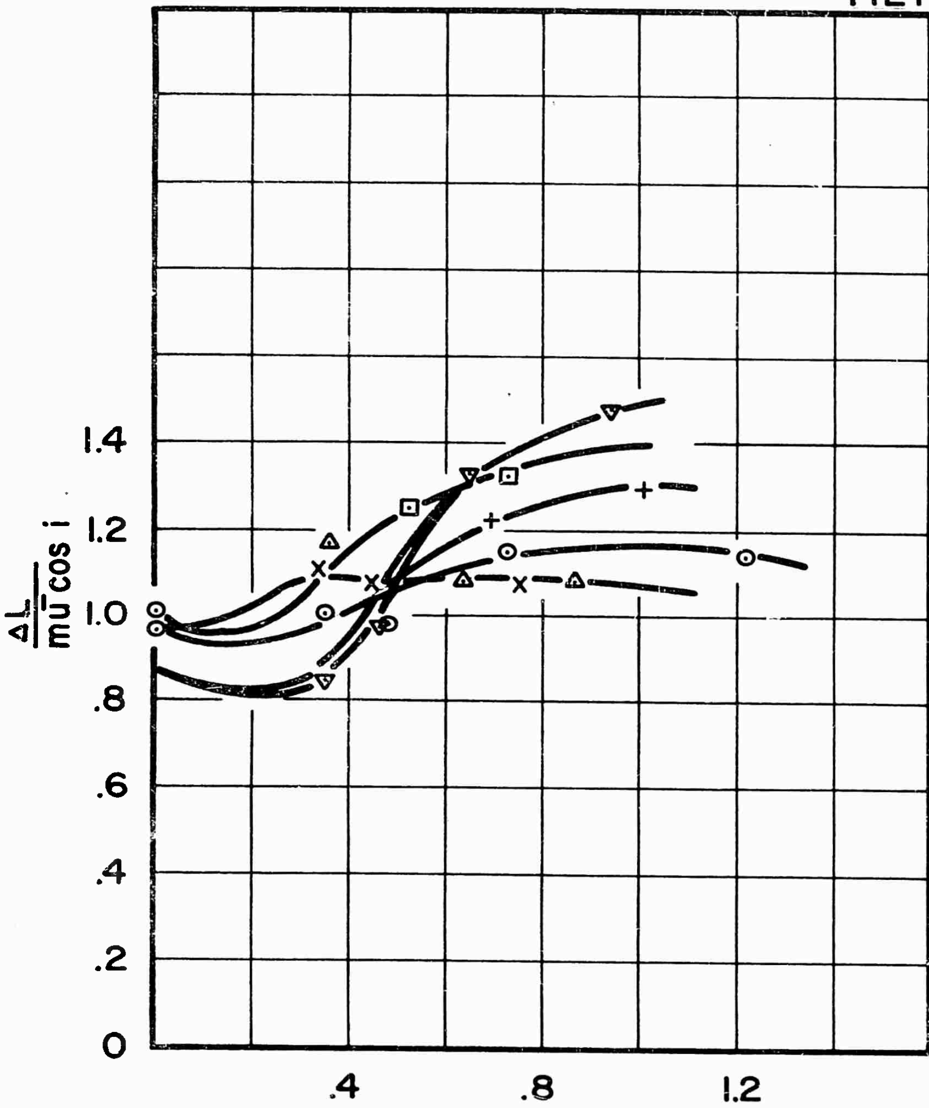

FIGURE 33

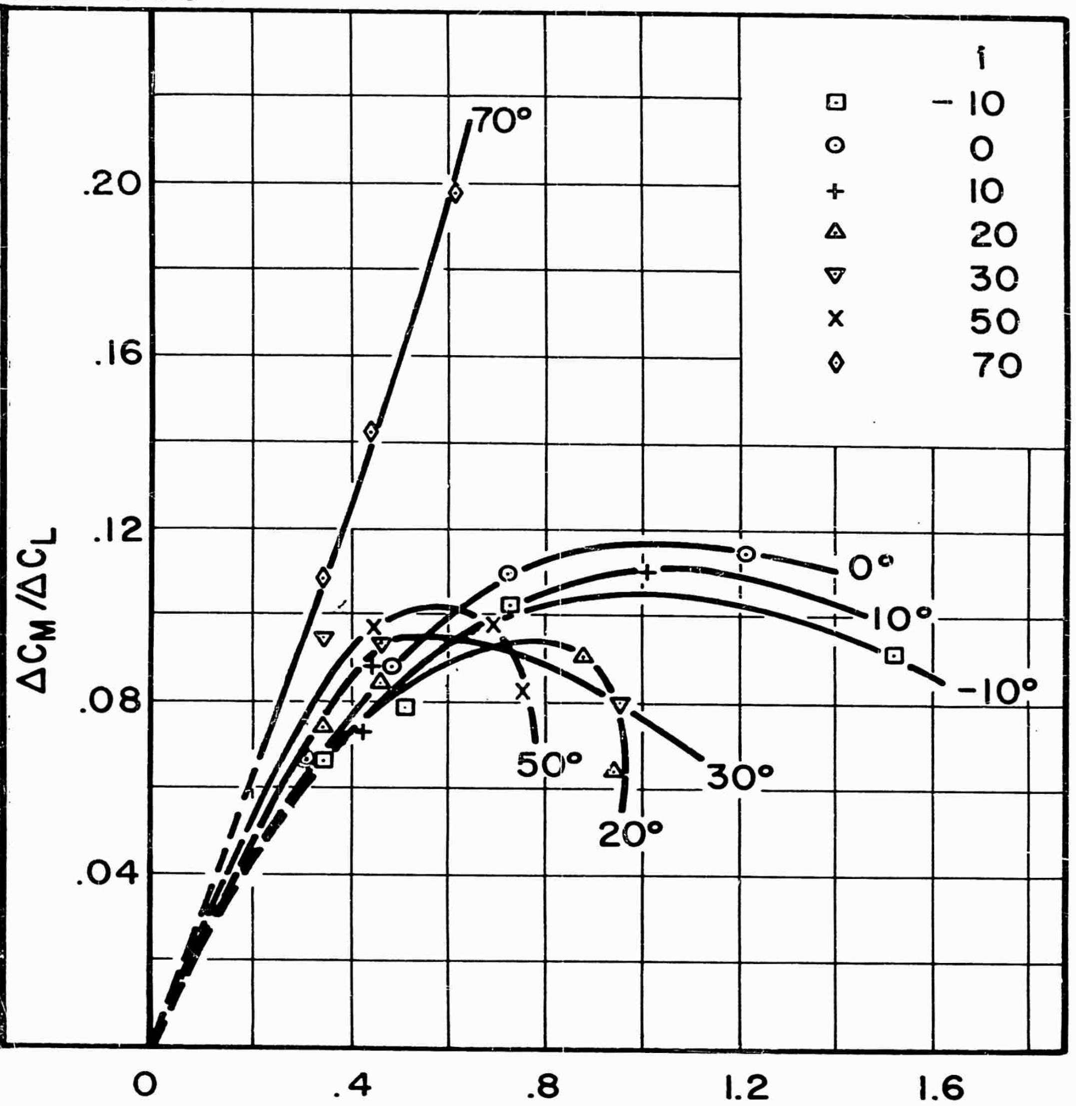

V/ū

FIGURE 34 INCREMENTAL MOMENT

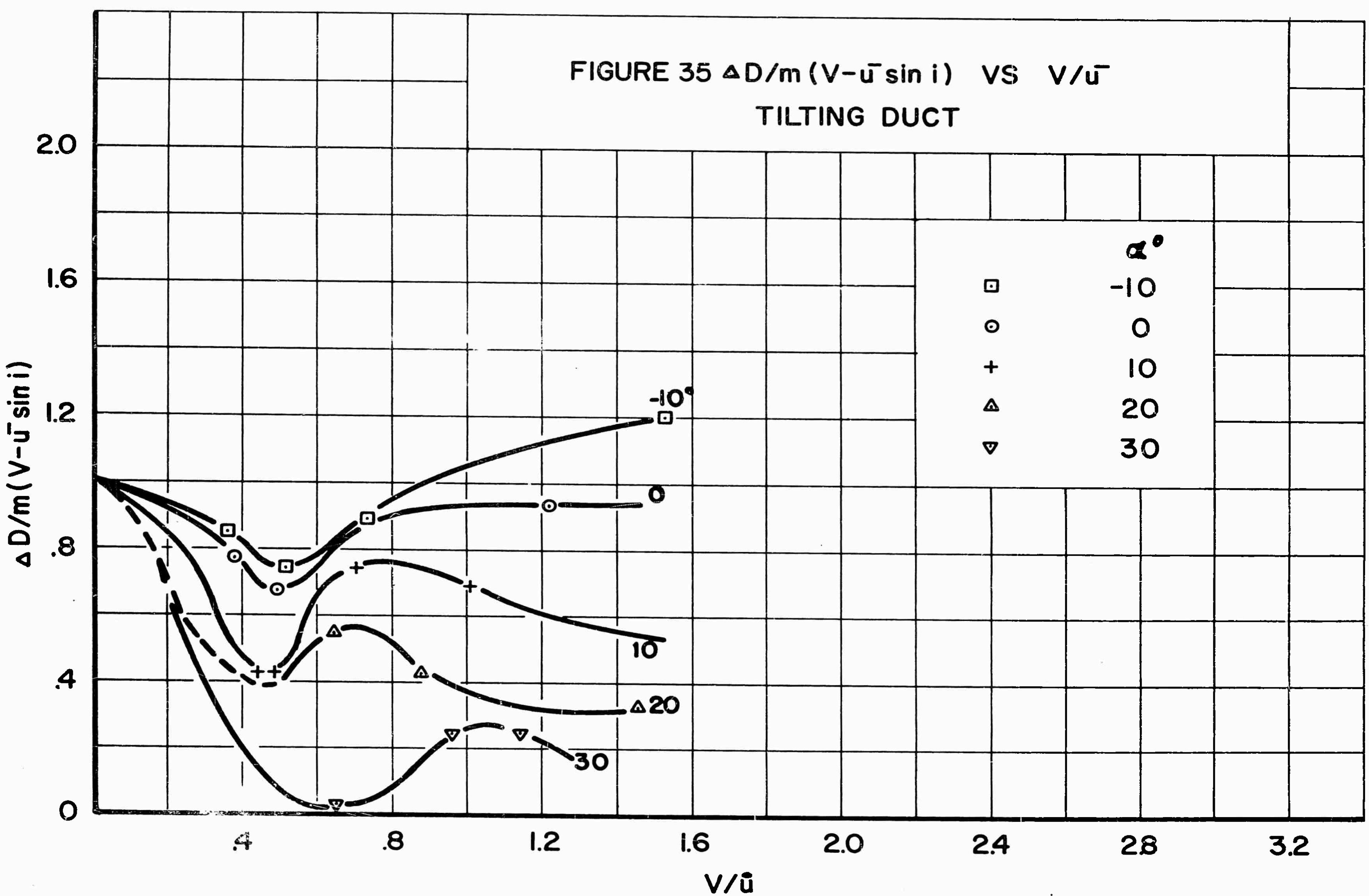

FIGURE 35 ΔD/m(V−ū sin i) VS V/ū
TILTING DUCT
α°
-10
0
10
20
30
-10°
0
10
Δ20
30
2.0
1.6
1.2
.8
.4
0
.4
.8
1.2
1.6
2.0
2.4
2.8
3.2
V/ū
ΔD/m(V−ū sin i)

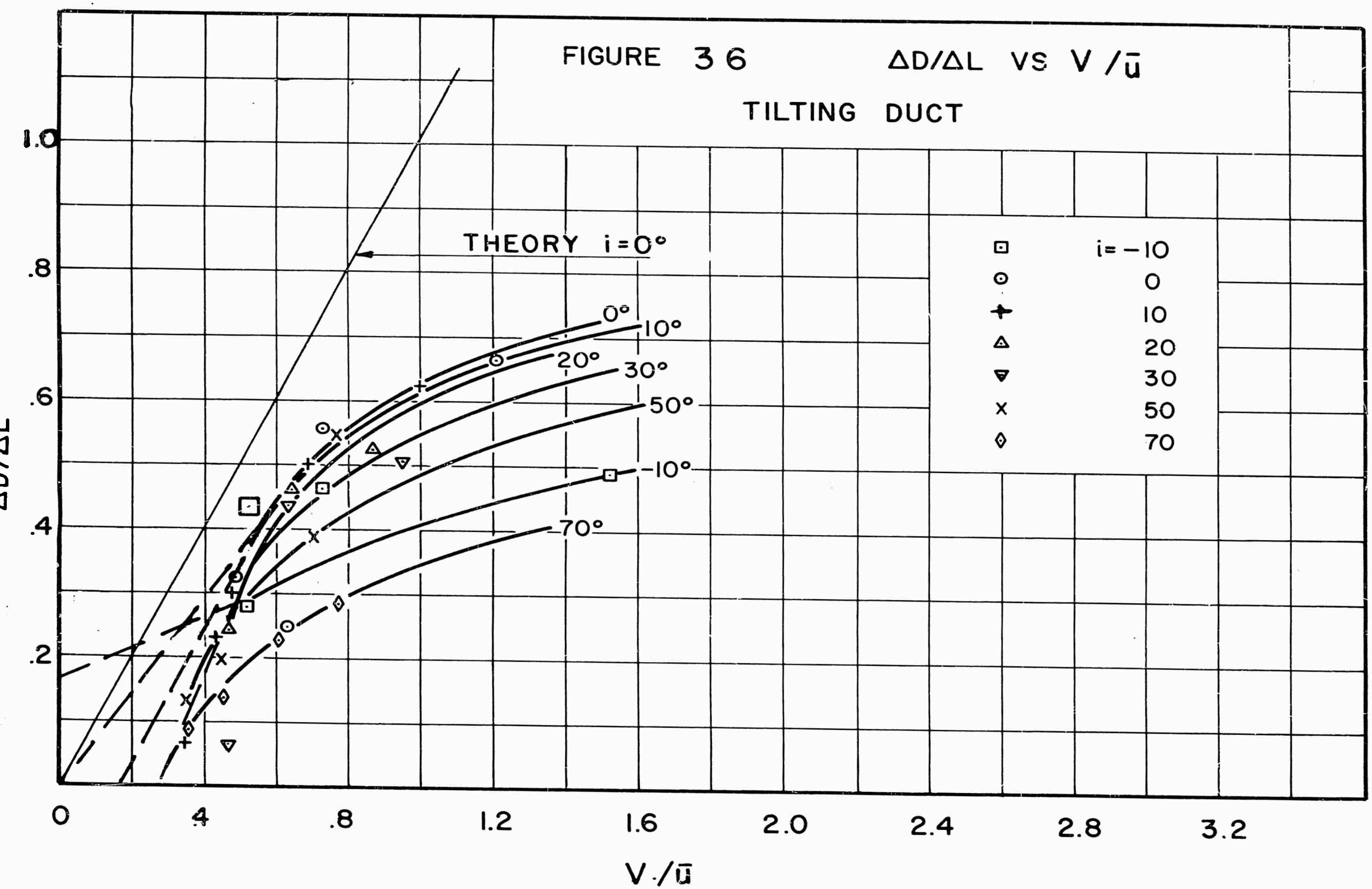

FIGURE 36 ΔD/ΔL VS V/ū
TILTING DUCT
THEORY i=0°
0°
10°
20°
30°
50°
-10°
70°
i= -10
0
10
20
30
50
70
1.0
.8
.6
.4
.2
ΔD/ΔL
0
.4
.8
1.2
1.6
2.0
2.4
2.8
3.2
V/ū

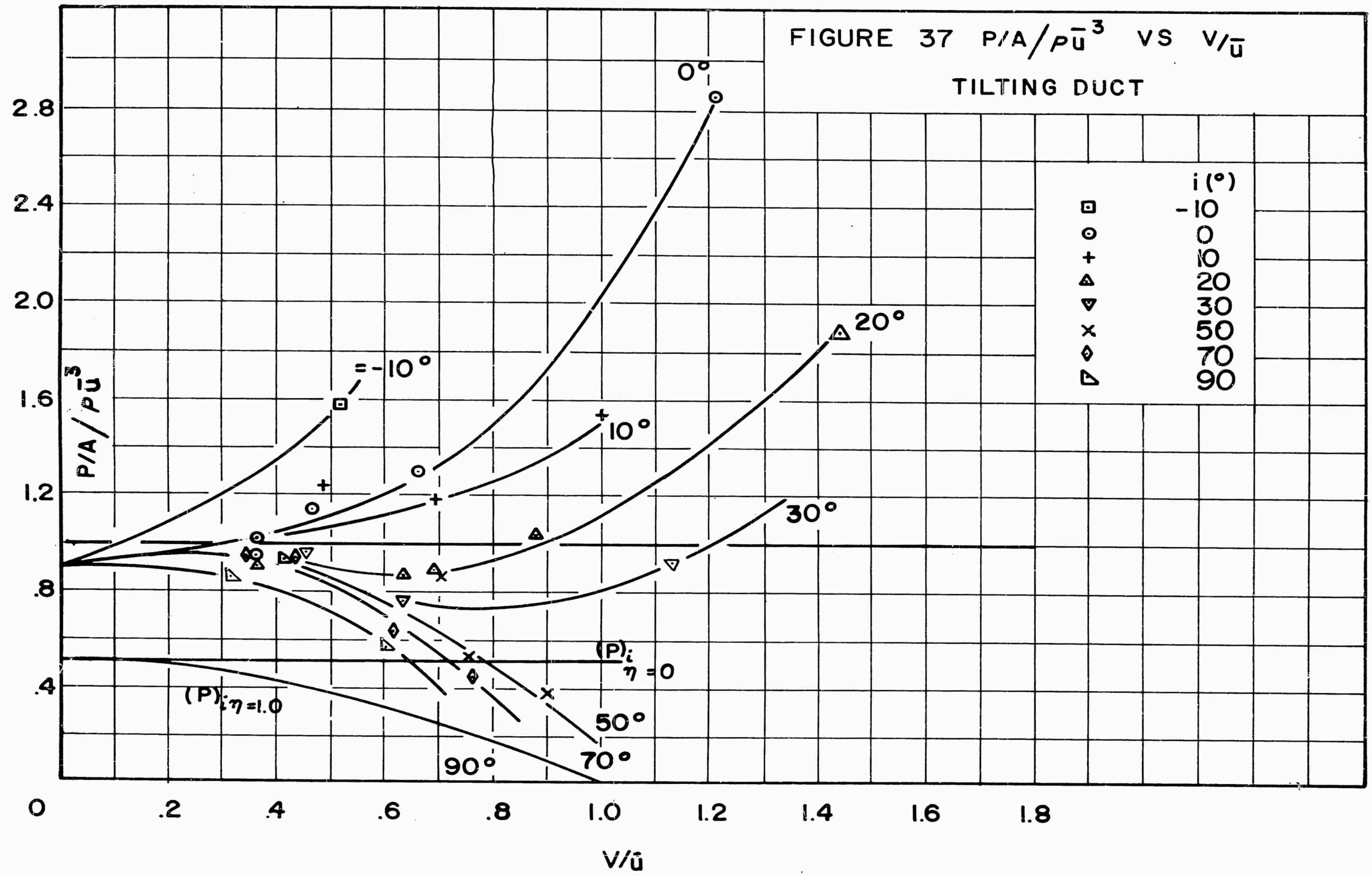

FIGURE 37 $P/A/\rho\bar{u}^3$ VS $V/\bar{u}$

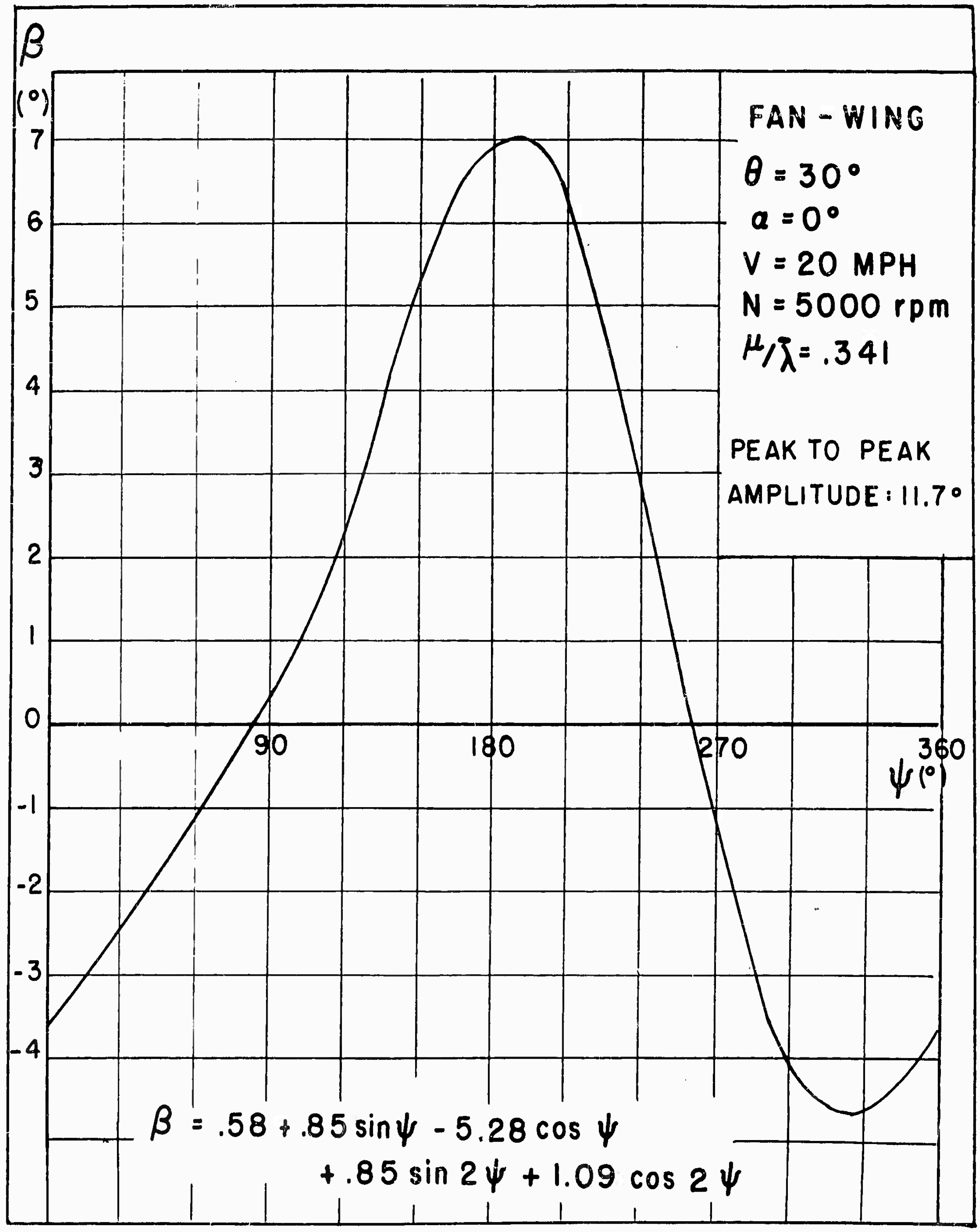

FIG.38 FAN BLADE FLAPPING ANALYSIS